

ABSTRACT

A detailed study was conducted on the tephra deposits that were found in several locations in the Peninsular Malaysia which are important time markers in the local Quaternary stratigraphy. Typically, these deposits consisted of aurally deposited, fine-grained < 100 μm , silica-rich volcanic glass shards and mineral grains, in layers ranging from 10 cm to 9 m in thickness, within quaternary lacustrine sediments. Few of these have been dated. In the literature, most, if not all, were attributed to the VEI 8 eruption at Lake Toba at 70-75 k.a., while, in actuality, there have been three other high VEI eruptions in Sumatra that might have been responsible - Mount Maninjau at 80 and 52 k.a. (proximal tuffs are exposed at Sianok Canyon near Padang Highlands, Sumatra) and Lake Ranau between 0.7 and 0.4 m.a. In this study, site reconnaissance, tephra age determination and geochemical fingerprint analysis have been carried out to provide scientific proves of the origins of Peninsular Malaysia tephra. Detailed field mapping of tephra distribution in the vicinity of Lenggong in Perak revealed that the tephra layers, covering 15 km², were deposited at a time when the local stream base level was 70 m above the current level, as most of the fresh tephra layers were found at that elevation. Tephra distribution was controlled by topography at the time of deposition since layers of fresh and reworked deposits of tephra had been discovered in the vicinity of the Perak River banks and on gentle slopes of palm oil estates. The presence of reworked ash under layers of fresh ash might indicated that more than one paroxysmal eruption were responsible. Fission track and optically stimulated luminescence (OSL) techniques were executed on two selected areas with fresh layers of tephra and correlated the results with published data of possible origins. Cluster analysis, bivariate analysis, Rare-Earth Element and trace element ratios analysis and spider diagrams were implemented to differentiate and recognize individual eruptions. The results of fission track dates of Lenggong tephra were 59 ± 7 k.a. and 59 ± 9 k.a., while Kuala Pelus tephra had luminescence dates of 58.5 ± 7.6 k.a and 75.5 ± 9.8 k.a. These dates could be correlated with the 52 k. a. Maninjau and 75 k. a. Toba eruptions. Major and trace element content of glass shards revealed similarities between those from the Peninsular Malaysia and the proximal tuff from the 75 k.a. Toba eruption. The majority of Gelok samples were correlated to Toba sample. Even though Lenggong and Padang Sanai major elements result showed that there were three populations in the same layer, chemical genetically it could not be related with Maninjau samples. Kg. Dong and Kuala Kangsar tephra showed the largest variations of SiO₂ and alkalies which were distinct from the other Peninsular Malaysia tephra. The Maninjau tuff was distinctly different from the Peninsular Malaysia tephra and from the YTT. This implies that Lenggong tephra could be originated from Toba and other possible source(s). The conclusion that could be drawn from this evidences that it is significantly proved that the tephra in Peninsular Malaysia is most likely originated from Toba and also possible from Maninjau and other eruptions.

ABSTRAK

Kajian secara terperinci telah dijalankan terhadap enapan debu gunung berapi yang dijumpai di beberapa kawasan di Semenanjung Malaysia yang merupakan penanda usia yang penting bagi stratigrafi Kuaterner tempatan. Secara amnya, enapan ini mengandungi enapan yang berbutir halus, berkaca syard dan butiran mineral, dengan lapisan berketebalan antara 10 cm hingga 9 m di dalam enapan tasik berusia Kuaterner. Hanya segelintir telah ditentukan usianya. Di dalam kajian terdahulu, kebanyakan penyelidik telah menyamakan kesemua debu ini dengan asalan Tasik Toba yang mempunyai Indeks Letusan Gunung Berapi 8, walaupun secara realitinya, terdapat tiga lagi letusan yang mempunyai VEI tinggi di Sumatra yang berkemungkinan besar menyumbang kepada enapan debu ini; iaitu Gunung Maninjau yang berusia 80 dan 52 ribu tahun di mana proksimal tuff tersingkap di Ngarai Sianok berdekatan Padang dan Tasik Ranau yang berusia 0.7 hingga 0.4 juta tahun. Dalam kajian ini, eksplorasi kawasan kajian, penentuan umur debu gunung berapi, dan kajian geokimia telah dijalankan untuk mendapatkan bukti saintifik bagi asalan debu gunung berapi di Semenanjung Malaysia. Kajian secara terperinci di kawasan Lenggong menyingkap bahawa lapisan debu gunung berapi yang merangkumi 15 km², telah dienapkan semasa paras air sungai 70 m lebih tinggi daripada paras waktu kini, oleh kerana kebanyakan debu 'segar' telah dijumpai di ketinggian tersebut. Taburan debu gunung berapi ini dipengaruhi oleh topografi semasa pengenapan berlaku kerana beberapa lapisan debu 'segar' telah dijumpai di tebing Sungai Perak dan di kecerunan landai di kawasan ladang kepala sawit. Kehadiran debu gunung berapi yang dikerja semula di bawah lapisan debu yang 'segar' menunjukkan berkemungkinan terdapat lebih daripada satu letusan gunung berapi yang menyumbang kepada enapan ini. Kaedah penentuan umur 'fission track' dan 'optically stimulated luminescence' (OSL) dijalankan di dua kawasan yang terpilih dan dikorelasikan dengan keputusan yang telah diterbitkan bagi sumber-sumber yang berkemungkinan. Analisis kluster, kajian bivariat, analisis unsur-unsur minor dan surih serta gambarajah spider telah dijana untuk membezakan dan mengenalpasti setiap letusan gunung berapi. Keputusan bagi umur 'fission track' bagi Lenggong adalah 59 ± 7 dan 59 ± 9 ribu tahun, manakala debu Kuala Pelus pula mempunyai umur 'luminescence' 58.5 ± 7.6 dan 75.5 ± 9.8 ribu tahun. Umur-umur ini dapat dikorelasikan dengan Maninjau yang berusia 52 ribu tahun dan Toba yang berusia 75 ribu tahun. Kandungan unsur-unsur minor dan surih menunjukkan persamaan di antara Semenanjung Malaysia dengan proksimal tuff bagi letusan Toba yang berusia 75 k.a. Secara majoritinya, sampel-sampel Gelok dapat dikorelasikan dengan sampel Toba. Walaupun unsur-unsur major menunjukkan terdapat lebih daripada tiga populasi di dalam satu lapisan debu gunung berapi yang sama di Lenggong dan Padang Sanai, secara genetik kimia ia tidak dapat dikaitkan dengan sampel-sampel Maninjau. Debu gunung berapi Kg. Dong dan Kuala Kangsar menunjukkan variasi SiO₂ dan alkali tertinggi menunjukkan perbezaan yang ketara berbanding debu-debu gunung berapi lain di Semenanjung Malaysia. Tuff Maninjau menunjukkan perbezaan yang ketara dengan debu-debu gunung berapi di Semenanjung

Malaysia dan Toba. Ini menunjukkan bahawa debu Lenggong berkemungkinan berasal daripada Toba dan sumber-sumber lain yang berkemungkinan. Berdasarkan bukti-bukti yang diperolehi, dapat dirumuskan berkemungkinan besar debu gunung berapi di Semenanjung Malaysia berasal daripada letusan Toba, dan berkemungkinan daripada Maninjau dan letusan-letusan gunung berapi lain.

Table of Contents

List of Figures.....	vi
List of Tables.....	viii
1. Introduction	1
1.1. Previous Studies and Research Motivations.....	8
2. Methods	18
2.1. Fieldwork	
2.1.1. Tephra Characterization	20
2.1.2. Glass Shards Morphology.....	21
2.2. Laboratory Methods	
2.2.1. Ages Determination	22
2.2.2. Fission Track on Glass Shards.....	22
2.2.3. Optical Stimulated Luminescence Dating (OSL).....	23
2.3. Geochemical Analysis	
2.3.1. Sample Preparation for Geochemical Analysis	24
2.3.2. Electronprobe Micro Analyzer (EPMA).....	25
2.3.3. Laser Ablation ICP-MS.....	26
3. Results	33
3.1. Tephra Distribution.....	34
3.1.1. Freshness Determination	42
3.2. Tephra Ages.....	44
3.2.1. Fission Track Ages	44

3.2.2. OSL Ages	44
3.3. Major, REE and Trace Elements Analysis.....	45
3.3.1. Peninsular Malaysia Major Elements Data.....	46
3.3.2. Sumatra Major Elements Data.....	46
3.3.3. Major Elements Plot.....	46
3.3.4. REE and Trace Elements Data.....	46
4. Discussion	49
4.1. Distribution.....	49
4.1.1. Tephra thickness	52
4.2. Tephra Ages.....	53
4.2.1. Previous Dating	53
4.3. Geochemical Analysis.....	55
4.3.1. Elemental Distribution.....	61
4.3.2. Modeling of Fractional Crystallization.....	66
5. Conclusions and Future Work	78
References	81
Appendix I.....	86
Appendix II.....	88
Appendix III.....	102

List of Figures

Figure 1-1: Documented localities of tephra found in Peninsular Malaysia.....	2
Figure 1-2: Rhyolitic tephra on Indian Ocean Floor	3
Figure 1-3: The volcanic history of Sumatra	5
Figure 1-4: Toba Caldera in Northern Sumatra.....	15
Figure 1-5: Maninjau Caldera in Central Sumatra.....	16
Figure 1-6: Danau Ranau in Southern Sumatra.....	16
Figure 3-1: Maninjau Bukit Tinggi Tuffs.....	34
Figure 3-2: Tephra distribution in Lenggong.....	37
Figure 3-3: Tephra deposits in Bukit Sapi.....	38
Figure 3-4: Tephra layers in Labit.....	38
Figure 3-5: Tephra strata in Gelok.....	39
Figure 3-6: Visualisation of depositional area of Lenggong Valley.....	39
Figure 3-7: Relationship between tephra distribution with vegetations.....	40
Figure 3-8: Relationship between tephra distribution with freshness	41
Figure 3-9: Relationship between tephra distribution with elevation and freshness	41
Figure 3-10: SEM photos of fresh and reworked glass shards.....	43
Figure 3-11: Box plot for REE data.....	47
Figure 4-1: Relationship of topography with tephra distribution in Lenggong.....	50
Figure 4-2: The distribution of tephra freshness in Lenggong.....	51
Figure 4-3: Chondrite Normalized REE profile.....	57
Figure 4-4: TAS diagram.....	59
Figure 4-5: Major elements cross plots.....	62

Figure 4-6: SiO ₂ vs Sr bivariate plot.....	64
Figure 4-7: K ₂ O vs bivariate plot.....	65
Figure 4-8: Ba vs Y bivariate linear plot.....	69
Figure 4-9: Ba vs Y bivariate log plot.....	70
Figure 4-10: Ba vs Nb bivariate log plot.....	72
Figure 4-11: Nb vs Y bivariate log plot.....	73
Figure 4-12: Ba vs Sr bivariate log plot.....	74
Figure 4-13: Rb vs Sr bivariate log plot.....	75
Figure 4-14: Ba vs Y bivariate log fin lot.....	76
Figure A3.1: Picture of Bukit Sapi (PM-S1) tephra.....	102
Figure A3.2: Picture of Gua Badak (PM-B1) tephra.....	102
Figure A3.3: Picture of Temelong tephra.....	103
Figure A3.4: Picture of Labit tephra.....	103
Figure A3.5: Picture of Lubuk Kawah tephra.....	104
Figure A3.6: Picture of Sena Halu outcrop at Luat Province.....	104
Figure A3.7: Picture of Padang Grus tephra.....	105
Figure A3.8: Picture of Kuala Pelus (KP1 and KP2) tephra.....	105
Figure A3.9: Picture of Kg. Talang (PM-T1) tephra.....	106
Figure A3.10: Picture of Kg. Dong (PM-D1) tephra.....	106

List of Tables

Table 1-1: List of major eruptions in Sumatra	4
Table 2-1: List of sites visited.....	18
Table 3-1: The distribution of samples profile in Lenggong	35
Table 3-2: The distribution of samples profile in Peninsular Malaysia.....	36
Table 3-3: The distribution of samples profile in Sumatra	36
Table 3-4: Fission track ages of Gelok tephra.....	44
Table 3-5: OSL ages of Kuala Pelus tephra.....	45
Table A1-1: Glass fission-track ages of tephra beds from the Gelok and Serdang	86
Table A2-1: Peninsular Malaysia Major elements data.....	88
Table A2-2: Sumatra Major elements data.....	92
Table A2-3: Rare Earth Elements raw data from LA-IP-MS	94
Table A2-4: Mineral/melt partition coefficient.....	99
Table A2-5: Chondrite Normalizing Standards	101
Table A2-6: Normalizing Standards to MORB.....	101

CHAPTER 1

"A person who leaves home in search of knowledge, walk
in the path of God"
- Prophet Muhammad (P.B.U.H).

1.0 INTRODUCTION

Tephra layers played an important role as a time marker in establishing a chronology for the Quaternary, because they occurred within very short period intervals and widely distributed. Individual tephra, however, vary significantly, and were restricted spatially by factors such as the magnitude and direction of prevailing wind and the particle size of the tephra. Consequently, tephra was useful for local and regional stratigraphy (Machida, 2002). Many extraordinary large tephra, such as the 75 k.a. Toba eruption, have been recognized as very powerful tools for correlating stratigraphic sequences and extensive landforms, particularly for land-sea correlation.

Tephra has been used since 1940s as time stratigraphic marker for both site-specific and regional geologic studies and often provided absolute age constraints for sediments, structural features, depositional rates, biostratigraphic datum levels, and soil developments (Sarna-Wojcicki, 2000; Ward et al., 1993). Tephra has also been used to determine the timing and rate of movement along faults. Soil scientists used tephra for the development of time lines in soil formation and to control the biostratigraphic datum levels (Ward et al., 1993).

Dispute in the origin of distal tephra layers have been reported in numerous parts of Peninsular Malaysia (Fig. 1-1). Very few of these tephra units have been dated and some of the dated tephra were not published. Many of the previous researchers

simply reported that the age of these tephra were approximately 70 -75 ka originated from the Toba super eruption in Sumatra. Despite clear field evidence for multiple more



Fig. 1-1. Documented localities of tephra found in Peninsular Malaysia (modified from www.divezone.net)

than Volcanic Explosive Index (VEI) 8 have occurred in multiple volcanic regions of Sumatra, newer publications have attributed all near superficial tephra from India to the South China Sea, including Peninsular Malaysia, to Toba as the single source. (Tjia and R.F Muhammad, 2008).

Wind blown tephra deposits from Sumatra was first recorded by Scrivenor (1931) in Peninsular Malaysia. The thickest tephra deposit ever recorded in Peninsular Malaysia was about nine metres, and it was found at the confluence of Kuala Pelus and Perak River. Widespread tephra layers have been recorded as far as the North East Indian Ocean and the Bay of Bengal (Ninkovich et al, 1978) (Fig. 1-2).

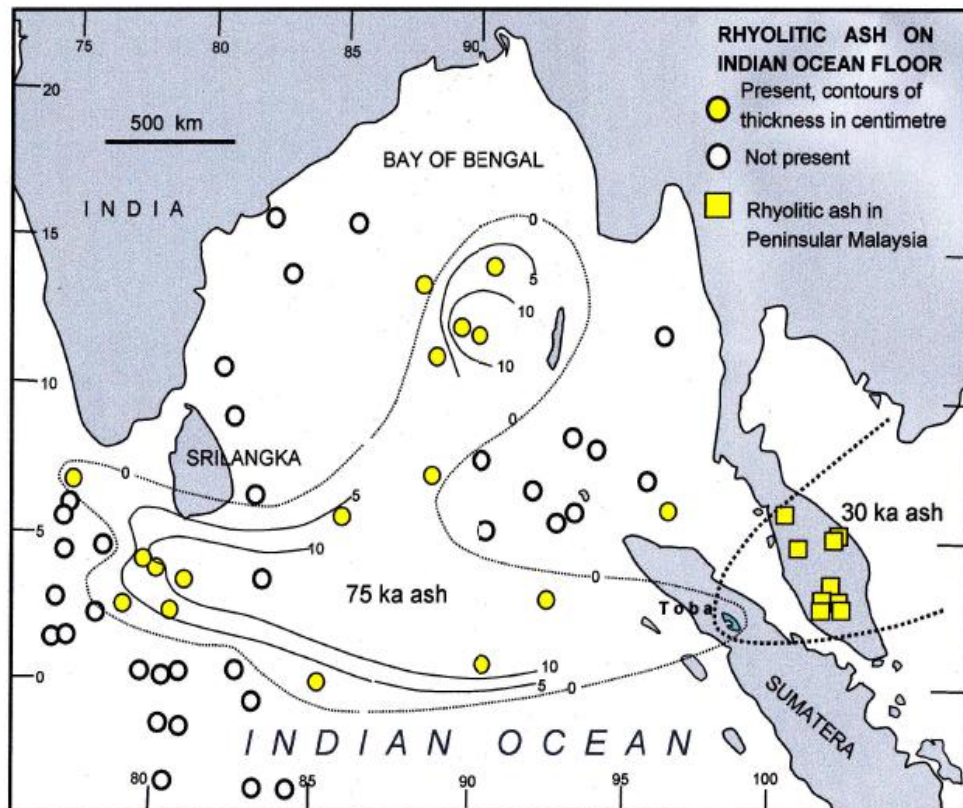


Fig. 1-2. The distribution of rhyolitic tephra on Indian Ocean Floor (Tjia, 2008).

The Lake Toba eruptions were considered to have been the largest explosive eruption ever documented throughout the Quaternary age. The available "absolute" dates of the multiple Toba eruptions were summarized in Table 1-1. Apart from Bukittinggi, the other five acid tuffs belong to Toba. All of the samples were dated by fission track, except for the sample from Tuktuk Siadong.

Tuff Name	Age
Youngest uppermost acid tuff layer 9 km South of Parapet	30,000 years
Acid tuff at Siguragura	100,000 years
Upper acid tuff at Parapet Pass	100,000 years
Lower acid tuff at Parapet Pass	1.2 my
Ignimbrite (welded acid tuff) at Tuktuk Siadong (K/Ar)	1.9 my
Acid tuff at Bukittinggi, Padang Highlands	70,000 years

Table 1-1: List of major eruptions in Sumatra from Nishimura, (1980).

Other Sumatra volcanoes like Maninjau and Ranau in South Sumatera have also had multiple paroxysmal events (Kastowo, 1996). Maninjau volcano in Bukittinggi was believed to have at least three multiple paroxysmal events at 70 ka and 80 ka (Tjia and R. F. Muhammad, 2008). Therefore, it was very plausible that Lenggong valley acid tephra could be originated from Sumatra volcanoes other than Toba. The Toba-like caldera associated with superficial acid tephra deposits were also known found at Bukittinggi area (known as Fort de Kock in Dutch Colonial times). They were exposed in the deep "Karbouwengat", nearby the Maninjau Lake, and at further southern area of Ranau (Figure 1-3). The 70 ka Bukittinggi tephra could be well

correlated with the reported 74 ka – 75 ka Toba tephra mentioned in the recent articles (Alloway, 2004).

This study will concentrate on the tephra found around Lenggong, Perak. This site is home to the Tampanian Paleolithic stone tool sites and the 11,000 years old "Perak Man"(Zuraina, 1988), previously dated at 31,000 based on ^{14}C ages of organic material in close association with acid tephra at Ampang and Serdang and are corroborated by the age of the uppermost tuff layer near Parapet (see Table 1-1). However, more recently, it was shown that the dating of the stone tools was dependant on tephra dating (Tjia and R. F. Muhammad, 2008). By correlation with the Toba Tephra, the tephra that belonged to the tools was agreed to be of the great 75,000 years-old Toba Eruption.

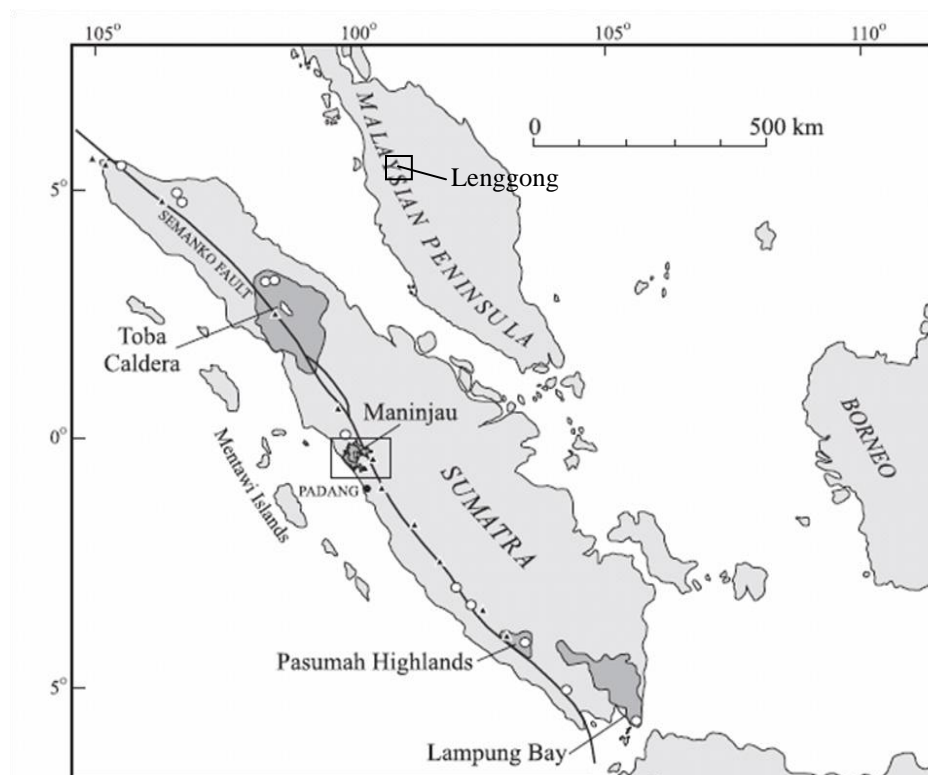


Fig. 1-3. The volcanic history of Sumatra. (Modified from Alloway, 2004)

1.1 OBJECTIVES

The main objectives of this study were:

- To determine the distribution of tephra deposits in Peninsular Malaysia, particularly in Lenggong Valley area.
- To provide a detailed geochemical data and precise ages determination for tephra layers of Peninsular Malaysia. This research will investigate whether the trace element compositions of these ash beds will be distinctive enough to recognize individual eruptions.
- To establish the tephra correlation between Peninsular Malaysia and Sumatra.
- To establish the time marker in the stratigraphy for the Late Pleistocene of Peninsular Malaysia region.

This study attempted to delineate the source and age of tephra found in Peninsular Malaysia. The focuses of this research were on the Lenggong and Kuala Kangsar tephra that have not yet been correlated to any eruption source. Both places were the ideal locations for study due to three main reasons: 1) Abundance of tephra localities. 2) Kuala Kangsar tephra was thought to be similar to that of Kota Tampan tephra based on their proximity and the similarity of their chemical composition and 3) Both areas have a substantial number of undifferentiated tephra and are simply described as the “Toba Tephra”(Chesner, 1991, 1987, Basir, 1987, Ninkovich, 1978). This research attempted to investigate whether the trace element compositions of these tephra beds were distinctive enough to discriminate individual eruption. Using laser ablation inductively coupled plasma

mass spectrometry (LA-ICP-MS), the rare-earth elements (REE) and other trace-element concentrations were obtained and to the established Youngest Toba Tuff (YTT) and Sianok (Maninjau) tephtras.

A detailed investigation on the source of tephra in Peninsular Malaysia could be established by comparing geochemical signatures of tephra in Peninsular Malaysia that of ejecta from Sumatra volcanoes. Previous researchers were mainly focused on analyzing the major elements of the tephra, however, major elements alone has proved to be inconclusive in many cases (Pearce, 2004) and such has been the case here. An example was the attempt to use major elements signature to determine the source of a widespread deposition of rhyolitic tephra deposits along Padang Terap river made by Debaveye, J. et al. (1986). Given that the silica-rich volcanic tephtras from Sumatra region have very similar major element composition, major element signatures cannot distinguish between them (Pearce, 1998). Minor and trace elements analysis could possibly be proven more useful than major elements alone.

There were substantial amount of tephtras in Peninsular Malaysia that remained undifferentiated. Part of the reasons were the lack of research, unpublished results and insufficient geochemical data analysis. Based on Toba's super magnitude intensity, all of these undifferentiated tephtras were speculated to be originated from super volcano YTT (Westgate et al, 1998). Referring to Ninkovich (1972), a Toba origin might still be considered most likely. Eruptions of the Toba Caldera have been frequent (Dehn et al, 1991) and without isotopic ages and geochemical characterization of the glasses in the distal tephtras, correlation to a particular eruption could not be confirmed (Shane et al, 1995).

Geochemical data analysis showed apparent variables among Peninsular Malaysia's tephra, YTT (Toba) and Sianok (Maninjau) data suggesting disparate sources for Perak tephra. Volcanics from Maninjau caldera, had been dated at 52 ± 3 ka. (M. M. Purbo-Hadiwidjono, 1979). The Maninjau tuff deposits were distributed over 8500 km^2 and have a volume of $220 - 250 \text{ km}^3$. However, Sumatra eruption volumes have often been underestimated, and only 0.5 % of known Indonesian eruptions have been dated by other than historical techniques (Simkin and Siebert, 1994).

The major, trace and rare earth elements analysis used for fingerprinting study were able to differentiate the glass shards population and it gave better understanding on the magmatic fractionation of the origins of Peninsular Malaysia tephra. The results of this study can be used to advance the understanding of the Paleolithic archaeology of the Lenggong area and will further contribute to Peninsular Malaysia Pleistocene stratigraphic in correlation.

In addition, this study would hopefully be beneficial in establishing one or more time markers in the stratigraphy of the Late Pleistocene in Peninsular Malaysia. Establishing an effective time frame for the tephra found in Peninsular Malaysia could benefit various fields of research, such as soil science, geology, paleoclimatology, stratigraphy, paleontology and archeology.

1.2 PREVIOUS STUDIES AND RESEARCH MOTIVATION.

Multiple super-volcanic eruptions have occurred in Sumatra for the last 65 million years. As a result of the eruptions, tephra were deposited over a broad area in Peninsular Malaysia. As early as 1930s, pioneer studies tephra deposits in Peninsular Malaysia were

carried out by J. B. Scrivenor. Tephra in Peninsular Malaysia was first recognised by this researcher in Kota Tampan area in 1930. He subsequently found up to 9 m of tephra at Kuala Pelus in 1931 and it was considered by Van Bemmelen (1949) to be originated from Toba. The tephra overlain the top of several metres thick of sand and gravel containing Palaeolithic chopper tools and flakes, which in turn mantled by about a metre thick of soil (Ninkovich et al., 1978b). Westgate et al., (1998) suggested that the chemical composition of the tephra was indeed the YTT.

Stauffer's (1973) study on Late Pleistocene age for tephra in West Malaysia suggested the Ampang Lake allowed 500 years for deposition of the roughly 0.5 m of peat between the tephra and two dated underlying wood fragments, taking 34,500 B.P as the middle of their age overlap, he estimated the actual age of the tephra as approximately 34 ka B. P. He considered the maximum age for the tephra as the 73 ± 12 ka yrs reported for the Toba ignimbrite deposits in Sumatra, determined using the potassium-argon method (Ninkovich, et al, 1971). He stated that there was no evidence that the tephra in Peninsular Malaysia was related to the Toba eruption. However, since there was no evidence of any other eruption of comparable magnitude in Sumatra (Ninkovich, et al. 1978b), a Toba origin might still be considered most likely. Dating of this tephra was in progress when this paper was published, with expectation to resolve the remaining ambiguity. However, the result for ^{14}C age determinations for this area have not been published.

Stauffer (1978) found fresh Serdang tephra in Selangor deposited in clear separate layers in a stratigraphic sequence. The topmost layer was a fine grained tephra, underlain by the coarse biotitic tephra, whereas the bottom layer constituted fine grained tephra, suggesting different eruption events. The relatively undisturbed nature of the tephra also

supported the idea that the deposition took place in an open-water (lacustrine) environment, as had previously been suggested for Ampang tephra (Stauffer, 1973). This writer planned further studies on the dating of the tephra and associated wood and peat. Serdang zircon fission track age of 30 ± 4.5 ka was determined for the tephra (Nishimura and Stauffer, 1981).

This finding is contrary to (Chesner, 1991) age of fission track 68 ± 7 k.a. that supported the conclusion of Rose and Chesner (1987) that tephra in Malaysia originated from the 75 k.a. YTT eruption. Based on that, Chesner (1991) believed a large explosive eruption originating from Toba at 30 k.a. as postulated by Stauffer et al. (1980) seems unlikely. This theory was supported by (Dehn and Chesner, 1991) as large Pleistocene eruptions in the last 30 to 40 k.a. were not known for the Toba Caldera and it was assumed that the zircon and ^{14}C age the Peninsular Malaysia tephra were in error (Taylor, 1982). Recent archeological publication reported on the $^{40}\text{Ar}/^{39}\text{Ar}$ age of 73.88 ± 0.32 ka for sanidine crystals, extracted from Toba deposits in the Lenggong Valley, 6 km from an archaeological site with stone artifacts buried by tephra (Storey, 2012).

Tjia (1976) stated that if Terengganu tuff originated from Toba, it had been flown about 500 km, which is more than 150 km compared to Perak Tuff. He found tephra in Sungai Bekok, Terengganu was deposited at the elevation of 30 m and the distribution of plant remains at the lower layer could be interpreted as lagoonal deposit with dense plantations. Generally, all Quaternary experts believed that during the last interglacial sea level reached 6 m higher than at present, as glacial ice melted back a bit more than it has today.

Debaveye (1986) studied on a widespread deposition of rhyolitic tephra deposits along the axis of Padang Terap river. The tephra was thought to be originated from the Toba area, North Sumatera based on microscopy and major elements analysis. This area has been correlated with uncertain age of Toba eruption which is 75 k.a. or a 30 k.a. eruption. Debaveye (1986) summarized the origin of this tephra deposits were from tuff erupted at a centre just north of the Toba depression called Sibuatan Tuff. However, he was uncertain whether the tephra originated from the 75 k.a. Toba eruption or from 30 k.a. Sibuatan eruption. A second possible source is Krakatau, located in the Straits of Sunda near Southeast Sumatra. Sunda Strait tuffs were believed to be erupted throughout the Late Miocene to the Pleistocene time. This is based on the major elements composition (glass shards) and minor elements (on topsoil) analysis result in Padang Terap that has been correlated with Toba's ignimbrites chemical composition that is chemically identical. Electron probe X-ray microanalyser, X-ray diffractions (clay fraction) and physico-chemical characterization of a soil developed on rhyolitic tephra. Yet the K-Ar dates on glass shards of this area has not yet published.

Basir (1987) suggested that the age of Kuala Kangsar tephra deposits were of similar age to tephra in the Kota Tampan area and its age as claimed by (Ninkovich, 1978) on the basis of proximity of occurrence and similarity of two samples of tephra major elements chemical composition by using X-ray fluorescence spectrometry, is 75 k.a. years (Ninkovich et al, 1978). Kuala Kangsar tephra deposits was located approximately at 30 km from Kota Tampan area in Lenggong. The tephra was deposited as sub aerial fallout on the river-bank of Sungai Perak. The reverse graded bedding found in the deposit was attributed to the progressive increase of the initial gas velocity during eruption, which was responsible

to eject the coarser fragments to a greater height in the later phase, thus promoting a wider wind dispersion. The finer tephra was rapidly dispersed and deposited earlier followed by the deposition of coarser tephra. The occurrence of six layers indicated the fluctuation of wind energy as a transporting agent. He assumed that the source of the tephra might possibly be originated from Toba eruption based on its largest magnitude explosive eruption ever documented in Quaternary age and its widespread tephra layers have been recorded in the North-East Indian Ocean and Bay of Bengal (Ninkovich et al, 1978). However, no dating determination has been done on the Kuala Kangsar tephra. Basir (1987) showed no scientific evidence that would suggest a relationship exists between the different isolated deposits in Lenggong. His notions of similarities were solely based on its proximity to Kota Tampan area and results of two major elements analysis acquired by X-ray Fluorescence Spectrometry.

Eruptions of the Toba caldera have been frequent (Dehn, 1991) and without precise isotopic ages and geochemistry characterization of the glasses in the distal tephras, correlation to a particular eruption could not be confirmed (Shane, 2000). Collectively, in the literature, most of the tephras were attributed to the VEI 8 eruption dated at Lake Toba at 70-75 k.a. However, there were three other high VEI eruptions in Sumatra that might be responsible to the tephra deposits, the Mount Maninjau dated at 80 k.a. and 52 k.a. (its proximal tuffs were exposed at Sianok Canyon near Padang, Sumatra) and Lake Ranau dated from 0.7 mya to 0.4 mya. (Bellivier et al., 1999). Consideration should also be given to other eruptions such as Pulau Weh in North Sumatra which was presumed to be Pleistocene age (Bennett et al., 1981). However, based on the volcanology highlights in Volcanology of Indonesia, only few stratigraphic studies of older volcanic deposits were established in Indonesia and only 0.5 % of the known Indonesian eruptions were dated by

other than historical records, emphasizing the need for more study on the prehistoric record in this region (Simkin, 1994).

To date, much of the volcanological researches conducted in Sumatra were largely focused on the eruptive history of Toba caldera (Alloway, 2004). Maninjau was a volcanic edifice situated in Padang Highland, located about c. 300 km to the south of Toba and c. 15 km to the west of Bukit-Tinggi town at west-central Sumatra. Purbo-Hadiwidjoyo et al. (1979) estimated that the Maninjau tuff deposits were distributed over 8500 km² and have a volume of 220–250 km³ with VEI 7. Undoubtedly at that magnitude, Maninjau that located approximately 600 km from Lenggong could possibly contributed to the Peninsular Malaysia tephra deposits. The c. 52 k.a. age for the paroxysmal Maninjau PDC deposit was supported by the occurrence of an underlying silicic tephra bed which was geochemically indiscriminated from the c. 75 k.a. Toba. The Volcanic Explosivity Index (VEI) of the Toba super-eruption was the largest possible for a volcanic eruption. The magnitude of Toba eruption was an order larger than the Maninjau VEI 7, which produced ca. 2500–3000 km³ of dense rock equivalent to pyroclastic ejecta (Rose and Chesner, 1987) compared to that of the 220–250 km³ pyroclastic from 52 k.a. Maninjau eruption (Alloway, et al, 2004). Despite its high magnitude eruption, the Maninjau eruption has been ignored and lack of research. Other enormous eruptions during Tertiary Quaternary periods such as the Ranau eruption should also be considered as source of Peninsular Malaysia tephra deposits (Table 1-1).

Previous researchers have focused primarily on analyzing the major elements of the tephra. Silica-rich volcanics from the Sumatra region have very similar major elements composition. Hence, they were not easily discriminated from each other using these

elements. The result from minor and trace elements analysis could be used to discriminate the origin of the tephra layer.

Pattan et al. (2002) agreed that the origin of tephra in the Central Indian Ocean Basin (CIOB) was in dispute. The in-situ silicic volcanism and Indonesia arc volcanism have been proposed as the potential sources of tephra in the basin. A detailed study on the morphology and chemical composition (10 major, 20 trace and 14 Rare Earth Elements) of the glass shards were carried out from 8 sediment cores in the CIOB to gain insights and provided a new tephra volume estimation. The major, trace and REE composition and morphology of the shards suggested that Youngest Toba Tuff (YTT) dated at ~74 k.a. of Northern Sumatra as the source of the tephra. The YTT shards contained higher concentration of Ca, K, Al, Cs, Ba, Ta, Th, U and heavy REE and lower amount of Fe, Rb, Sr, Y and light REE compared to that of the Middle Toba Tuff tephra, The YTT tephra contained higher level of Si, K, Hf and light REE, and lower amount of Ti, Fe, Mn, Mg, Ca, Na, Rb, Sr, Y, Nb, Th, U and heavy REE compared to that of the Oldest Toba Tuff tephra.

Pearce et al. (1995) studied on a proximal sample of the Toba tephra from Sumatra, and analysed it by both solution and laser ablation ICP-MS techniques. Samples UT1068, UT1069, UT1070, UT1134, and UT1135 were collected from the northern part of the Indian sub-continent. Based on the acquired data, Pearce demonstrated that there could be little doubt that these samples were the distal members of the Toba tephra. On the basis of EPMA, data these distal samples were compositionally similar to the proximal Toba tephra from Sumatra. A range of trace elements were determined from the proximal and distal samples of the Toba tephra using LA-ICP-MS. LA-ICP-MS offered a rapid trace element analytical technique with low detection limits for small samples of volcanic glass

shards. It could be used with confidence to correlate or distinguish the separate tephra deposits, when the EPMA data alone were inadequate. This approach has been applied in this study.

Tjia and R.F. Muhammad (2008) stated that the multiple paroxysmal volcanic outbursts of Toba character occurred at multiple locations in Sumatra throughout the Quaternary age. At Toba, four such events might be occurred between 1.9 Ma and about 30 k.a. age. Maninjau and Ranau eruptions, which were included in the top rank of the Volcanic Explosivity Index (VEI), could be considered as a possible prime contributor to tephra distribution in Peninsular Malaysia. Figs. 1-4, 1-5 and 1-6 showed calderas that were formed in Toba, Maninjau and Ranau due to the high magnitude of these ancient eruptions. Based on this notion, Tjia (2008) suggested that the contention that the widely distributed (from India to the South China Sea) rhyolitic tephra of 75 k.a. attributed to a single Toba paroxysm was highly improbable.

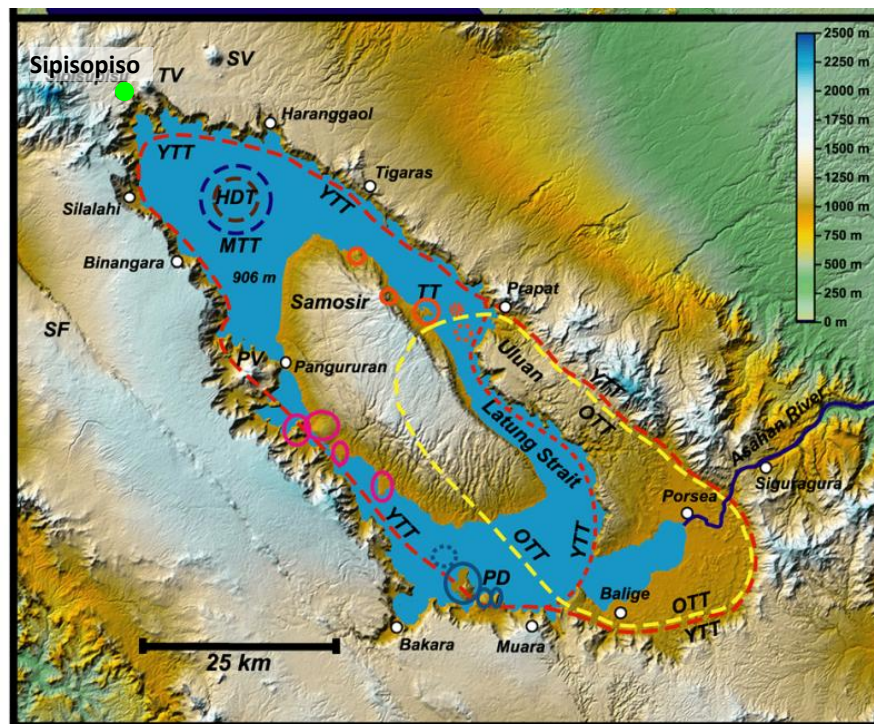


Fig. 1-4. Toba caldera complex in northern Sumatra from Chesner, (2012). The Sipisopiso YTT location was highlighted in green circle.

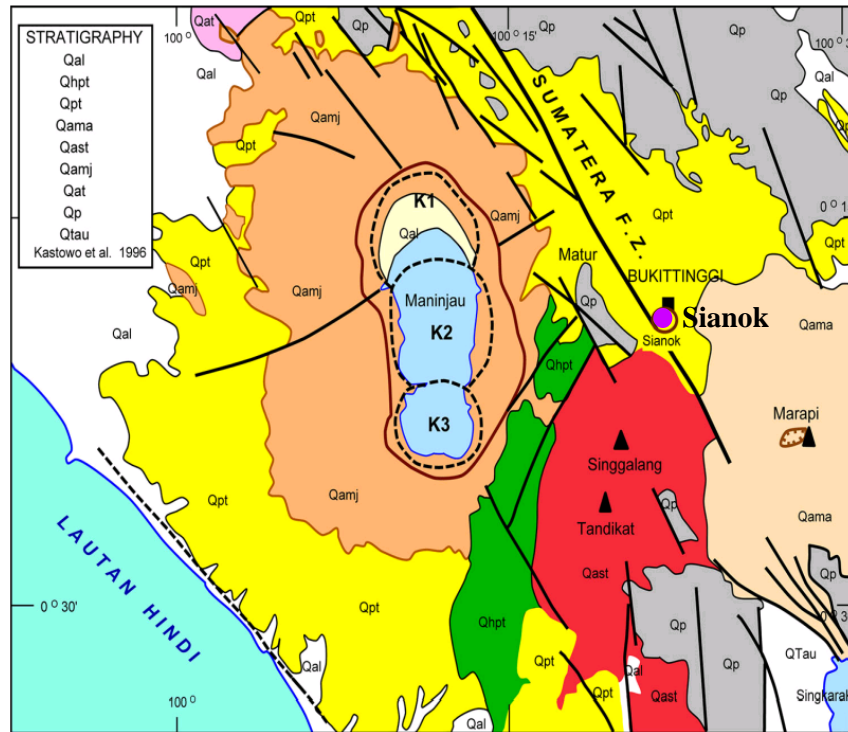


Fig. 1-5. Maninjau Caldera in Central Sumatra from Tjia (2008). K1, K2 and K3 were the Maninjau craters. Sianok valley location was highlighted in purple colour.

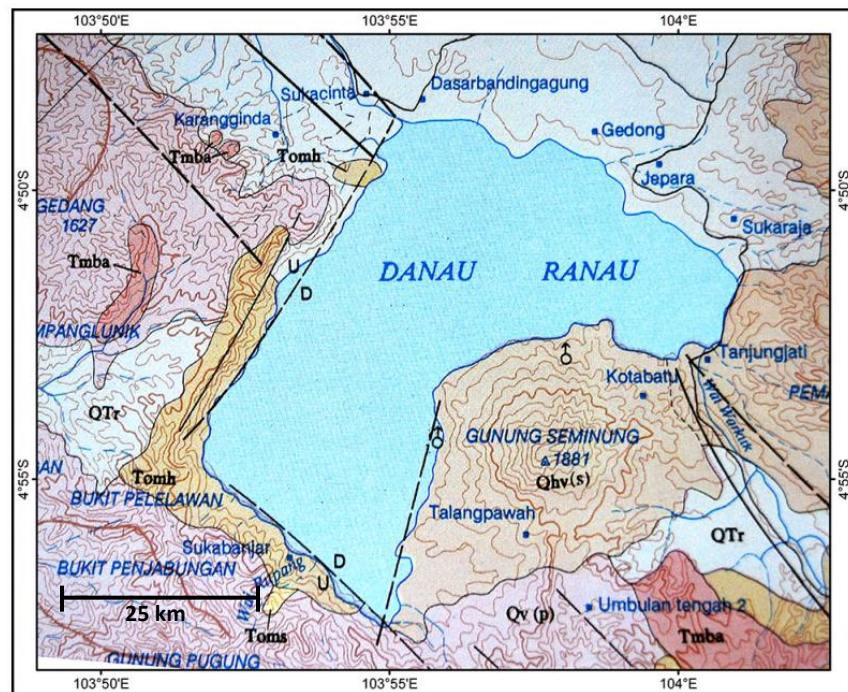


Fig. 1-6. Danau Ranau in Southern Sumatra from Gafoer et al. (1993).

Collectively, most of the tephra deposits in Peninsular Malaysia were insufficiently dated. The lack of geochemical data unable to prove that all of these deposits were solely originated from the 75 k.a. Toba eruption. However, the Ampang tephra dated at 34 ka (Stauffer, 1973) and Serdang tephra dated at 30 + 4.5 k.a. by zircon fission track. (Nishimura and Stauffer, 1981) showed that there was more than one possible sources of eruption. The major elements analysis by Basir (1987) was not distinctive enough to discriminate each tephra. This research attempted to address the lack of dated tephras. By conducting detailed geochemical analysis (trace elements and rare earth elements), tephras from Peninsular Malaysia could be discriminate and correlated to the Sumatra's tephra.

CHAPTER 2

“Knowledge is not what is memorized.
Knowledge is what benefits”
– Imam ash-Shafi’e.

2.0 METHODS

The investigation of tephra samples from Peninsular Malaysia and Sumatra was conducted in two phases. The first phase consisted of fieldwork and the second phase consisted of laboratory work. Fieldtrips were carried out at Lenggong, Kuala Pelus, Kuala Kangsar, Kg. Dong, Padang Sanai, Ampang, Serdang and Kg. Sungai Taling and samples were collected for dating and geochemical analysis. Samples collections were also included a number of Toba tuffs and Maninjau tuff, collected from Sumatra. The list of sites visited, with the corresponding analyses conducted was shown in Table 2-1.

Sample Name	Code Name	Field Work	Sample Collection	SEM	EPMA	LA-ICP-MS
Gelok 1	PM-G1	√	√		√	√
Gelok 2	PM-G2	√	√		√	√
Gelok 3	PM-G3	√	√		√	√
Gelok 4	PM-G4	√	√		√	√
Gua Badak 1	PM-B1	√	√		√	
Gua Badak 2	PM-B2	√	√		√	
Bukit Sapi	PM-S1	√	√	√	√	
Kg. Pisang	PM-M1	√	√	√		
Kg. Kuah	PM-M2	√	√	√		
Chegar Galah	PM-M3	√	√	√		
Kuala Pelus 1	PM-P1	√	√		√	
Kuala Pelus 2	PM-P2	√	√		√	
Kuala Pelus 3	PM-P3	√	√		√	
Kuala Pelus 4	PM-P4	√	√		√	
Kg. Talang 1	PM-T5	√	√		√	
Kuala Kangsar	PM-K1	√	√		√	
Kuala Kangsar	PM-Q5	√	√		√	
Kg. Dong	PM-D1	√	√		√	
Padang Sanai	PM-3C	√	√		√	√
Sianok 1	SM-4A	√	√		√	√
Sianok 2	SM-4B	√	√		√	√
Sipisopiso (YTT)	SM-5A	√	√		√	√

Table 2-1. List of sites visited, with the corresponding analyses conducted. PM= Peninsular Malaysia; SM=Sumatra; SEM= Scanning Electron Microscope; EPMA= Electron Probe Micro Analyser; LA-ICP-MS=Laser Ablation Inductively Coupled Plasma Mass Spectrometry.

2.1. FIELD WORK

A detailed mapping of tephra distribution was conducted in Lenggong at Kota Tampan area due to the abundance of tephra localities. A continuous samples collection was conducted within the Peninsular Malaysia area included collection of Lenggong tephra, Padang Terap tephra, Kuala Pelus, Kuala Kangsar, and a number of samples in Kg. Dong, Pahang. A number of Sumatra pumices and tephra samples were also collected for comparison. Approximately 500 to 1000 g of fresh tephra and more than 1000 g for reworked tephra samples were collected from each outcrop. The Sumatra samples were collected from Sipisopiso (YTT) and Sianok Canyon tephra. They were to be compared to the Peninsular Malaysia tephra.

Field observations and mapping were carried out in the study areas with the aid of Lenggong topographic base map, compass, sketch notebook, global positioning system (GPS) to locate tephra spots with elevations based on Datum Malay Peninsula Kertau 1948, measurement tape, hand lens, hammer and shovel for sample collections. The samples were sealed to avoid contamination and amalgamation with other samples. Each bag was labeled with area name code, to be synchronized with more detailed field note. Camera was used to capture tephra outcrop images for documentation purposes. Generally, the tephra has a yellowish-white to ochre colour and made up of silt to sand-sized particles. Tephra was identified primarily by its whitish color, the nature of its boundary, its hardness, gritty, abrasive and its weight was lighter than fluvial sediments. Some of the local people in Lenggong claimed that fresh tephra tasted like milk powder. The tephra samples were identified in the field before it was collected and subsequently be confirmed in the laboratory using petrographic study or the X-Ray Fluorescence (XRF) technique.

The samples collection focused primarily on the freshness of the tephra. However, most of the tephra found in Lenggong area were reworked. A detailed GIS mapping were constructed based on 94 localities in Lenggong area. Fresh tephra was characterized by its light color and light density whereas the reworked tephra normally was mixed, compacted and cemented to terrigenous material.

Field data were extracted to produce surface mapping using a geographic information system (GIS) that allows us to view, understand, interpret, and visualize data. It was used to reveal Lenggong tephra relationships, patterns, and trends in the form of maps, and contour maps were used in producing the map. The geospatial datasets such as stream, soil, rock from JUPEM data source were used in producing the map.

2.1.1. Tephra Characterization

The quick identifications could be made by noting the variation of grain size, colour and thickness of the different tephra layers. However, colour and other field-observable properties might be misleading. Therefore, recourse has to be made to geochemical analysis or other more reliable laboratory tests to define the chemical composition and physical properties of the tephra layers (Westgate and Gordon, 1981)

In Peninsular Malaysia, where tephra was distally deposited from its source, glass shards were not visible to the naked eye and some of the samples were extremely low concentrations of shards, particularly in the lacustrine sediments. Some of the early researchers in tephrochronology relied upon visible properties of tephra deposits where, for example, colour and the characteristic of shard morphology were assumed to be sufficiently diagnostic. For instance, the Laacher See Tephra constituted the high amount of vesicular shards whereas the Vedde Tephra was commonly referred as containing ‘butterfly’-shaped

(three-winged) shards (Wohlfarth et. al., 1993). Shard shape and color were, however, rarely sufficient to distinguish between individual eruption events, because these two characteristics might be common to tephra derived from the same eruption centre, or from different eruption centres but have similar lithologies. Care has to be exercised, therefore, when distinguishing between such materials and glass shards. For these reasons, more comprehensive examinations of tephra-derived components was required, including the mineralogy and chemical composition of glass and other mineral (crystals), if present (Shane, 2000).

2.1.2. Glass-shard Morphology

Glass shards could be distinguished from crystalline siliceous material by their isotropy, whereby grains of glass, which was non-crystalline and isotropic, become black under a polarizing microscope with both analyzers in place (Lowe, 2011). Shards exhibited a range of morphologies and hence in favourable circumstances might provide a means for helping to distinguish one tephra from another, typically using scanning electron microscopy (SEM), in addition to optical microscopy. A useful method for mounting glass for morphological study by SEM, which also enables to run the subsequent geochemical analysis from the same grains, was described by Kuehn and Froese (2010).

This research used four samples from Bukit Sapi, Chegar Galah, Kg. Pisang and Kg. Kuah for glass shards morphology study was shown in table 2-1.

2.2. LABORATORY METHODS

2.2.1. Age Determination

Majority of the tephra ejected between 1.5 M.a. and 50 k.a. have been dated by radiocarbon methods. However, this method has its own limitation. The calibration system

to obtain calendar years for AMS ^{14}C dating has not yet been fully established (Machida, 2002). The use of fission track and optical simulated luminescence ensured that the tephrocronological approach could be employed both within and beyond the limit radiocarbon dating.

2.2.2. Fission Track on Glass Shards

Fission-track dating was uniquely appropriate for determining the low-temperature thermal events using common accessory minerals over a very wide range of geological age, typically from 0.1 M.a. to 2000 M.a. This method has made a significant impact on understanding the thermal history of continental crust, and to determine the the timing, sources and age of volcanic events. The usefulness of this dating technique stems from the tendency of some materials to lose their fission-track records when heated, thus producing samples with the fission-tracks produced since they last cooled down. The useful age range of this technique was from 100 years to 100 million years before present (BP), although the estimated error were difficult to assess and rarely given. Generally it was thought to be most useful to date in between 30,000 and 100,000 years BP (Garver, 2008). In this study, two samples from Gelok at Lenggong were dated using fission track. The selection criteria for this analysis were based on the freshness, thickness and stratigraphy of the tephra samples. The Gelok dating samples were taken from second and fourth layers of total 2.8 m for tephra deposits. Padang Sanai tephra was not suitable for the fission track analysis since it was deposited as a single paddy soil layer. The fission track analysis for tephra samples in Peninsular Malaysia were performed by J. A. Westgate at the University of Toronto, Canada.

2.2.3. Optical Stimulated Luminescence Dating (OSL)

Luminescence dating has now become an established method for providing chronologies for sedimentary deposits containing sand- or silt-sized mineral grains. In particular, the fast component of the OSL signal from quartz has been used extensively for dating deposits ranging in age from a few decades to 100 ka (Wintle, 2008). Volcanic tephra has its own signature for each eruption. In a sedimentary sequence the associated material within the tephra layer could be dated, giving a date for the eruption. If this tephra is found anywhere else in the world, a date will already be known.

Geochronology was the science of determining the age of rocks, fossil and sediments, within a certain degree of uncertainty inherent to the method used. Tephrochronology was the study of volcanic tephra deposits, combining petrology, geochemistry, and isotopic dating methods correlation of unknown volcanic tephra to geochemically-fingerprinted, dated tephra. This study promoted correlation of marker horizons. The optically stimulated luminescence (OSL) signals currently used were appropriate for mineral grains that its previous radiation history was erased by exposure to sunlight immediately prior to deposition. In the case of TL, zeroing was achieved by heating. In the case of OSL, it was achieved by light exposure, with both procedures being relevant to the way in which the signal was zeroed in the past (Liritzis, 2011). In this study, two fresh tephra from Kuala Pelus samples were taken from the first and third layer of total 9 m thickness for tephra deposits. Padang Sanai tephra was not selected for OSL since the depositional area had been exposed to human and animal activity.

The OSL analysis for the tephra samples were performed in Luminescence Dating Laboratory School of Geography, Environment and Earth Sciences, Victoria University of Wellington in New Zealand.

2.3. GEOCHEMICAL ANALYSIS

2.3.1. Sample Preparation for Geochemical Analysis

The collected tephra samples that have been collected were prepared for electron probe & laser ablation analysis. Glass shards were concentrated by using the heavy liquid Sodium Polytungstate (SPT) (Savage 1988). Special efforts were made to avoid cross contamination.

Initially, tephra samples were crushed using a mortar. A precaution needed to be taken not to grind the samples, to avoid destroying the glass shard. The ultrasonic analysis was then performed to clean the glass shards surfaces from any clay coating (Hanan et al. 1998). Samples were wet sieved using 60 to 230 mesh screens and the material coarser than 20 micron was free from clay-minerals. The resulting material was a combination of glass shards and the silt-sized quartz and feldspar.

A heavy liquid separation of glass shards was performed to sink the higher density quartz and feldspar from the glass shards using Savage (1988) method. The SPT heavy liquid of SG 2.42 was prepared by dissolution in distilled water. A piece of obsidian was placed into 500 ml glass beaker as standard glass density. SPT powder was added to the distilled water and the liquid was stirred gently with plastic stirring rod until the obsidian floated to the surface. It was advisable to start at higher densities and work down to the

desired value by adding distilled water a few drops at a time. The specific gravity of the solution should be adjusted only when it was at ambient temperature, since temperature affected its density (Krukowski, 1988).

Samples were then mixed with SPT and were left undisturbed for a few hours since some samples were heavily cloudy and the heavy minerals needed time to sink. The floated glass shards were filtered through the filter paper and rinsed many times with distilled water. The samples were then air dried or dried in the oven at low heat, preferably around 65° C to 75° C for 24 hours to ensure any remaining distilled water added during cleaning phase was removed.

The dried glass shards were then inserted into the resin block for further steps. Approximately after two days or when the resin mixture was completely hardened, the sample blocks surface were ground and polished. The individual glass shards were identified and mapped using optical microphotographs. However, the samples needed extra polishing if the glass shards were invisible under the microscope, indicating the low relief of glass shards. Before the blocks were carbon coated, the photographs were used as probe maps and each shard was analyzed for major elements and then later for trace elements.

2.3.2. Electronprobe Micro Analyzer (EPMA)

An electron probe was the primary tool for major elements analysis of solid materials at small spatial scales. Although electron probes have the ability to analyze for almost all elements, they were unable to detect the lightest elements of minor and trace elements (Jansen, 1982).

All of the glass shards from Peninsular Malaysia and Sumatra were analysed with total of 40 to 50 points per sample using beam size of 50 µm. The electron probe data were

then saved in the Microsoft Excel format and was sent together with the sample blocks for laser ablation ICP-MS analysis. A data quality control was conducted for major elements data from this analysis to eliminate possible data contamination from feldspar or feldspar inclusion. This was done by comparing data obtained with the alkali feldspar and plagioclase standard major elements composition. Sixteen samples from Gelok, Gua Badak, Bukit Sapi (Lenggong, Perak), Kuala Pelus, Kg. Talang, Kuala Kangsar, (Perak), Kg. Dong (Raub, Pahang), Padang Sanai (Kedah), Sipisopiso (proximal YTT, at Lake Toba) and two layers of proximal Maninjau tuff at Sianok Canyon (Sumatra) (Table 2-1) were used for EPMA study.

Major element analysis of volcanic shards was conducted by J.A. Westgate at the University of Toronto, and by the author and supervisors at University of Malaya using a Cameca SX100 microprobe and at Nanyang Technical University (NTU) in Singapore using a Jeol JXA-8530F Field emission microprobe. In all cases, natural mineral standards were used for calibration.

2.3.3. Laser Ablation ICP-MS

Trace element analyses of volcanic shards were conducted at the University of Aberysthwyth, Wales, by N.J.G. Pearce using Laser Ablation ICP-MS, using techniques described in Pearce et al. 2004. As this is a destructive process, it was carried out after major element analysis by microprobe. Electron Microprobe samples with oxide totals around ~ 90% were selected for LA-ICP-MS analysis.

Trace element data was only available for Gelok (Lenggong, Perak), Padang Sanai (Kedah), Sipisopiso (proximal YTT, at Lake Toba) and two layers of proximal Maninjau tuff at Sianok Canyon (Sumatra) (Table 2-1).

2.3.3.1. LA- ICP-MS Vs Other Methods

Geochemical ‘fingerprinting’ of glass shards could be based on X-Ray Fluorescence (XRF) (Norrdahl and Haflidason, 1992) and inductively coupled plasma mass spectrometry (Pearce et. al., 1995; Eastwood et. al., 1999). These methods also have their limitations, however, because large sediment samples were required because small samples were susceptible to contamination effects (Shane, 2000). Furthermore, analytical targets must be focused on the sufficient surface size to be able to represent the original magmatic components (Shane, 2000),

Particle-induced X-Ray Emission (PIXE) was ideal for nondestructive surface analysis at trace levels, but it would not be appropriate for heavy elements analysis. On the other hand, XRF does not need an accelerator and was more appropriate for trace element investigations, especially for medium weight and certain light elements in small-scale laboratories in developing countries. ICP-MS complements PIXE and XRF by providing heavy elemental analysis. Laser ablation was preferred over FIA because time was saved by avoiding lengthy sample preparation procedures. Detection limits in ICPMS were about three orders of magnitude lower than PIXE or XRF (Pillay, 2001).

2.3.3.2. LA-ICP-MS

Laser Ablation ICP-MS was a suitable method for minor & trace elements analysis. Rare earth element concentrations are likely to be of help in either confirming or refuting correlations of the origin(s) of the tephra layer. Trace elements were used in geochemical and petrological studies because these elements were more capable in discriminating petrological processes than major elements (Rollinson, 1993). Trace elements were often classified into groups for geochemistry and petrology studies since the behavior of the elements were related to a particular group. The main groups of trace elements were

divided into the following; 1) the first transition series, 2) the platinum group elements, and 3) the rare-earth elements (REE). A number of other elements were also considered important in discussing trace elements, they were Rb (atomic number 37), Sr (38), Y (39), Zr (40), Nb (41), Cs (55), Ba (56), Hf (72), Ta (73), P (15), Pb (82), Th (90), and U (92) (Rollinson, 1993).

The elements in first transition series were Sc, Ti, V, Cr, Mn, Fe, Co, Ni, Cu, and Zn (atomic numbers 21-30). The first transition series included two major elements of Fe and Mn. The platinum group elements were of Ru, Rh, Pd, Os, Ir, Pt, and Au (atomic numbers—44-46, and 76-79, respectively). The REE constituted Sc (atomic number 21), Y (39), La (57), and the lanthanides, constituted 14 elements that range from Ce (58) to Lu (71). However, in geochemical and petrological studies, the REE were often limited to Y (39), La (57) and the lanthanides (58-71) (Henderson, 1996). Thus, this study followed the REE limitation according to Henderson (1996).

The purpose of grouping trace elements was to show the similar chemical behaviour, which means, they also share similar chemical properties. Any deviation of normal group behavior indicates some petrological process change or systematic changes of behavior in a rock (Henderson, 1996).

The rare-earth elements (REE) were the most useful trace elements and demonstrated important applications in igneous, sedimentary, and metamorphic petrology (Rollinson, 1993; Henderson, 1996). The REE were usually sub-divided into the light REE and heavy REE. The light REE consisted of elements with atomic numbers 57-62 (La-Sm) and the heavy REE atomic numbers were 64-71 (Gd-Lu).

The REE have very similar chemical behaviour and resulted in similar physical properties. This similarity was attributed to the fact that all of the REE were able to form stable 3+ ions that were of near equal size. However, there were a small number of REE

that existed in oxidation states other than 3+. The most important REE for geological processes were Ce^{4+} (relative oxidizing condition) and Eu^{2+} (relative reducing condition). The difference in size between these two elements and their 3+ counterparts was significant enough to cause changes in chemical behavior (Henderson, 1996).

However, despite having similar behaviour the REE still have some small subtle differences that were directly attributed to the ionic size of each REE. These subtle differences rendered the REE to fractionate from one another. The REE were decreased in ionic radius with the increase of atomic number. However, special attention must be given to the fact that geological processes took advantage of the subtle chemical differences and could fractionate elements from one group to another.

Rare-earth elements (REE) should be normalized to a standard of reference and in most cases chondritic meteorites was used to normalize the igneous systems (Rollinson, 1993; Henderson, 1996). The reason for using chondritic meteorites was because they were thought to represent the unfractionated primitive solar system. There were two main reasons for normalizing REE. The first reason was to remove the Oddo-Harkins Rule effect and the second reason was to identify any REE fractionation relative to chondritic meteorites.

This research used the Sun and McDonough (1989) reference set standard for normalizing REE. Normalization using the chondritic meteorites presented a number of problems. The notion that chondrite meteorites were a bit varied in composition was delusive, when in fact there often was great variability in composition. This lends itself to some authors approaching the normalization process by averaging chondrite meteorites and others by assuming that the C1 chondrites were the most the representative composition of the original solar nebula (Rollinson, 1993).

The multi-element spider diagram was typically used in data analysis to display the overall incompatible element characteristics of a rock (Saunders, 1998). In a spider diagram, the elements were ordered to give a smooth curve for average mid-ocean ridge basalts (MORB; Sun, 1980), which in effect means an increasing incompatibility of the elements in lherzolite during incipient partial melting from right to left. The total concentrations of the elements in spider diagram needed to be normalized against a primitive mantle standard (Sun and McDonough, 1989).

The source analysis in this study used reverse approach, the ANOVA cluster analysis to minimize variability within clusters of Peninsular Malaysia and Sumatra data. Cluster analysis was a major technique for classifying a 'mountain' of information into manageable meaningful piles (Garson, 2012). It was a data reduction tool that created more manageable data subgroups than individual datum. Like factor analysis, it examined the full complement of inter-relationships between variables. Both cluster analysis and discriminant analysis were concerned with classification. Subsequent multi-variate analysis could be performed on the clusters as groups (Garson, 2012).

The REE patterns seen in the REE plots or what were referred to sometimes as Masuda-Coryell diagram, were the result of the chemical behaviour of the REE and was controlled by the magma source and the crystal-melt equilibria that has occurred during the evolution of the magma chamber (Rollinson, 1993; Henderson, 1996). The chemical behaviour of REE in magmatic systems did not allow the larger sizes of REE ions to incorporate readily into common minerals. REE tended to have small mineral-melt partition coefficients (partition coefficient K , was the concentration of the element in the mineral divided by the concentration of the element in the coexisting melt) for minerals that have small cation coordination sites (Henderson, 1996). In a non-eccentric cooling magmatic system that contained minerals with small cation coordination sites, REE tended to be

incompatible. Thus, REE preferred to remain in the melt portion of a magmatic system (Henderson, 1996; Rollinson 1993). The overall partitioning of REE between a mineral and the melt did not only depend on the ionic radius but also depended on the ionic charge, temperature, pressure, and composition of the magmatic system (Henderson, 1996).

Europium (Eu) existed in both a divalent (2+) and a trivalent (3+) oxidation state depending on the redox potential in the magmatic system. The divalent state of Eu has a much larger ionic radius than the trivalent state. Despite its larger ionic radius, the partition coefficient of the divalent Eu into some minerals was greater than that of the trivalent state. A good example of the Eu partitioning behaviour could be seen in plagioclase feldspar mineral and a non-eccentric magma.

The relative partitioning difference in the divalent and trivalent state of Eu could lead to Eu anomaly. The Eu anomaly was defined as the deviation from the general REE trend or patterns when the normalized REE data were plotted. In the diagram, negative Eu anomaly showed a sharp decreased below the other REE pattern, a positive anomaly showed a sharp increased above the other REE pattern. The Eu anomaly was the measured difference between the actual measured Eu value and a predicted Eu* anomaly value. The predicted Eu* value was calculated by averaging the Sm and Gd values—i.e., $(Sm + Gd)/2 = Eu^*$. The actual Eu anomaly was determined by dividing the actual measured Eu by the predicted Eu*.

Westgate et al. (1994), Pearce et al. (2004), and Knott et al. (2007) demonstrated that the inductively coupled mass spectrometry (ICP-MS) was an effective method for measuring trace element concentrations in tephra correlation.

In attempting to establish tephra correlation between Peninsular Malaysia and Sumatra tephra deposits, the glass major, REE and trace elements chemistry must be examined and correlated using analytical precision for all elements. The major element,

REE and trace element discrimination diagrams were plotted using the diagrams demonstrated in Pearce, (1995, 2004); Alloway (2004). Characteristics multivariate analysis using bivariate plots of selected major, REE and trace element data, chondrite normalized REE concentrations were plotted to discriminate all samples. All of the trace and REE concentrations were reported in ppm by weight. The analytical precision was typically ± 2.3 % for the more abundant trace elements (Ba, Zr, Rb, Sr, LREE) to around ± 10 -20 % for the less abundant elements, the odd atomic number HREE (Pearce, 2004). In Iceland, FeO/CaO and FeO/TiO₂ ratios were frequently the most useful indices for identifying particular tephra, although additional examination in particular MgO, FeO and CaO offered further assistance (Machida, 2002).

The analysis of Rare-Earth Elements (REE) and trace elements for Peninsular Malaysia and Sumatra glass shards were performed by Nicholas J. G. Pearce at University of Aberystwyth using a Coherent GeoLas ArF 93nm Excimer laser ablation system coupled to a Thermo Finnegan Element 2.

CHAPTER 3

“Do not let your difficulties fill you with anxiety;
after all, it is only in the darkest nights that the stars
shine more brilliantly”
– Ali Ibn Abi Talib (R.A).

3.0 RESULTS

A total of ninety four tephra localities were identified in the detailed study of the tephra distribution in Lenggong. Ten tephra localities were previously reported (Ruslan, 2008) in this area. Two samples from Gelok (Gelok 2, Gelok 4) and another two samples from Kuala Pelus (Pelus 1, Pelus 2) were taken for age determination. Four EPMA data were obtained from Gelok (PM-G1, PM-G2, PM-G3, PM-G4), two from Gua Badak (PM-B1, PM-B2), one from Bukit Sapi (PM-S1), Kg. Jawa (PM-M1) and Kg. Kuah (PM-M2). All of these data represented Lenggong tephra. Four samples were obtained from Kuala Pelus (PM-P1, PM-P2, PM-P3, PM-P4), one from Chegar Galah (PM-M3), Kg. Talang (PM-T5), two from Kuala Kangsar (PM-Q5, PM-K1), one from Kg. Dong (PM-D1), one from Padang Sanai tephra (PM-3C), one from Toba tephra (SM-5A) and two Sianok tephra (SM-4A, SM-4B) from Sumatra for geochemistry analysis. These twenty two samples were labeled using code names based on location in this study (Table 2-1). PM code name referred to Peninsular Malaysia samples whereas SM code name referred to Sumatra samples. Sumatra tephra samples were taken from Sipisopiso located at the north of Toba Caldera (fig. 1-4), while Sianok valley located at the east of Danau Maninjau (figs. 1-5 and 3-1).

However, Kg. Sg. Taling tephra were unsuitable for geochemistry analysis because the size of the glass shards were too small for EPMA analysis. In addition, Sg. Bekok tephra could not be collected during fieldtrip, since it was believed to be deposited deep underneath Bekok River. No tephra deposit was found in Ampang and Serdang too due to

intensive land clearing and development in those areas. However, Serdang fission track data and tephra samples from supervisor data collection were able to be used in this study.

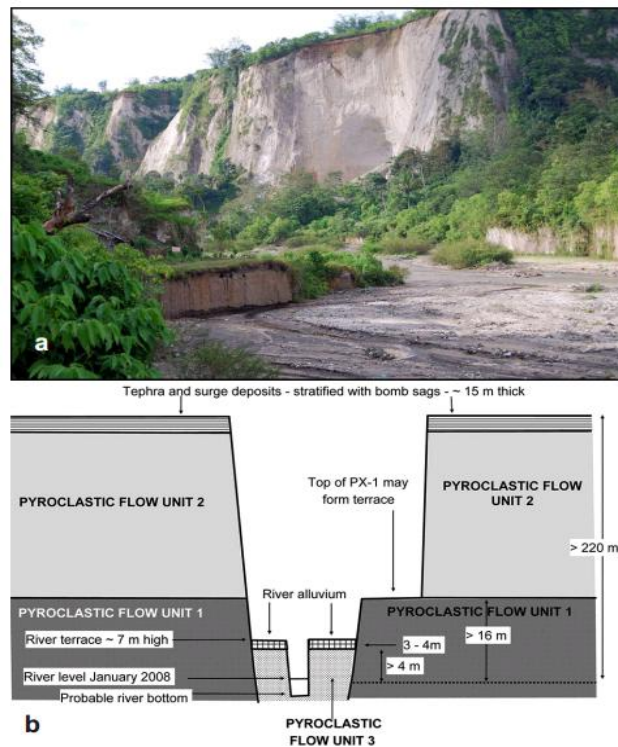


Fig. 3-1 showed a) The samples taken from Maninjau at Bukit Tinggi Tuffs in the Sianok ravine, by Tjia and R.F. Muhammad, (2008). b) The Morphology of the Bukit Tinggi in the Sianok Valley indicated three pyroclastic flow units (Tjia and R.F. Muhammad, 2008).

3.1. TEPHRA DISTRIBUTION

The distal and fine grained ($< 200 \mu\text{m}$) fallouts of Sumatra tephra were wind blown more than 300 km to Peninsular Malaysia. The Lenggong study area consisted predominantly of sediments that were interbedded with fresh and reworked tephra layers. The details of tephra distribution in Lenggong area were displayed in table 3-1 and fig. 3-2

Localities	Number of Spots & Descriptions	Area	Tephra Layer Thickness (m)	Tephra Freshness
Bukit Sapi	4 spots of fresh layers, 6 spots reworked Total: 10 spots.	100 m ²	0.2 - > 2.0 (fig. 3-3)	Fresh and reworked. One of the freshest tephra quality in Lenggong (refer SEM photos fig. 3-10A and B). Reworked tephra layer overlay fresh tephra. Reworked tephra in patches & layers. Fluctuations groundwater level mark (fig. A3-1).
Gua Badak	1 spot of fresh patches, 2 reworked. Total: 3 spots.	300 m ²	0.7 - > 3.0	Fresh tephra was deposited in patches & layers (fig. A3-2). Reworked tephra deposited in patches.
Temelong	15 spots of mixed fresh and reworked layers. 6 reworked. Total 21 spots	2 km ²	> 3.5	Fresh and reworked. Fresh layers widespread, well-preserved by paddy fields. Reworked deposits in patches. Some highly reworked & cemented (fig. A3-3).
Labit	6 spots of fresh layers, 7 reworked. Total: 13 spots.	5 km ²	1.4 - > 2.0 (fig. 3.4)	Fresh and reworked. Reworked overlain fresh layer, preserved by vegetations. Reworked in patches & highly reworked & compacted (fig. A3.4).
Gelok	8 mixed reworked layers, fresh deposits in patches. Total: 8 spots	2 km ²	0.1 - > 1.0 (fig. 3-5)	Reworked deposits highly compacted & almost impossible to be removed. Fresh tephra was deposited in patches.
Chepor	Total 3 reworked spots.	50 m ²	0.1 - > 2.0	Reworked tephra deposited in patches.
Kota Tampan	2 fresh spots, 14 reworked Total: 16 spots	5 km ²	0.6 - 1.2	Fresh tephra in layers and patches, preserved by vegetation (fig. A3-5). Reworked in patches and layers (refer SEM photo fig. 3-10b and c).
Luat	3 fresh spots 14 reworked Total: 17 spots	400 m ²	0.5 - > 4	Fresh and reworked. Exposed fresh thickness up to more than 4 m, 4 layers. (fig. A3-6). Reworked tephra in layers and patches.
Kg. B. Belimbing	1 spot mixed fresh & reworked	100 m ²	0.4	Fresh and reworked in patches.
Padang Grus	2 fresh spots	50 m ²	2.0	Fresh tephra well preserved by vegetation but some destroyed by animal activities (fig. A3-7).

Table 3-1: The distribution of samples profile in Lenggong (refer to fig. 3-2 for localities map).

Localities	Number of Spots & Descriptions	Area	Tephra Layer Thickness (m)	Tephra Descriptions and Freshness
Kuala Pelus	5 fresh layers	400 m ²	3 - > 4.8	Tephra located at 'labu sayong' quarry. 9 m total thickness of tephra could be the same tephra of Scrivenor (1931). Two fresh samples from layer 1 and layer 4 were taken for dating analysis (OSL) (fig. A3.8)
Kg. Talang	5 layers of fresh tephra	300 m ²	0.7 - > 1.0	Fresh tephra were deposited at Kuala Kangsar quarry area (fig. A3.9)
Kuala Kangsar	5 spots of mixed fresh and reworked layers.	2 km ²	> 3.5	Fresh and reworked. Reworked deposits in patches. Some highly reworked & cemented (fig. A3.3).
Kg. Dong	3 spots of fresh patches, 1 reworked. Total: 4 spots.	2 km ²	in patches	Reworked sample hardened and cemented. Wet samples deposited at an abandoned paddy field, the land was about to be developed during sample collection (fig. A3.10).
Padang Sanai	Widespread fresh tephra at paddy field and at police station.	2 km ²	0.1 - > 1.0	Brown and greyish, very fine grained with clay texture like, medium sorting, compacted and loose grained. Sample mixed with roots and other organic materials.
Bahau	2 layers of fresh tephra.	50 m ²	in patches	Light brown, very fine-grained with clay alike texture, well-sorted, consisted quartz and compacted tephra. Sample mixed with roots.

Table 3-2: The distribution of samples profile in Peninsular Malaysia (except Lenggong) (refer to fig. 1-1 for localities map).

Localities	Number of Spots & Descriptions	Tephra Descriptions and Freshness
Sianok 1	1 sample of fresh layer	Light brown-greyish colour, fine-grained, well-sorted and loose grained, consisted of dark minerals fragments (mica). Tephra sample consisted of lapilli with size 2-10mm.
Sianok 2	1 sample of fresh layer	Dark brown colour, fine-grained, -well-sorted and loose grained consisted dark minerals (mica).
Sipisopiso (YTT)	1 sample of fresh layer	Brown-fine-grained, sand-like texture-well-sorting and very loose grained-Sample mixed with soft pumice-pumice consisted mica fragments with quartz quartz 25-30%.

Table 3-3: The distribution of samples profile in Sumatra (refer to fig. 1-3 for localities map).

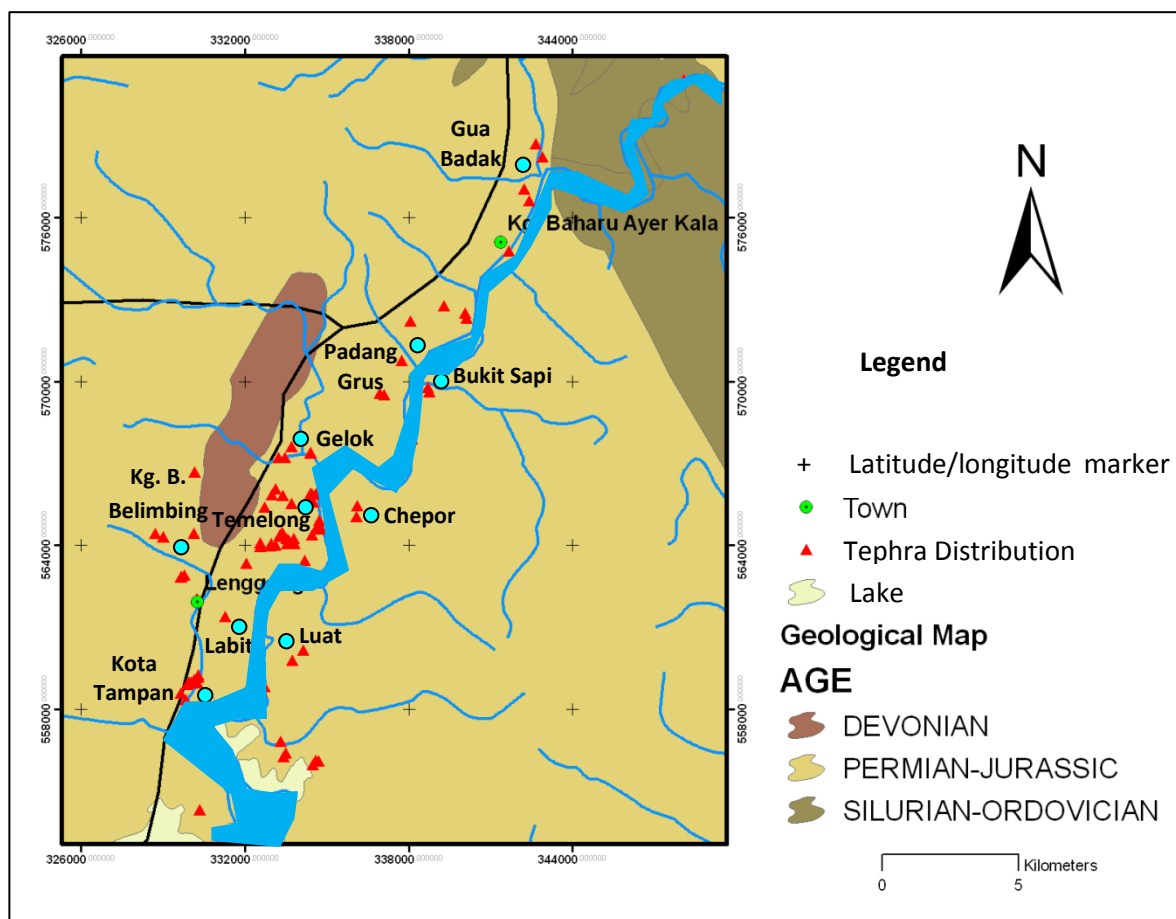


Fig 3-2: Tephra distribution in Lenggong.

showed the overall tephra localities in Lenggong area. Some localities showed intercalation of the reworked tephra layer overlain by the fresh layer, which was preserved by vegetations. Fig. 3-3 showed the oxidization marks of sediments that indicated the possibility of groundwater fluctuation level in tephra deposits in Bukit Sapi. Fig. 3-4 showed tephra layers descriptions in Labit. The Labit tephra consisted of five layers of tephra deposits, in which three of these layers were around 40 cm to 60 cm thick. The tephra layers have turned to purplish color due to reworking and mixed with coarse-grained quartz and pyrite (Ward, 1993). Bukit Jawa tephra sample in Gelok consisted of four layers of compressed and consolidated tuff with thickness from 50 cm to 1.10 m (fig. 3-5). The uppermost layer was very dense flaky tuff which was underlaid by silty flaky tuff layer.

The third layer consisted of hard, dense and consolidated tuff (fig. 3-5). In field, the fresh tephra were easily recognized by its whitish color and tasted like milk powder. However, the weathered tephra were not easily identified by its color, but by its hardness and the nature of its boundary. The tephra samples were later on confirmed in the laboratory using petrographic study or the X-Ray Fluorescence (XRF) technique.

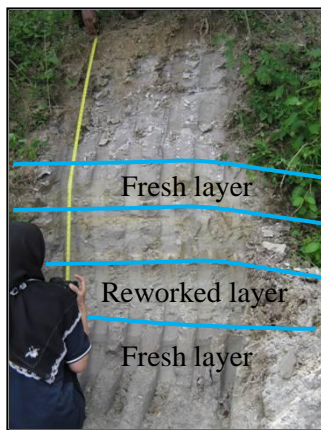


Fig. 3-3. Tephra deposits in Bukit Sapi.

- i) Note the oxidization marks (blue lines) of tephra deposits showed possibility of fluctuations of groundwater level in tephra deposits.
- ii) Intercalations of fresh-reworked-fresh layers.

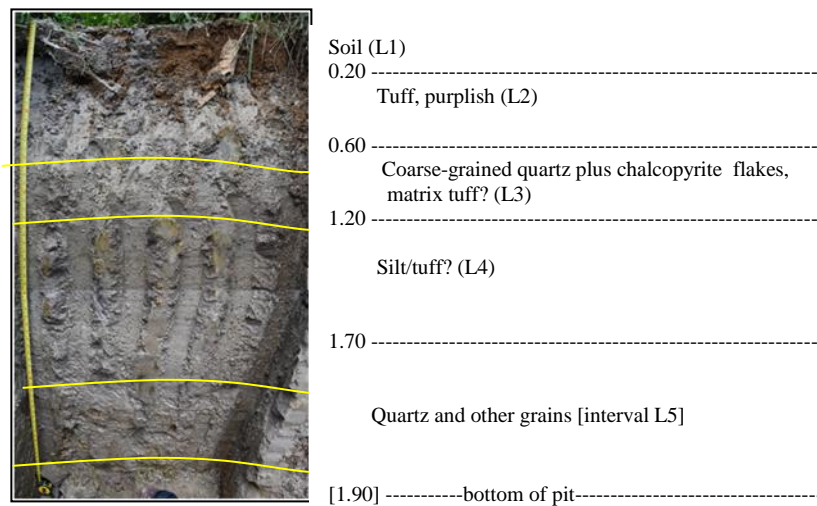


Fig. 3-4: Tephra layers in Labit.

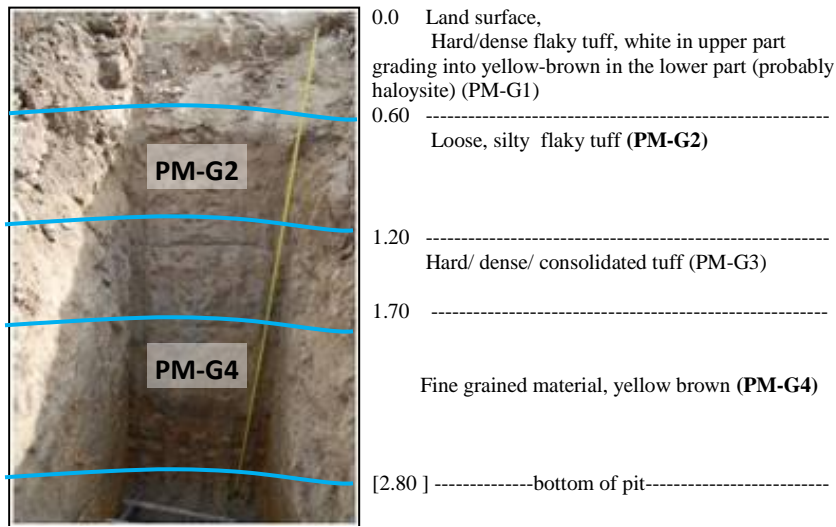


Fig. 3-5. Tephra strata in Gelok.

Fig. 3-6 demonstrated the relationship of topography of Lenggong area with the distribution of tephra. Based on the landslide scars observed at Gunung Hong, there is possibility that the tephra was washed out from these two highlands and finally deposited in the river valley.

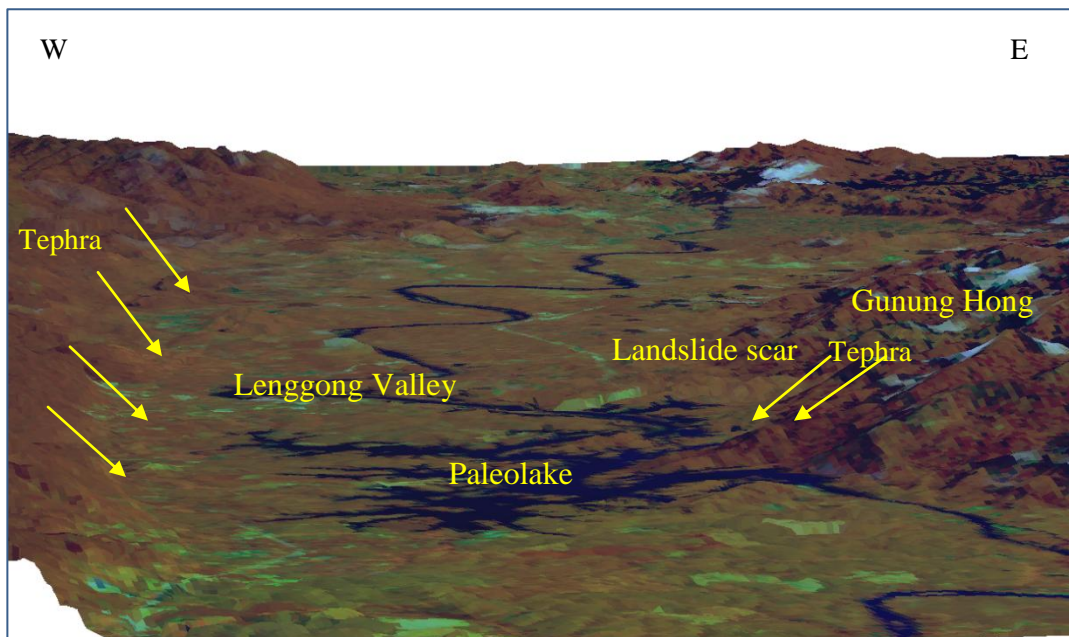


Fig 3-6: Visualization of depositional area of Lenggong Valley.

Fundamentally, Lenggong was covered with plantations that were particularly good medium for trapping and preserving tephra, as their surfaces was well vegetated. The surface maps in fig. 3-7 showed the distribution of tephra and the relationships between the topography and vegetations with the freshness of tephra in Lenggong. Fresh tephra was most widespread at the central of the valley at higher elevation areas, followed by the northern and southern parts of Lenggong at lower elevation areas (figs. 3-6-3-8).

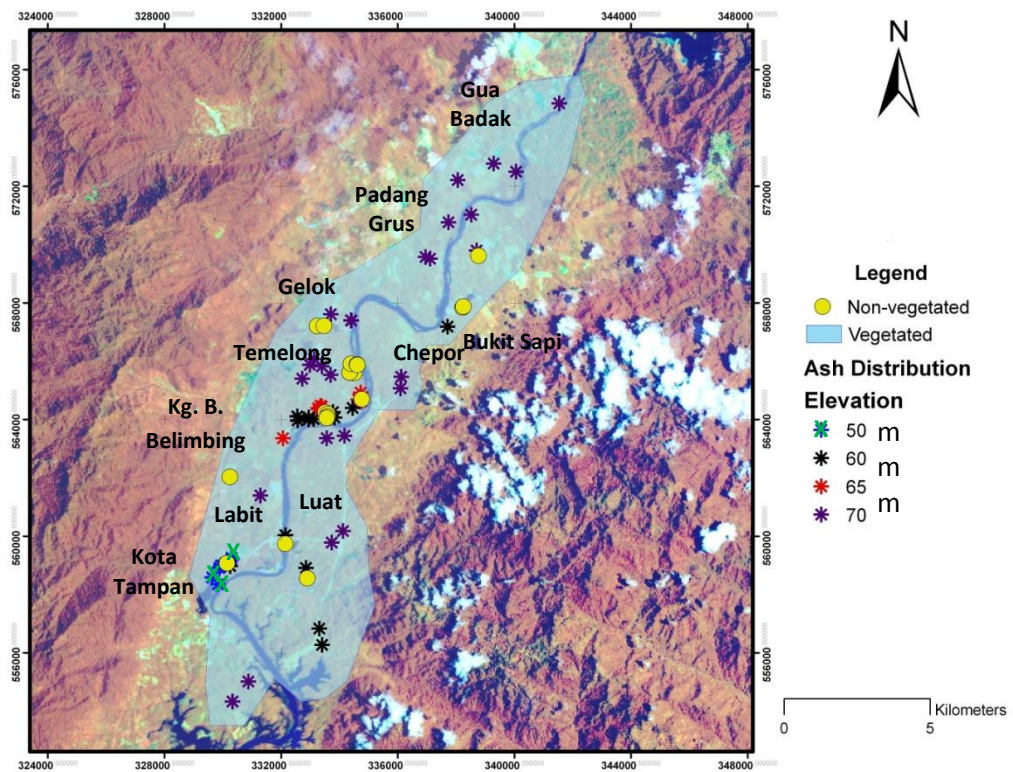


Fig 3-7: Relationship between the distribution of tephra with vegetated and non-vegetated area in Lenggong Valley.

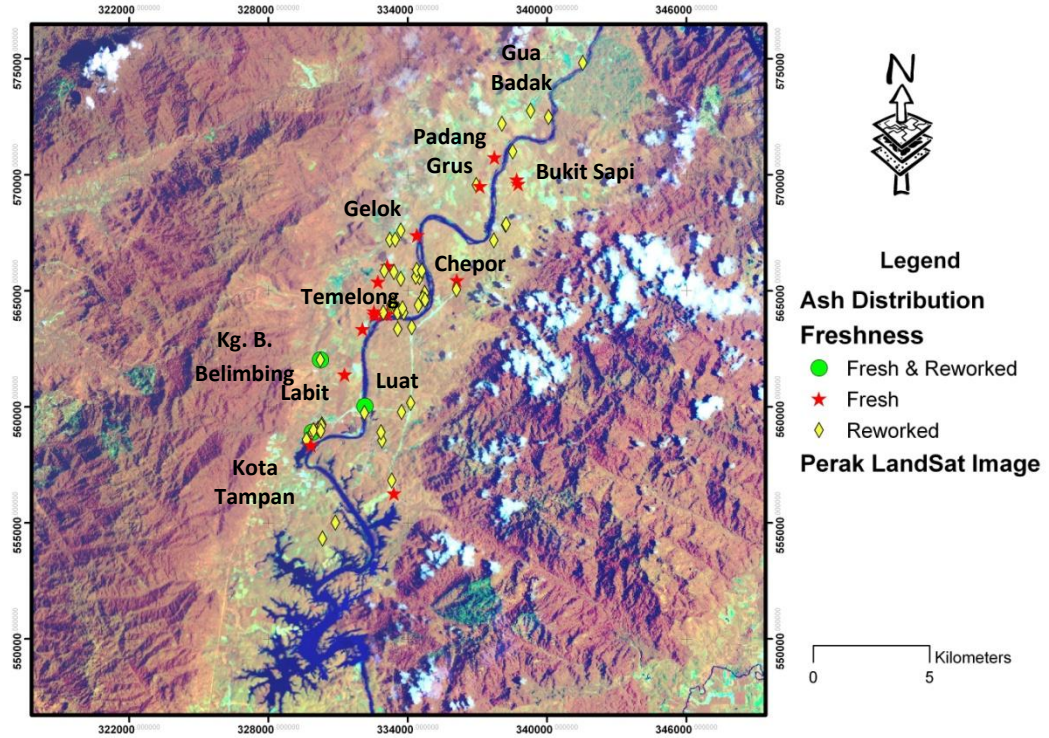


Fig. 3-8: Relationship between tephra distribution and freshness in Lenggong Valley

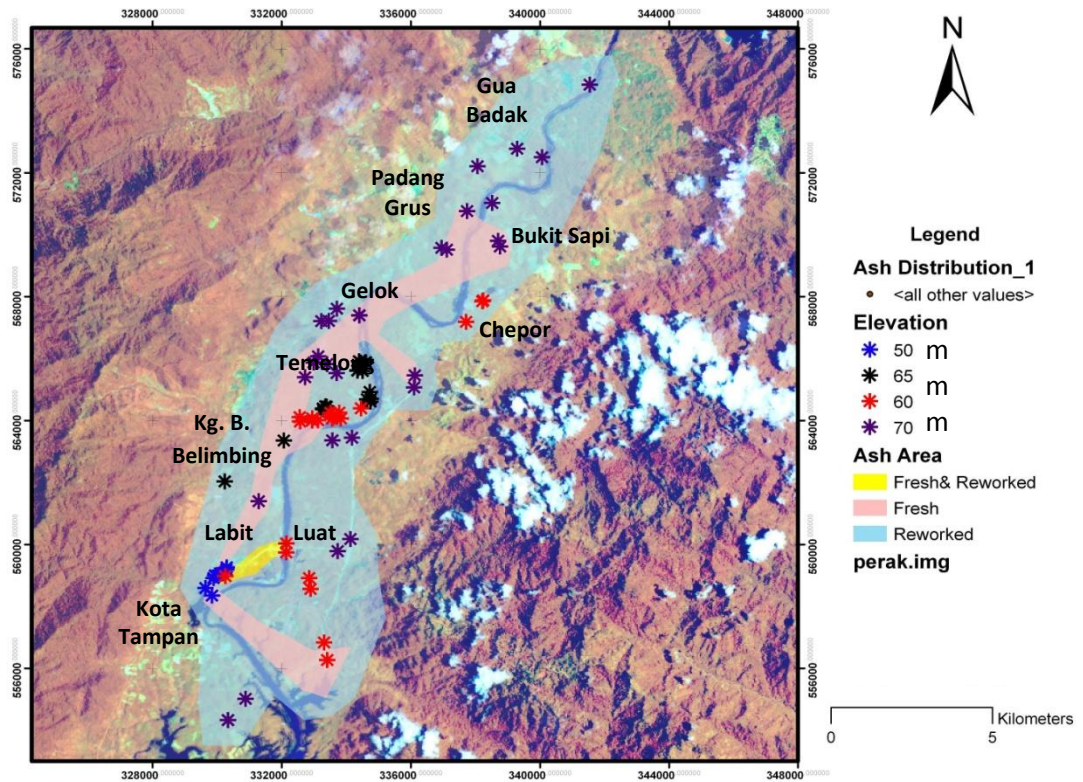


Fig 3-9: Relationship between distribution with elevation and freshness.

3.1.1. Freshness Determination

3.1.1.1. Macroscopic features of tephra layer

The freshness of tephra samples was determined based on field inspection at the representative sample points. Most of fresh deposits located at the centre of Lenggong Valley, followed by northern part and few spots at the southern part (fig. 3-9). Based on the elevation map, all of these fresh deposits were located at higher elevation compared to that of reworked deposits. Patches of fresh tephra were transported in small volume and eventually disappeared in formation.

3.1.1.2. Microscopic Features of Tephra Layer – Scanning Electron Microscope (SEM) Images

Four selected samples from Bukit Sapi (PM-S1), Kg. Jawa (PM-M1), and Kg. Kuah (PM-M2) and Chegar Galah (PM-M3) (Table 2-1) based on their freshness under SEM. Bukit Sapi, Bukit Jawa and Kg. Kuah located at Lenggong whereas Chegar Galah located at Kuala Kangsar. Bukit Sapi was identified as representative sample for fresh tephra while Chegar Galah, Bukit Jawa and Kg. Kuah were representatives for reworked samples in Perak. These volcanic layers ranged in thickness from 30 cm to approximately 3 m. SEM images were taken from raw tephra materials directly from the field. SEM images of glass shards showed distinctive textures of glass shards for freshness comparisons. Bukit Sapi tephra that represented fresh samples in Lenggong showed distinctive finer and cleaner textures compared to that of the other reworked samples (fig. 3-10A and B). The SEM photo showed the Y-shaped (circled in fig. 3-10A), bubble wall (circled in fig. 3-10B), highly vesicular glass shards with smooth and slightly curved shape. Some of the shards were very thin and constituted plane-type blocky glass (fig. 3-10D).

Bukit Jawa that represents reworked materials has a poorly vesicular shard in weathered material (fig.3-10B). The weathered tephra of Kg. Kuah showed bubble wall-type glass shards in weathered material (fig. 3-10C). The Chegar Galah tephra showed plane-type blocky glass shards that were covered with reworked materials (fig.3-10D).

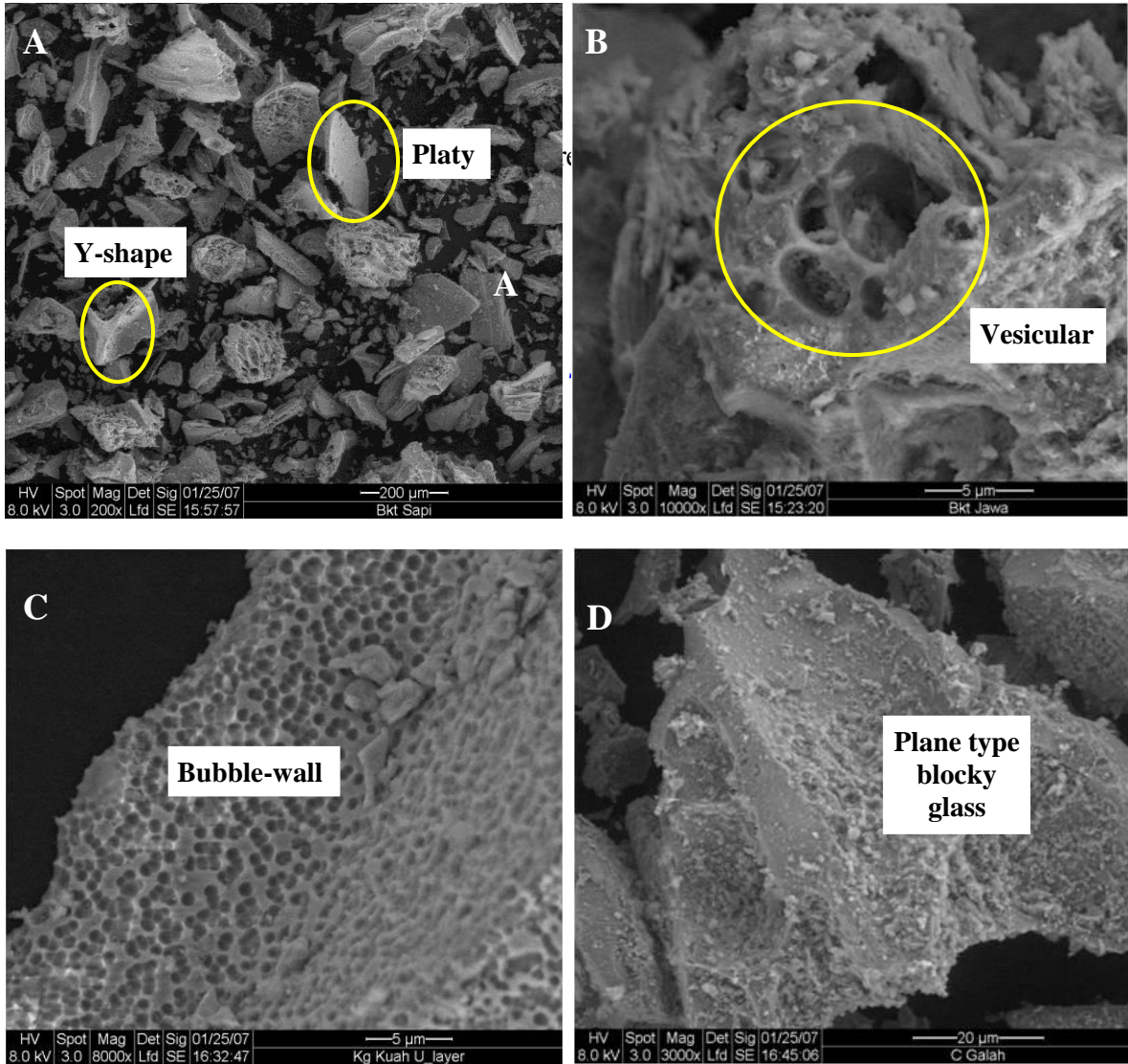


Fig. 3-10: SEM photos of fresh (A) and reworked (B-D) glass shards. Photos were taken on different time and scale.

Platy (circled in fig. 3-10A) or bubble-wall (fig. 3-10B) shards were much common than pumice shards in distal shards. Rose, (1987) reported that the widely dispersed Toba tephra composed entirely of bubble-wall shards. The glass shards particles were preserved in well-sorted layers that fell prematurely as aggregates and would possibly be carried thousands of kilometers farther if they had remained as simple particles (Rose, 1987).

More comprehensive work on Peninsular Malaysia distal tephra occurrence was needed because of their unusual shape characteristics.

3.2. TEPHRA AGES

In this study, two samples from Gelok at Lenggong were dated using fission track. The selection criteria for this analysis were based on the freshness, thickness and stratigraphy of the tephra samples. The Gelok dating samples were taken from second and fourth layers of total 2.8 m for tephra deposits. Padang Sanai tephra was not suitable for the fission track analysis since it was deposited as a single paddy soil layer. Table 3-4 showed the results of PM-G2 and PM-G4 ages using fission track approach (refer to fig. 3-5 for PM-G2 and PM-G4 outcrop descriptions).

3.2.1. Fission Track Ages

Sample Name	Age ($\pm 1\sigma$) ka
PM-G2	59 \pm 7
PM-G4	59 \pm 9
*Serdang 1	64 \pm 11
*Serdang 2	64 \pm 11

Table 3-4 showed glass fission-track ages of tephra beds from the Gelok and Serdang localities (refer to table A1-1 for details).

* Data from Westgate, 1998 as comparison.

3.2.2. OSL Ages

In this study, two fresh tephra from Kuala Pelus samples were taken from the first and third layer of total 9 m thickness for tephra deposits (Fig. A3.8). Padang Sanai tephra was not selected for OSL since the depositional area had been exposed to human and animal activity.

Sample Name	Luminescence Age (ka)
KP1	75.5 ± 9.8
KP2	58.5 ± 7.6

Table 3-5: Glass shards OSL ages of tephra beds from Kuala Pelus, Perak (refer to fig. A3.8 for tephra deposits picture).

3.3. MAJOR, RARE EARTH ELEMENTS (REE) AND TRACE ELEMENTS ANALYSIS

Major element data of glass shards were obtained using EPMA analysis for Lenggong, Padang Sanai and Sumatra. Samples were analysed using EPMA model Cameca SX100 at University of Malaya. However, the Kuala Kangsar and Kg. Dong samples were performed using a JEOL JXA-8530F Field Emission model at NTU. Electron Microprobe samples with oxide totals of less than ~ 90% were discarded. In this study, total as low as ~ 90% might be perfectly acceptable since volcanic glass typically absorbed water after deposition. Any cut-off point based on analytical total should be selected because this reflects the water contents where changes can be observed to start in the glass, and should not be some arbitrary selected number such as 95% total that was widely used by European tephrochronologists (Pearce, 2008). Values were then normalized to 100% for the purpose of comparison and plotting. Normalization has been criticized by Hunt and Hill (1993),

who argued that no adjustment of the original measures should be undertaken and that all samples yielding oxide measure total of less than 95 % be rejected, because the variance of the values obtained for individual oxide measures remains insufficiently precise to be reliable. Normalizing the data was, however, widely undertaken by New Zealand and North Amerika tephrochronologists (e.g. Shane, 2002; Westgate et. al., 2001; Newnham et al., 2003) have demonstrated through discriminant function analysis that the use of raw, normalized or otherwise transformed data made little difference in correctly assigning glass shards to their source volcano. In this study, normalization of major elements data was performed to remove the variable effects of hydration in different samples. Table A2.1 showed the major elements data of tephra that were used in this study.

Trace element and REE values for glass shards were obtained using Laser Ablation ICP-MS (LA-ICP-MS) at Aberystwyth University using the method described in Pearce, (1995).

3.3.1. Peninsular Malaysia Major elements Data

Table A2-1 showed the major elements data for Peninsular Malaysia whereas table A2-2 showed the major elements for Sumatra tephra that were used in this study.

3.3.2. REE and Trace Elements Data

The rare-earth and trace chemical data were preliminarily analyzed using cluster analysis. Cluster analysis was a classification technique that places samples into more-or-less homogeneous groups, so that the relationships between groups were revealed. The groups were determined only on the basis of geochemical similarities between samples. In the box plot diagram, the level of the branching point between two groups indicates the

similarity between these groups. Fig. 3-10 showed the box plot correlation for chemical composition between Peninsular Malaysia and Sumatra tephra. This particular trace element showed distinct correlation among Padang Sanai (PM-3C) and Sianok samples (SM-4A and SM-4B). However, this preliminary analysis is inconclusive. Samples which can be separated on bivariate or trivariate major oxide plots, using elements determined with good accuracy and precision, cannot be correlatives. Samples which cannot be separated on all possible combinations of bivariate or trivariate plots can be considered to be likely correlatives, but any suggested correlations must be consistent with all other stratigraphic, compositional and mineralogical information (Westgate, 2013). Where samples cannot be separated by the major element compositional data, trace element analyses are likely to be of help in either confirming or refuting correlations. A similar approach can be adopted for the graphical presentation and interpretation of trace element data from tephra deposits as is described here for erecting correlations based on trace element analyses.

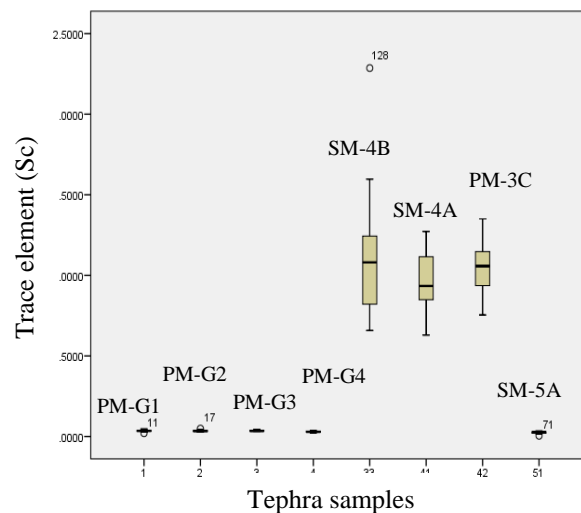


Fig. 3-11. Box plot showed the results of cluster analysis on the REE and trace elements geochemistry, and the separation into eight distinctive tephra compositions. These eight clusters of samples were identical to those subjectively recognized in the plots. Note the degree of similarity of the individual tephra samples within PM-3C with SM-4A and SM-4B.

Table A2-3 showed the rare-earth elements (REE) data for Lenggong (PM-G1, PM-G2, PM-G3 and PM-G4), Padang Sanai (PM-3C), Toba (SM-5A) and Sianok (SM-4A and SM-4B) that were used in this study. Concentrations were measured in ppm. Refer to table A2-4 in Appendix II for Chondrite Normalize Standards.

CHAPTER 4

“Where all think alike, no one thinks very much”
- Walter Lipman.

4.0 DISCUSSION

The tephra distribution study showed there was a site in Lenggong with five tephra layers with thickness of more than 4 m (fig. A3-6). The glass shards surface morphology could be correlated with distal glass shards study originated from Sumatra tephra that was found as far as Indian Ocean (R. F Muhammad, 2010). Dating results obtained from Lenggong and Kuala Pelus showed a correlation with Maninjau and YTT ages. The PM-G2, PM-G4 and KP2 results could be correlated with the 52 k. Maninjau while KP1 could be correlated with the 75 k.a. YTT. The geochemistry analyses focused on the glass shards population and chemically ‘fingerprint’ Peninsular Malaysia and Sumatra tephra to establish the sources of widespread Peninsular Malaysia tephra.

4.1. DISTRIBUTION

The abundance of tephra in vegetated areas and river banks, coupled with its depositional environment history, rendered Lenggong as an ideal region for tephra studies. Approximately 1137 km² of the Lenggong area has been studied for this research and approximately a total of 15 km³ of layers of dispersed tephra have been found there. Layers of fresh and reworked deposits of tephra have been discovered in the vicinity of the Perak River banks and on gentle slopes of palm oil estates. Reworked material suggested lacustrine environment in Lenggong.

The occurrences of reworked material under layers of fresh deposits indicate that the tephra layers were originated from more than one sources eruption. These

deposits have been subjected to a long history of weathering and reworking since their fall. The freshness and thickness of tephra were heavily influenced by topography and ancient river flow which was believed to have been 70 m higher than current water level during deposition across the study area. The relationship between topography, vegetated pattern and the distribution of Lenggong tephra were modeled with a geographic information system (ArcGIS).

The depositional of tephra in Lenggong area occurred in Perak River Valley, which was sandwiched between two highlands. Fig. 4-1 demonstrated the relationship of topography at Lenggong area with the distribution of tephra. There was possibility that the tephra was washed out from these two highlands and eventually deposited in the river valley. Another possibility was a large landslide at Gunung Hong had eroded the tephra to the Perak River, at the present artificial dam site during the formation of Chenderoh Lake (Tjia, 1990). There was also probability that the deposits were originated from the north area of Perak River due to the slope gradient which flooded Lenggong Valley area.

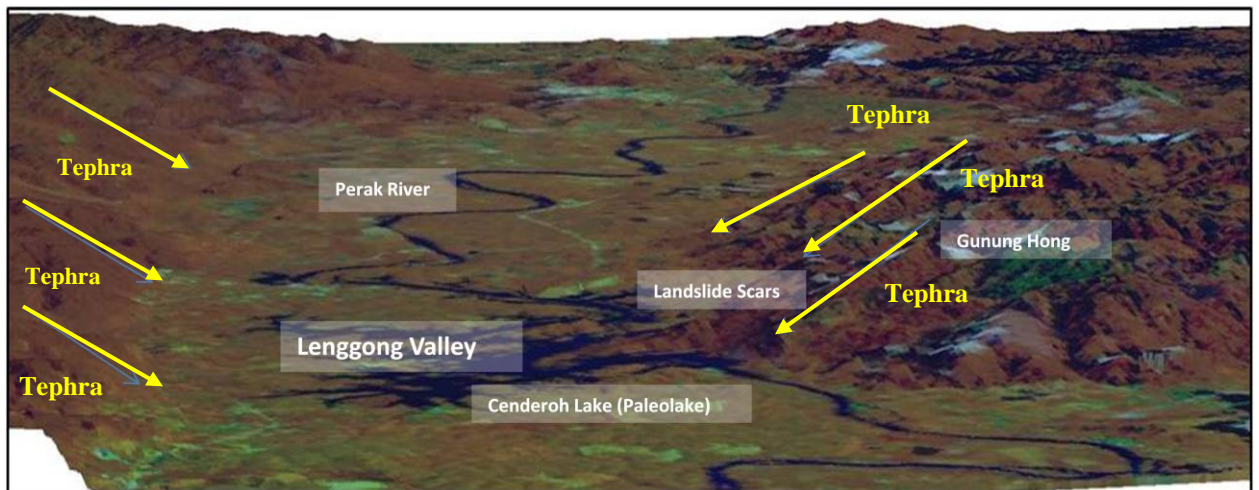


Fig. 4-1: The relationship of topography with tephra distribution in Lenggong.

The Lenggong area was covered with plantations, thus particularly good for trapping and preserving tephra, as their surfaces were well vegetated. The current situation might be different from the tephra were primarily deposited during late Pleistocene. The surface map shows the distribution of tephra and the relationships between the topography and freshness of tephra in Lenggong (fig. 4-2). Fresh tephra was more widespread at the centre of the valley at higher elevation areas, followed by northern and southern part of Lenggong in lower areas (fig. 4-2).

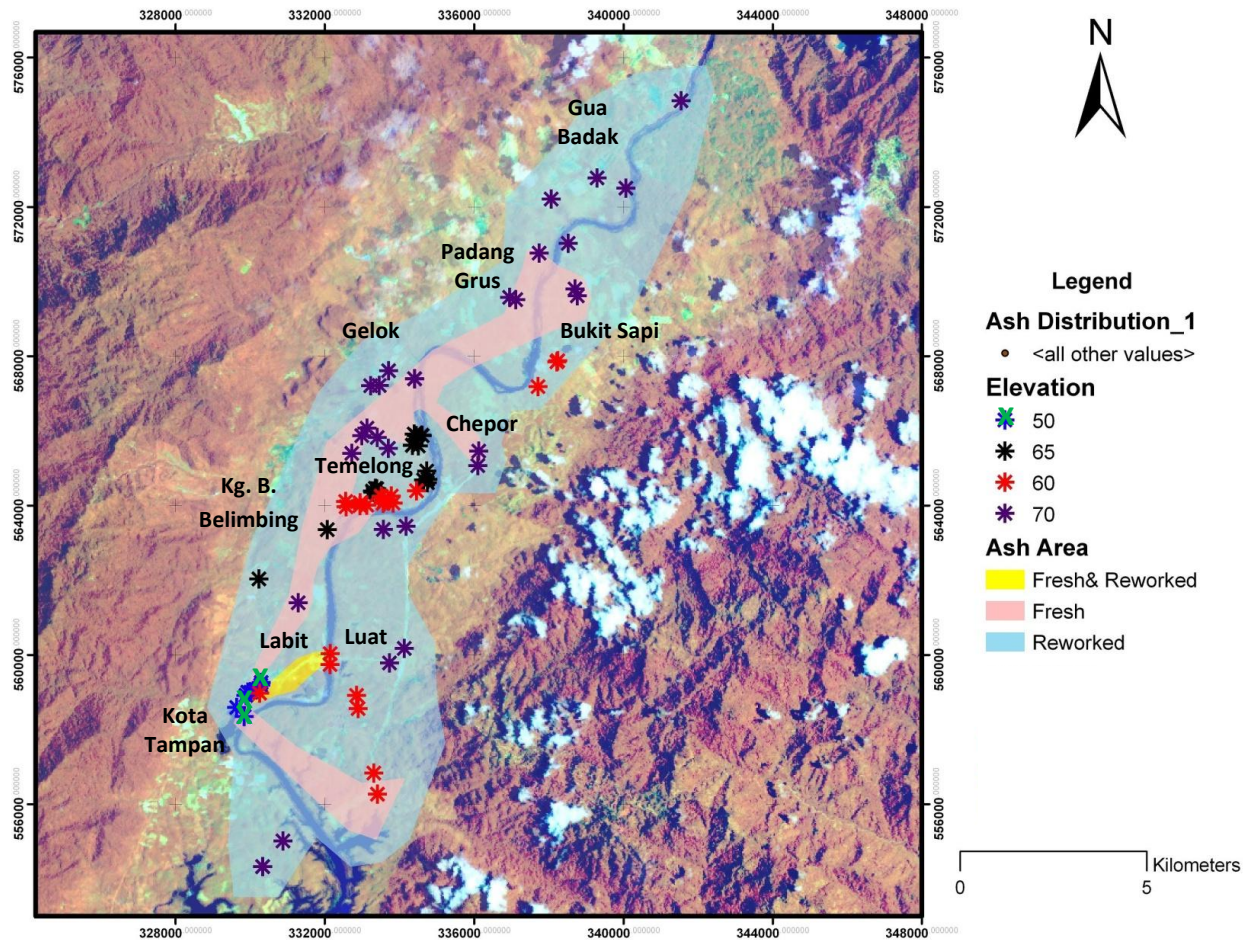


Fig. 4-2: The distribution of tephra freshness in Lenggong.

4.1.1. Tephra Thickness

The volume of the tephra in Lenggong has been suppressed and compacted by rain drops, fluctuation of ground water and overlain by recent sediments. Raindrops impacting on the tephra layer contributed to rapid compaction through decreasing porosity (Jackson, 1997). The compaction increased the bulk density of tephra deposit, sometimes by as much as 50 percent, within a few weeks of an eruption. Most tephra layers in Labit have been highly compacted and some of them have been proven to be hardened, making it impossible to be removed for land development (fig. A3-4).

The thickness of the tephra deposit in Lenggong might correspondingly decrease slightly over time. Within a few years of the eruption, much of the tephra was eroded from slopes of 50 degree or steeper, with re-deposition nearly always local and immediate. It was during severe rainstorms or flooding that the tephra was readily eroded from the steep slopes and swept into streams and rivers. Such erosion was similar to the behavior of soils on non-vegetated land during severe rainstorms (Jackson, 1997).

The advantage of wet tephra usually exhibits cohesive properties that could dramatically decrease reworking and disturbance. The resistance of compacted tephra to the wind erosion would increase as grains nest more tightly together (Jackson, 1997). There were evidences showing that the tephra had been deposited in lake and river environment during Pleistocene, which apparently affect the thickness of Lenggong tephra. The oxidization marks of tephra sample in Bukit Sapi showed a possibility of groundwater level fluctuations after the depositional of the tephra (fig. 3-2). The intercalations between fresh and reworked layers also lead to the possibility that these tephra layers derived from more than one eruption.

The maximum exposed fresh tephra thickness was in Kg. Sena Halu that was located in Luat province, where 4 m thick layer has been observed (fig. A3-6). Most of

these fresh deposits were located at higher topography and currently well preserved by community plantations. However, this might not represent the actual maximum thickness of tephra for this area because a deeper tephra layers might have been mixed with the terrigenous materials, compacted and cemented into hard materials that rendered it almost impossible to excavate (figs. A3-3 and A3-4). The field observation of this study is limited to surface observation. A few selected areas with important stratigraphy were excavated for dating analysis.

During Pleistocene, Kota Tampan area in Lenggong was located next to an ancient lake 70-75 m higher than current sea level (Zuraina dan Tjia, 1988). The existence of the lake was marked by a high terrace, ancient match valley, landslide scars and marks showing water flowed out of the ancient lake. A possible oxbow lake was also found at Banggol Batu in Kota Tampan to support the existence of the ancient lake. Landslide scars could be clearly seen from field where debris could be found in between Gunung Hong and Cenderoh Reservoir but due to insufficient data, it is invisible in surface map. Based on this study, Kota Tampan was a big island during the Middle Pleistocene period. The study has strengthened Zuraina and Tjia (1988) interpretations that Kota Tampan was influenced by the ancient Chenderoh Lake, Perak River and its tributaries. Kg Temelong Paleolithic site was related to that of Kota Tampan, and supports the theory of lake adaptation.

4.2. TEPHRA AGES

4.2.1 Previous Dating

A few attempts were made earlier to estimate the age of tephra in Peninsular Malaysia. The earliest was undertaken in Ampang, using ^{14}C , three wood samples in Ampang tephra were dated at 33.25 ± 1.8 k.a., 36.5 ± 2.5 k.a. and >39.9 k.a. (Stauffer

1973). The next effort was a fission track age of 30 ± 4.5 k.a. (Nishimura and Stauffer, 1981) on zircons from Serdang tephra. Nishimura (1980) also dated a 1 m thick consolidated tephra found at east side of Lake Toba, including Parapat Pass at 30 ± 0.3 k.a. that proved the most likely source for the 30 k.a. Serdang tephra. Although Stauffer et al (1980) suggested that these dates indicated the occurrence of another eruption at Toba, Chesner et al. (1991) considered tephra-shard chemistry (Ninkovich et. al., 1978a; Rose and Chesner, 1987), mineral chemistry and Sr isotopic ratios (Chesner, 1988) suggested the Malaysian tephra was correlated to the 75 k.a. YTT.

In general, early researchers of Peninsular Malaysia tephra lacked precise radiometric dates and made assumptions in their absence, e. g., Debaveye (1986) assumed that Padang Terap tephra could have been derived from the 75 k.a. Toba eruption or from the 30 k.a. Sibuatan eruptions based on microscopy and major elements analysis.

In this study, two samples from Lenggong and another two samples from Kuala Pelus were dated using fission track and optically stimulated luminescence (OSL) methods, respectively. The selection criteria for dating analysis were based on the freshness, thickness and stratigraphy of the tephra samples. The Gelok dating samples were taken from second and fourth layers of total 2.8 m of tephra deposits while Kuala Pelus samples were taken from the first and third layer of total 9 m thickness of tephra deposits. Padang Sanai tephra was not suitable for the dating analysis since it was deposited as a single paddy soil layer. The Lenggong tephra dates were obtained from Gelok area, collected from fresh layer Gelok 2 (PM-G2) and at the deepest of the fresh tephra layer which was Gelok 4 (PM-G4). PM-G2 and PM-G4 tephra were deposited at 59 ± 7 k.a. and 59 ± 9 k.a., respectively (fig.3-4). Fresh tephra in Kuala Pelus that were labeled as KP1 and KP2, was deposited at 75.5 ± 9.8 and 58.5 ± 7.6 k.a., respectively. These ages appeared in reverse order, that was the older sample was higher in the section, although there was possible

overlap within the ranges of uncertainty. There are several possible explanations; 1. The whole deposit could be from one single eruption, the discrepancy in the ages might only due to uncertainty. 2. There might be two events aged 75 and 58 k.a. Material from the 75 k.a. event was preserved in a body of aggregate which was later deposited on top of the younger 58 k.a. deposit without exposure to the sun. 3. The whole deposit could be from one single 75 k.a. eruption but 58 k.a. deposit might have been reworked and exposed to the sun, resetting the clock for OSL. Nevertheless, despite the abnormal reverse stratigraphy, the 58 k.a. KP2 data was the same age as PM-G2 and PM-G4 tuffs (Table 3-4). Presumably, the current dated tephra could be considered as valid since it could be correlated with one of the major event in Sumatra, which was the 52 k.a. Maninjau eruption (Kuna Raj, J., personal communication). Further detailed research should be done on Kuala Pelus tephra locality to find further information to explain the abnormal age sequence. The stratigraphy of the PM-G2 and PM-G4 is shown in fig. 3-4. The samples were taken at the depth of 1 m and 2.5 m for the PM-G4 (fig. 3-4). Kuala Pelus samples were acquired at the 2 m and 5 m depth (fig. A3.8). The ages of the PM-G2, G4 and KP2 could be correlated with 52 k.a. Maninjau volcanic event while KP1 was best correlated with 75 k.a. of YTT.

4.3. GEOCHEMICAL ANALYSIS

In this study, bivariate plots, Rare-Earth Element diagrams, trace-element ratios, and spider diagrams were constructed to determine if REE and trace elements could be used to fingerprint Peninsular Malaysia tephra and subsequently, correlate them with Sumatra tephra. EPMA was used to characterize a variety of tephra based on their major elements whereas all of the REE and trace elements data were obtained from laser ablation inductive coupled plasma mass spectrometry (LA-ICP-MS) on glass shards. This study described

how the REE and trace elements data from LA-ICP-MS method were able to discriminate between deposits, and the quality of the analyses was thus important in defining what could be recognized as different or regarded as the same (Pearce, 2004).

Based on the major elements plots in chapter 3, it could be concluded that population variability does exist in Peninsular Malaysian tephra. Spider plots for every samples of Peninsular Malaysia tephra have been constructed to identify the best discriminators, which are Sr, Ba, Ti and Y to prove the level of populations in every sample (fig. 4-3). Plots of CaO Vs Ba, Sr Vs Ba, Ti Vs Ba, Y vs Ba, population plots for Peninsular Malaysia, and comparison of population for PM and Sumatra plot were generated to confirm possible correlate trend. The glass compositional data support the presence of a compositionally zoned magma prior to eruption, produced by crystal fractionation. This multiple glass populations are due to disruption of the zone magma on eruption, produce some co-mingling (Westgate, 2013).

Crystal fractionation was a chemical process by which the composition of a liquid, such as magma, changes due to crystallisation. It was one of the three most important processes by which igneous differentiation occurs together with crustal contamination and magma mixing (Ukstins Peate, 2008). Crystal fractionation occurs since the formation of crystals within magma removes the chemical components of the crystal from the liquid and thus changes the composition of the liquid that remains. In a closed system crystal fractionation does not change the bulk composition of the crystal-liquid mixture. At equilibrium the liquid and crystals react with each other and the compositions of both will change together with temperature and pressure (Ukstins Peate, 2008).

Spider diagram of Peninsular Malaysia was constructed to identify which elements that show the greatest variability in the plots. Overall, PM-G1, PM-G2 and layer PM-G4

showed more than two populations while PM-G3 was almost homogenous. The elements that show greatest variability in the spider plots are Ba, Sr, Ti and Y due to crystal fractionation.

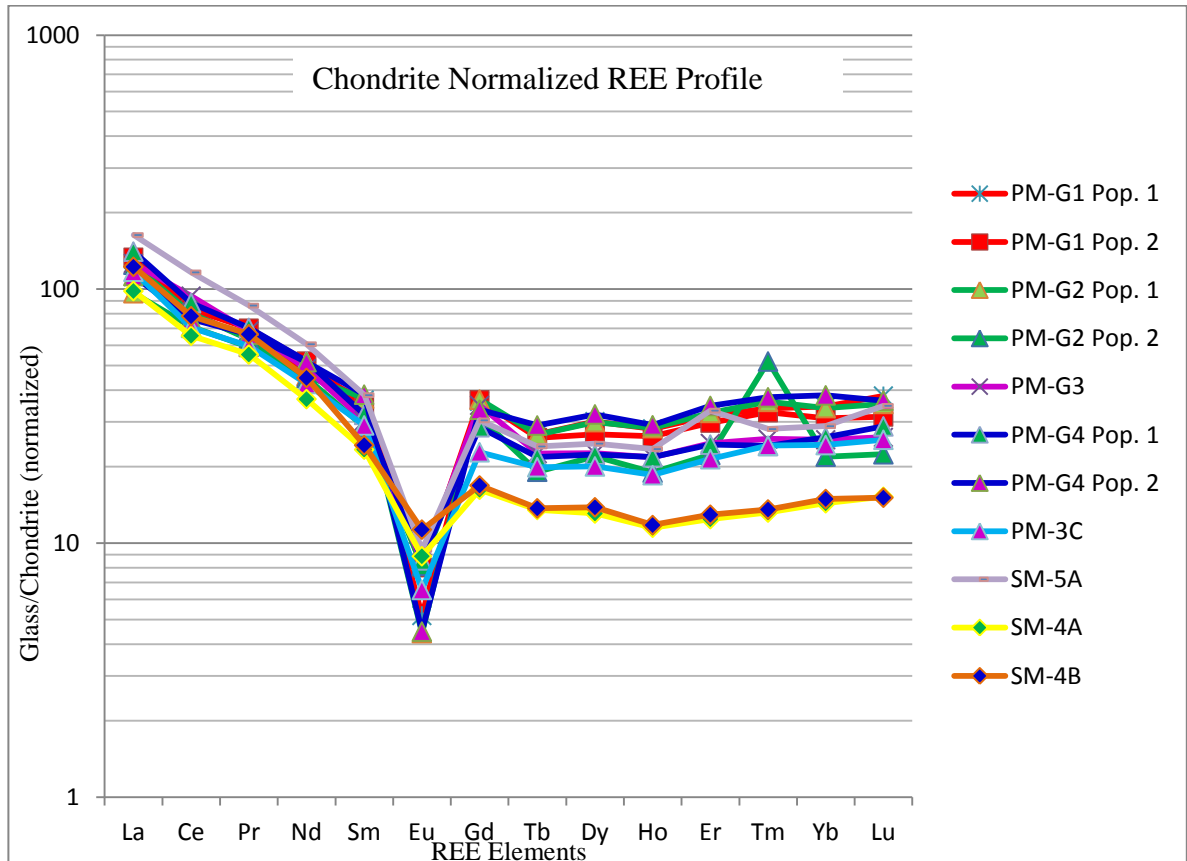


Fig. 4-3. Chondrite normalized REE profile for Gelok group, Padang Sanai, YTT and Sianok correlatives. This plot shows minimal variation among the mobile elements between the SM-5A, PM-G1, PM-G2, PM-G3, PM-G4 and PM-3C Tuffs; and SM-4A, SM-5A, PM-G1, PM-G2, PM-G3, PM-G4 and PM-3C Tuffs. It was clearly shown the distraction between YTT and Sianok in Heavy Rare Earth Elements (HREE). Note the significant variation in HREE among PM-G1 - Population 1 and 2, PM-G2 - Population 1 and 2 and PM-G4 - Population 1 and 2.

This strongly suggested that a correlation exists between YTT, Gelok, and Padang Sanai Tuffs. However, the less mobile elements of YTT, Gelok, Padang Sanai and Sianok (SM-4A and SM-4B) show a great amount of variability in the plot. The less mobile REE

anomalies help distinguish the individual eruptions. The HREE showed there was more than one population in PM-G1, PM-G2 and PM-G4. Elements normalized to the MORB standards of Pearce, 1983.

Analysis using Rare-Earth Element (REE) chemistry, trace element ratios, and spider diagrams become apparent that these samples could be separated from each other (figs. 4-3 to 4-8). In total, only five undifferentiated Peninsular Malaysia samples and 3 Sumatra samples were analyzed using REE and trace-elements ratios (figs. 4-6 to 4-15), and Spider Diagram (fig. 4-3). Based on this analysis, all Gelok samples and Padang Sanai samples could be correlated with the Toba eruption. (figs. 4-4b to 4-15). There are slight variations in the fractionation of the light rare earth elements (La-Sm) between the eruptions (fig. 4-3). Each eruption appears to have a distinct negative Eu anomaly, controlled mainly by early crystallization of feldspar.

TAS plots were used to classify volcanic rocks. In this case, all tephra samples (other than a few outliers) plot far into the Rhyolite field, as one would expect. However, it shows there are distinct differences between tephra from different locations. The most alkali metal ($\text{Na}_2\text{O}+\text{K}_2\text{O}$)-rich samples are the YTT from Sipisopiso and the tephra from Gelok. Padang Sanai samples also show a restricted, if slightly less alkali-rich, distribution of values. The other locations (K. Kangsar, Kg. Dong, and Sianok) show a wider range in both silica and alkalis. Taken together, there is a negative correlation between SiO_2 and alkali metals. The Kuala Kangsar samples plot on a shallower gradient than the others, however (see fig. 4-4b).

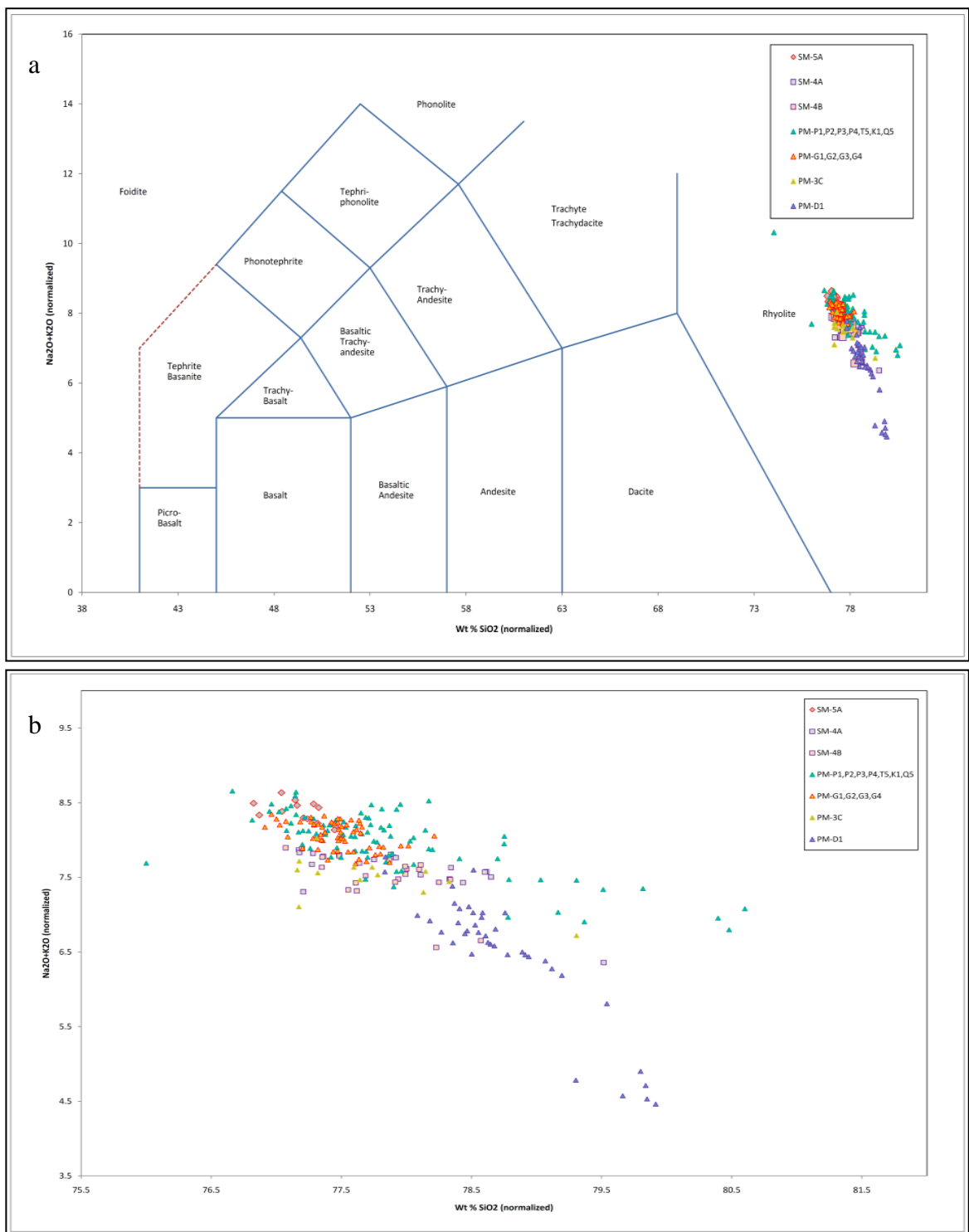


Fig. 4-4. a) TAS diagram: TAS diagram (after Le Maitre et al. (1989)). All data from glass shards plot as an elongated cluster in the rhyolite field. An expanded version (b) shows the negative correlation between SiO_2 and $\text{Na}_2\text{O}+\text{K}_2\text{O}$. Proximal YTT and samples from Gelok and Padang Sanai plot together, but Kg. Dong and Kuala Kangsar samples plot differently, in very elongated clusters. Samples from Sianok plot close to the YTT, Gelok and Padang Sanai samples, but contain lower total alkalis.

Major and trace elements data were presented in Appendix II. Major element data was presented as water-free normalized compositions, with H₂O by difference, as discussed in Pearce et al. (2008). In this paper, the authors argue that rhyolitic magmas could already contain 7-8% water, and after deposition, could absorb an additional few percent before devitrification and loss of cations results. Since water in unaltered glass shards serves as a diluent, calculations and plots should be based on water-free normalized values.

The amount of water in the glass shards differs markedly by location – the tephra at Gelok and the proximal YTT collected at Sipisopiso contains shards with little water (< 0.2%) while Padang Sanai shards could contain up to 10.5% water. Examination of Padang Sanai shards under the optical microscope did not reveal devitrification, however.

In igneous rocks, major and trace element compositions were affected by a myriad of processes, including crystallization, assimilation, and melt segregation. Crystallizing solids would remove elements from the melt in different proportions than what was present in the melt, causing the melt composition to change as crystallization proceeds. Some elements (i.e. “compatible elements”) are selectively absorbed by crystallizing phases while others are excluded (“incompatible elements”).

Glass shards represented the magmatic liquid present at the time of eruption. Different eruptions of the same magmatic system, or from a different magmatic system, will produce tephra deposits containing differing concentrations of elements. Theoretically, if the magma was homogeneous at the scale of the glass shards (in the micrometer range) then all (unaltered) glass shards produced by one eruption will have the same major and trace element compositions, no matter where they end up being deposited. In reality, short-range diffusion around crystallizing mineral grains will introduce inhomogeneity at the millimeter or centimeter scale, and this will be reflected in a range of compositions within the population of glass shards in a tephra deposit.

4.3.1 Elemental distribution

All volcanic shards analyzed for this study fall within a small range of SiO₂ values, from 76.9 to 80.6%. On a TAS diagram (fig. 4-4a), they plot far into the Rhyolite field, in a tight cluster. An expanded TAS diagram (fig. 4-4b) resolves the tight group into smaller groups, the groups taken together show a negative correlation between SiO₂ and K₂O + Na₂O (alkalies). The Kuala Kangsar and Kg. Dong tephra show the largest variations of SiO₂ and alkalies. The other locations are more restricted - except for a few outliers, to < 77.8% SiO₂ and to > 7.4% alkalies. As in many rhyolitic glasses, concentrations of Fe and Mg are extremely low.

It could be seen from fig. 4-4b that the Kg. Dong and Kuala Kangsar tephra were distinct from the other Peninsular Malaysia tephra. The Kg. Dong tephra contained less Na₂O than the others, while the Kuala Kangsar tephra contained less Al₂O₃ (figs. 4-5a, 4-5b, 4-5c and 4-d).

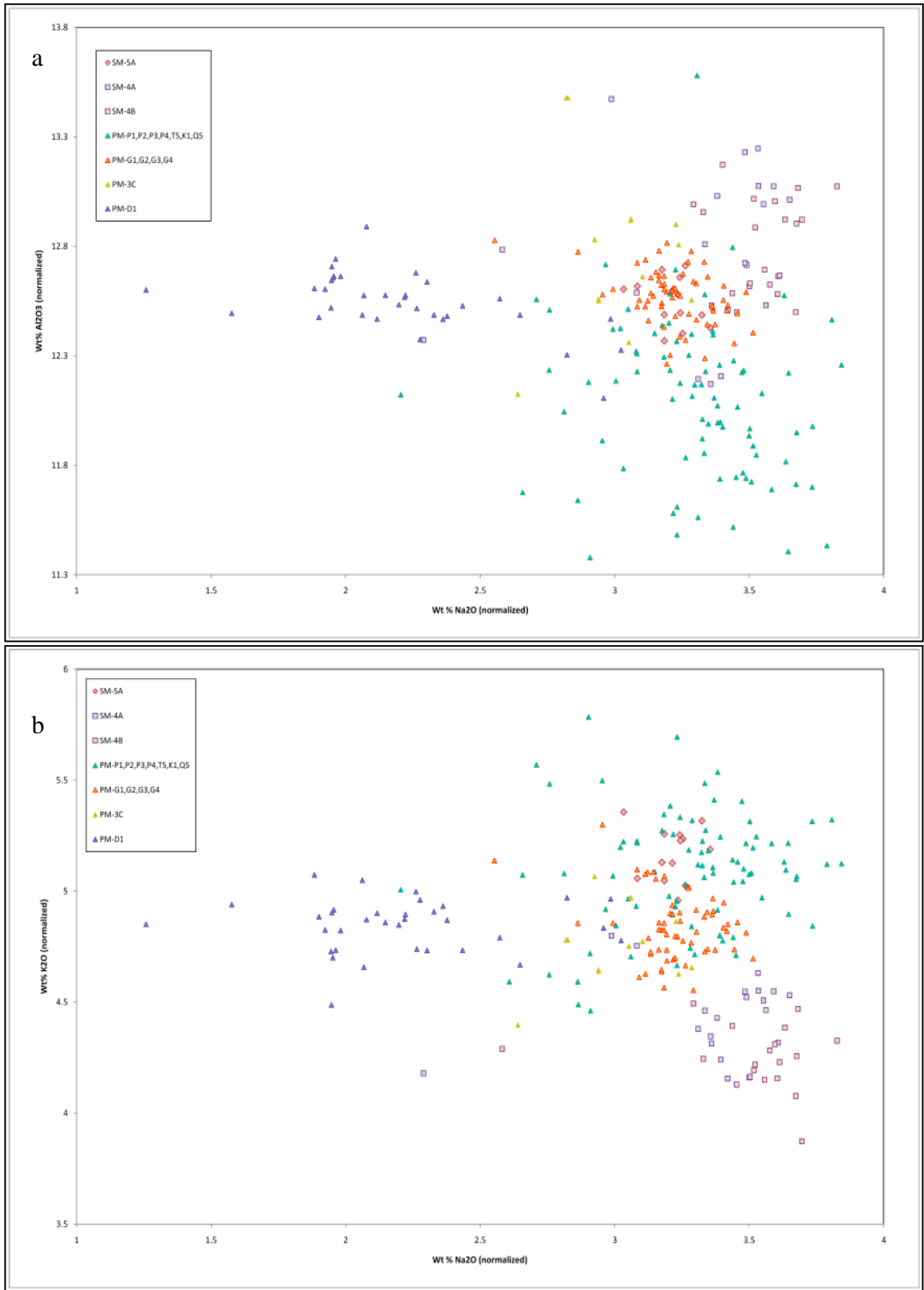


Fig. 4-5. Major element cross plots a) Na₂O-K₂O, b) Na₂O-Al₂O₃.

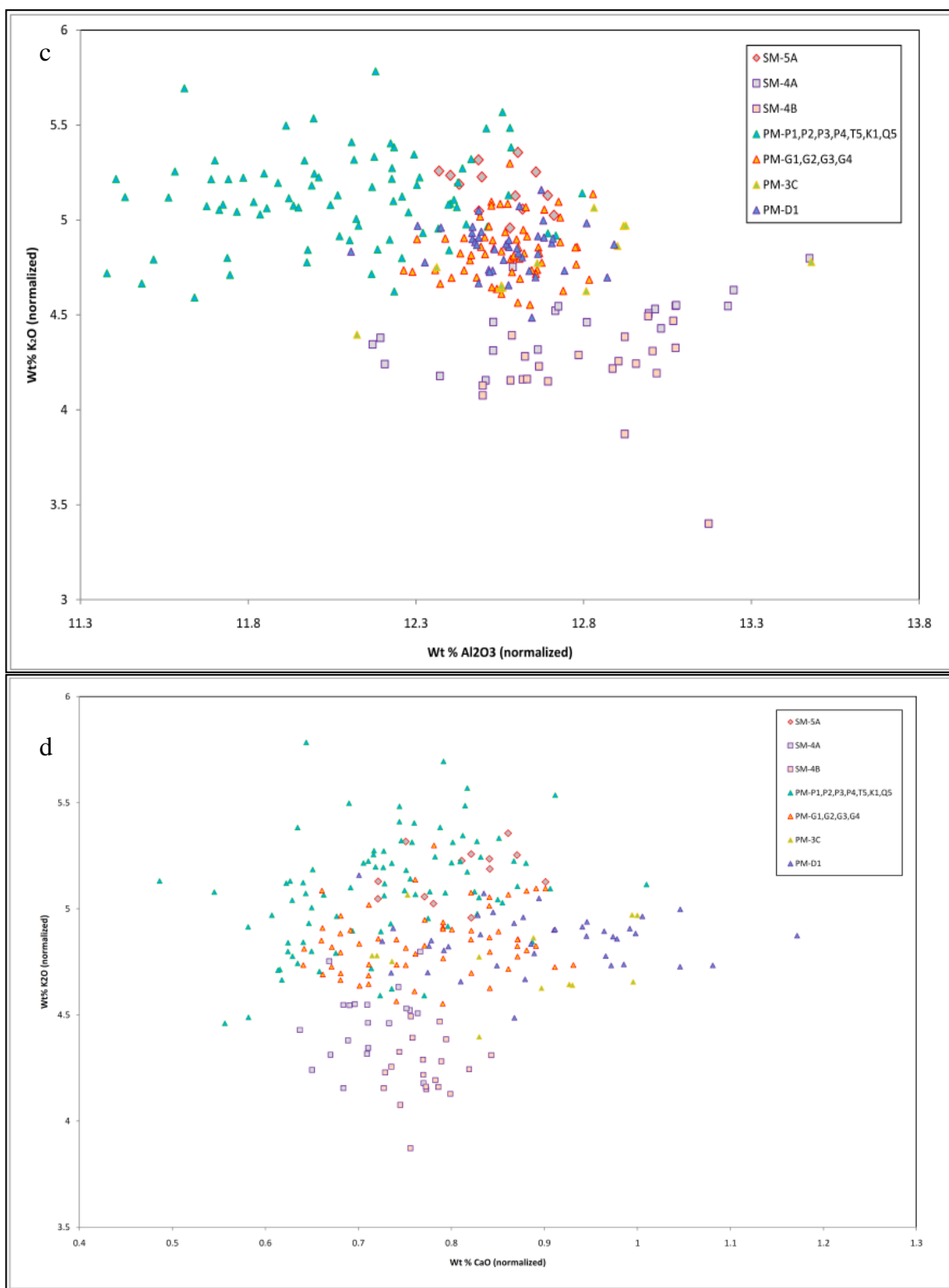


Fig. 4-5. Major element cross plots. c) CaO-K₂O, d) Al₂O₃-K₂O. Of the tephra from Peninsular Malaysia, the Kg. Dong and Kuala Kangsar samples were markedly different from the Gelok and Padang Sanai samples, which plot together with the proximal YTT ash from Sipisopiso. The Sianok Canyon tuff was distinctly different from the Peninsular Malaysia tephra and from the YTT, containing less K, and more Ca and Al.

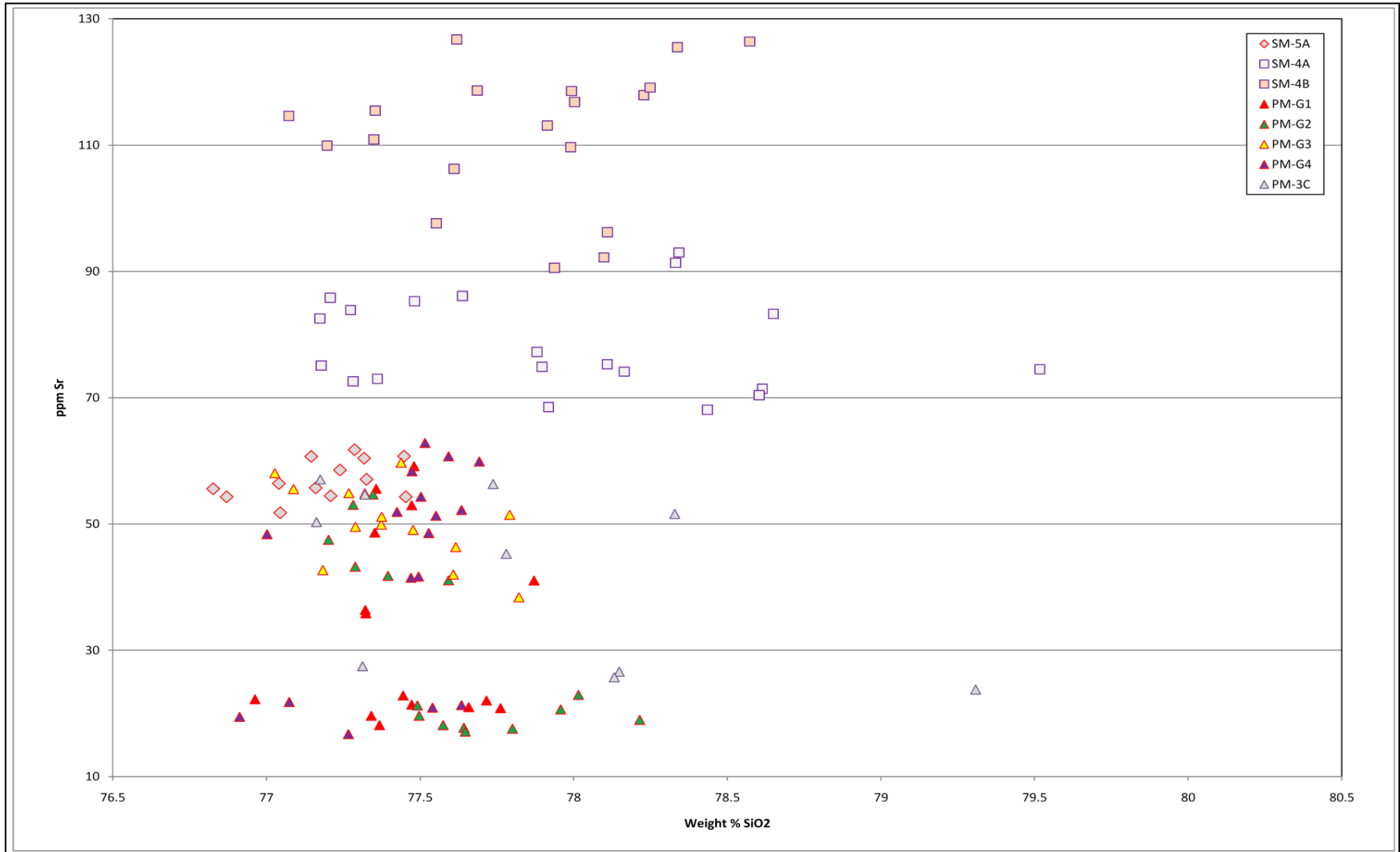


Fig 4-6: SiO₂ vs. Sr bivariate plot.

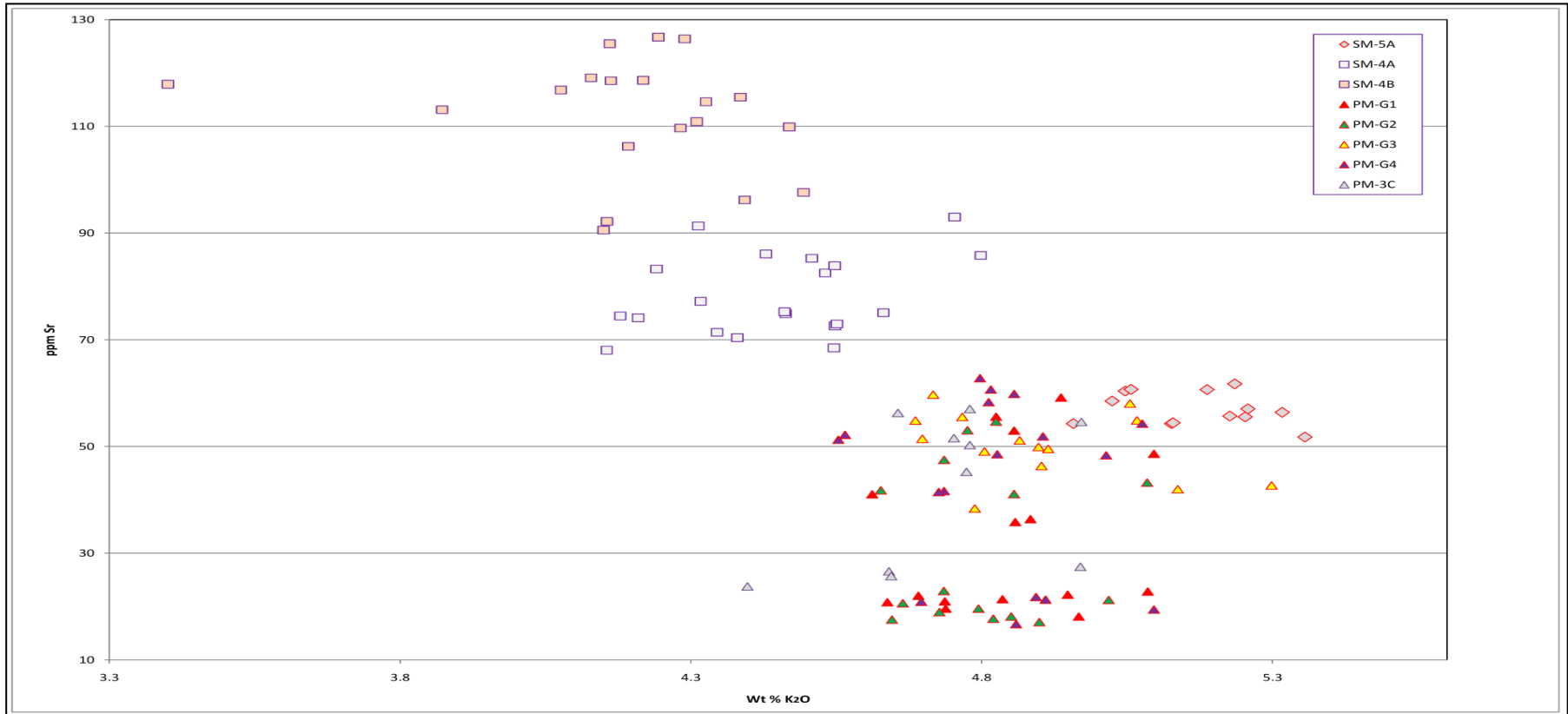


Fig 4-7: K₂O vs. Sr bivariate plot.

Here in figs. 4-6 and 4-7 it was abundantly clear that there could be no correlation between Sianok Canyon tuff and any of the Peninsular Malaysia occurrences of tephra analyzed for this study. Sianok tuff contained distinctly more Sr than does any of the tephra samples from the Peninsular Malaysia. Note that the two Sianok layers also plot differently, suggesting that additional fractional crystallization took place in the time between the two eruptions.

Based on over 700 analyses of glass shards from proximal YTT tuffs and distal YTT-derived tephra deposits from India, the Indian Ocean and Peninsular Malaysia, Westgate et al. (2013) found four distinct populations of glass shards, with contrasting concentration ranges of trace elements. This was best seen in a plot of Ba vs. Y (fig. 4-8). Not all populations are present at all locations.

The samples from Gelok and Padang Sanai plot within the range of compositions for Westgate's Populations I, II and III, a strong indication that these were distal ash derived from YTT. Population IV was missing at these locations. The one sample from Sipisopiso only contains shards belonging to Population III.

4.3.2 Modeling of fractional crystallization

Magmatic processes such as fractional crystallization could be modeled based on the partitioning of elements between melt and solid phases. Glass shard trace elements cross plots on logarithmic scales fig. 4-8 show linear trends. The linearity of these trends indicated that the dominant process controlling these trace element concentrations is fractional (Rayleigh) crystallization.

When plotted on logarithmic cross-plots for two elements the evolutionary path of the liquid will follow a straight line if fractional crystallization is taking place (Rollinson, 1993). This is because the concentration of an element in the liquid phase follows this equation:

(modified from Rollinson, 1993, eq. 4.18)

Where

$D = \text{Partition Coefficient} = C_l/C_s$

C_l = concentration of the element in the liquid

C_s = concentration of the element in the solid

C_o = initial concentration of the element before crystallization

X = Fraction crystallized

Glass shards are samples of the liquid existing at the time of eruption. The trace element crossplots of any given sample show a range of trace element concentrations, which means the liquid phase was locally inhomogeneous at the time of eruption. Such inhomogeneity could be caused by the short range influence of phenocrysts crystallizing within the melt. The melt closest to a given phenocryst would be the most depleted in elements compatible with the phenocryst (Pearce, pers. comm.), the degree to which this inhomogeneity is achieved would be a function of time vs. the rate of diffusion. Diffusion would be slower at lower temperatures or higher viscosities.

Westgate et al. (2013) has shown that proximal and distal YTT deposits contain four distinct shard populations, each displaying a distinct trace element range. Not all samples or all localities contain all four populations, for example, the proximal YTT tuff at Sipisopiso analyzed for this study only contained Population III, and the tuffs from Gelok and from Padang Sanai contain Populations I, II and III with the Gelok G3 layer only containing Populations II and III. On a Ba vs. Y cross plot, the populations appeared as elongated clusters, each with a distinct range of Ba values with little overlap. In contrast, the range of Y values is common to all populations. Westgate et al. (2013) stated that the most Ba-rich population (Population IV) was the least evolved, while the most Ba-poor (Population I) was the most evolved.

The existence of four discrete populations points to the existence of four separate reservoirs, each achieving its own level of magmatic evolution, with no chemical mixing between them. It has long been recognized that the contents of magma chambers

undergoing fractional crystallization can develop density-based stratification, and that instability-induced overturn and mixing induces eruptions (Kent et al., 2010). The sheer size of the magma chamber underlying Lake Toba, and the highly viscous nature of rhyolitic magmas would promote the formation of these domains, which reached different degrees of crystallization. The existence of shards belonging to more than one population in a given sample suggested simultaneous eruption of several reservoirs, and possible mechanical mixing without chemical homogenization before or during eruption. While the eruption of the YTT was seen as being geologically instantaneous, the presence of several horizons of ash at several locations suggested that the eruption might have taken place in stages that might perhaps have stretched out over months or even years. Each eruptive event might have tapped differing sets of reservoirs, resulting in the absence of one or more populations from a given tephra horizon.

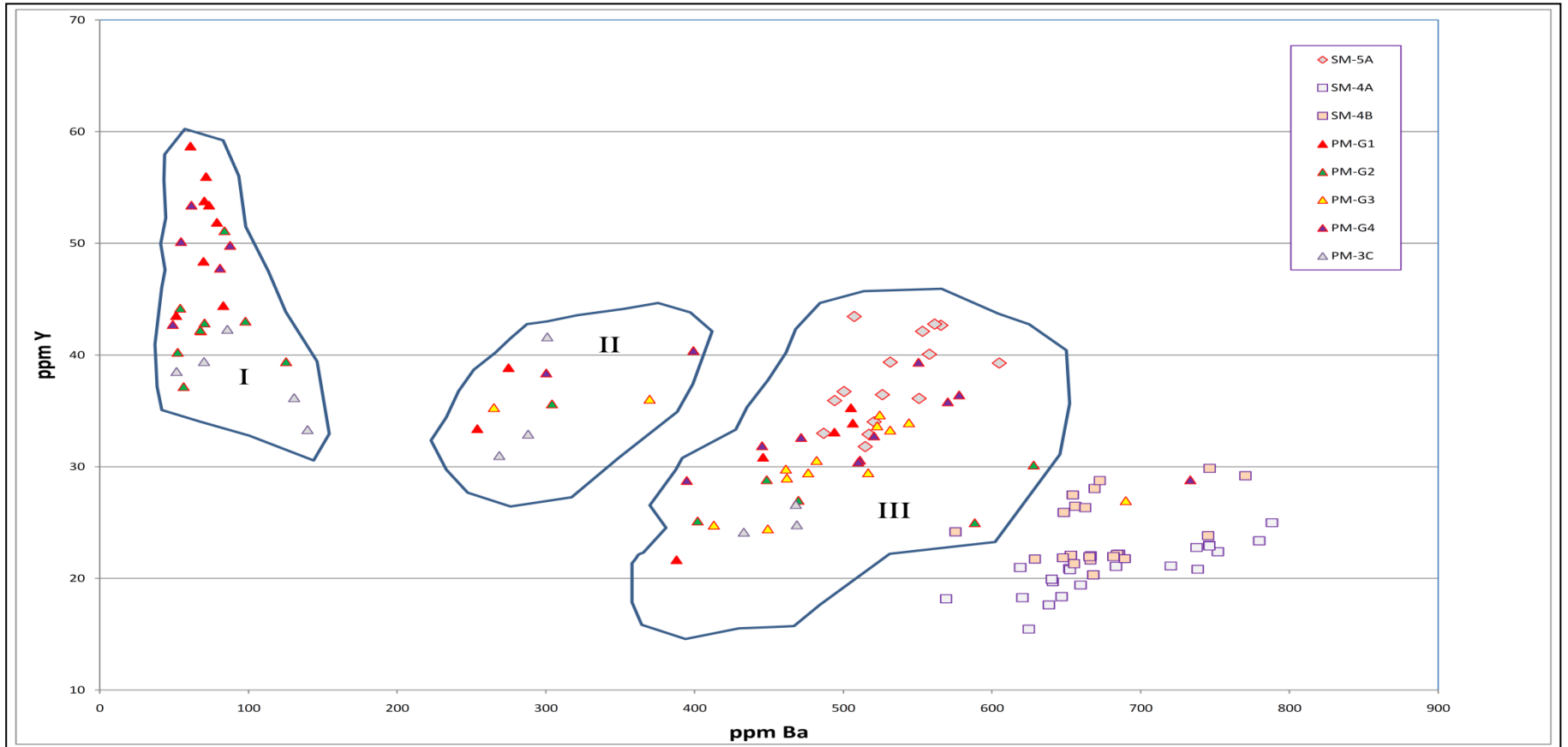


Fig. 4-8. Ba-Y bivariate linear plot: This plot revealed that Gelok (PM-G1,G2,G3,G4) and Padang Sanai (PM-3C) tephra fall within Populations I, II and III which is characteristic of YTT-derived ash (see Westgate et al. 2013). Population IV is missing, and should plot off-scale to the right (Ba > 1000ppm). Note that the PM-G3 layer from Gelok does not contain any Population I shards. Sianok Canyon tuffs (SM-4A and SM- 4B) fall between Populations III and IV.

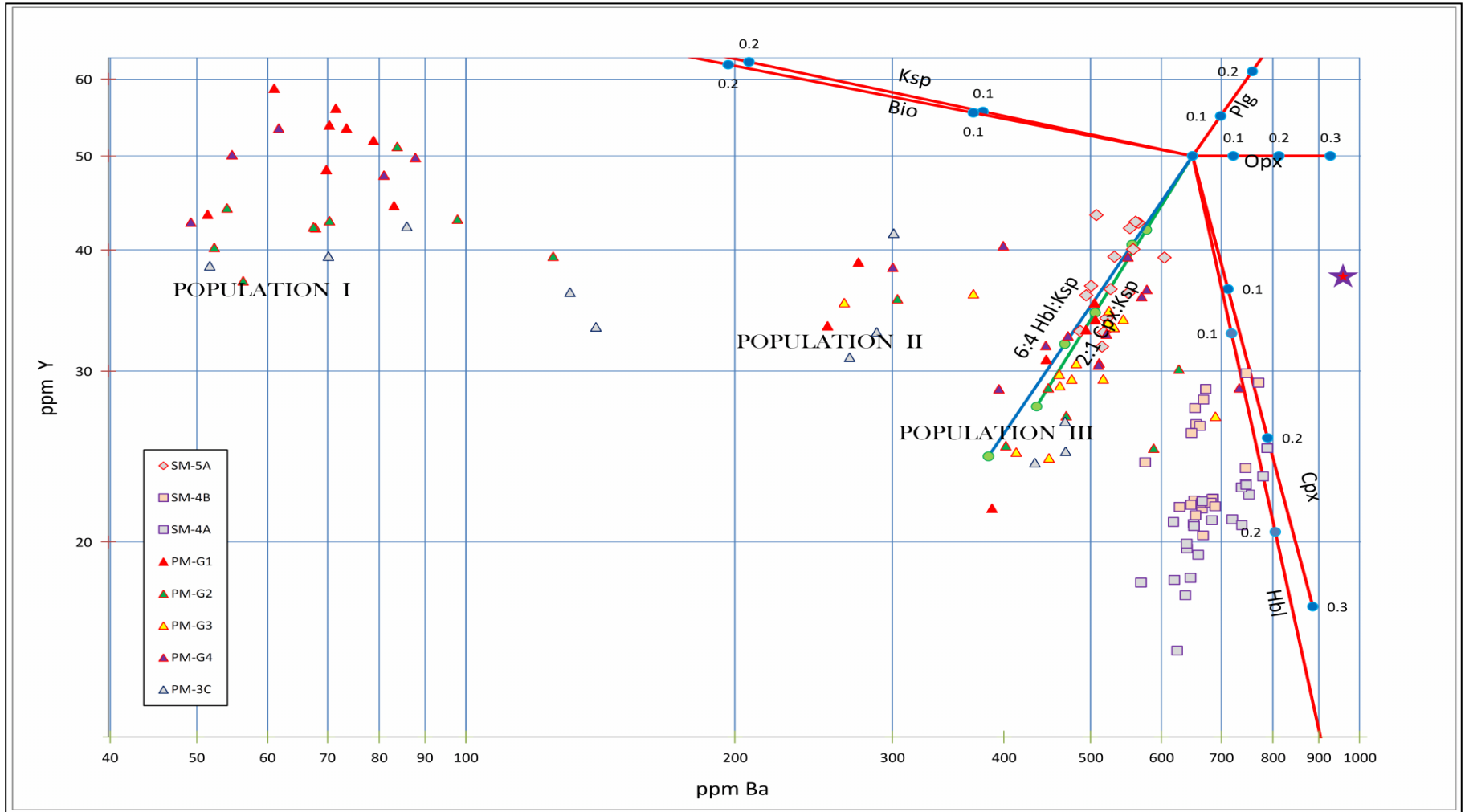


Fig. 4-9. Ba-Y bivariate log plot. Liquid line of descent vectors are superimposed on a plot of Ba vs. Y. Populations II and III show a negative correlation between Ba and Y, which corresponds to the fractional crystallization vector for a mixture of K-feldspar + Clinopyroxene or K-feldspar + hornblende.

These plots showed the populations described in Westgate (2013). Note that the Sipisopiso sample only plots in Population III. Gelok PM-G3 also was predominantly Population III. The other Gelok layers, and Padang Sanai, contain Populations I, II and III. Westgate's Population IV was missing. Implications: The presence of four populations indicated that fractional crystallization took place in two distinct stages. By the end of the first stage, which involved the crystallization of a Ba absorber (probably K-feldspar) the magma chamber had become segregated or stratified. The second stage acted on these separate domains, and involved both a Ba-absorber and a Y-absorber (garnet, allanite, monazite or apatite). The fact that populations are missing in certain layers (and in samples of the proximal tuff) indicate that the eruption tapped various domains or reservoirs within the magma chamber without mixing, perhaps at different times. The VEI8 eruption might have actually consisted of several smaller eruptions that took place over a matter of days, or months, or even years. These sub-eruptions might have tapped one or more unmixed reservoirs within the magma chamber, and temporal wind conditions would have governed whether the ash from that eruption would have been deposited within a locality.

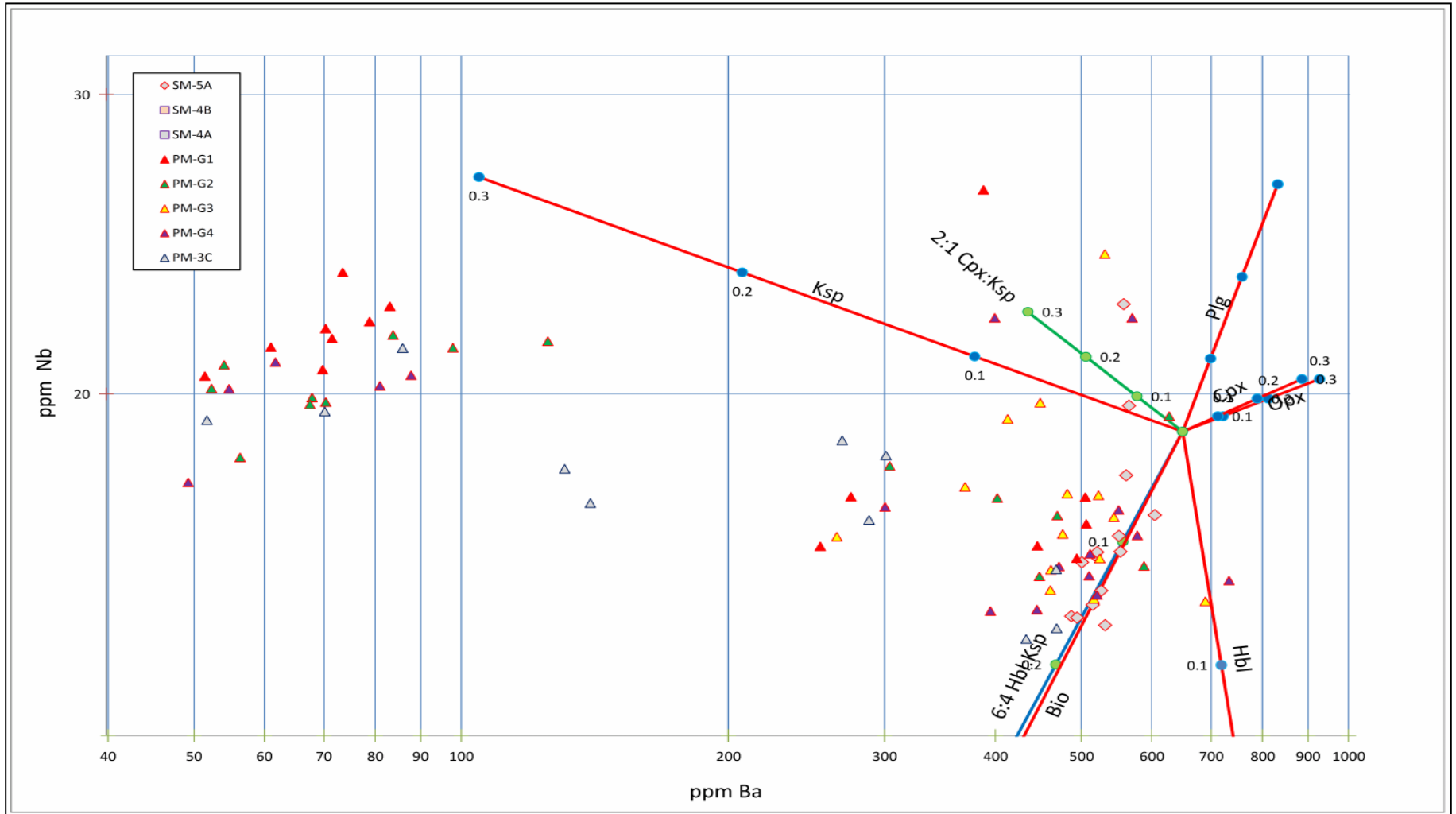


Fig. 4-10: Ba-Nb log plot. Ba concentrations plotted against Nb showed that the trends in Populations II and III follow the K-feldspar + hornblende vector (molar fractions 5:4) rather than the K-feldspar + clinopyroxene vector.

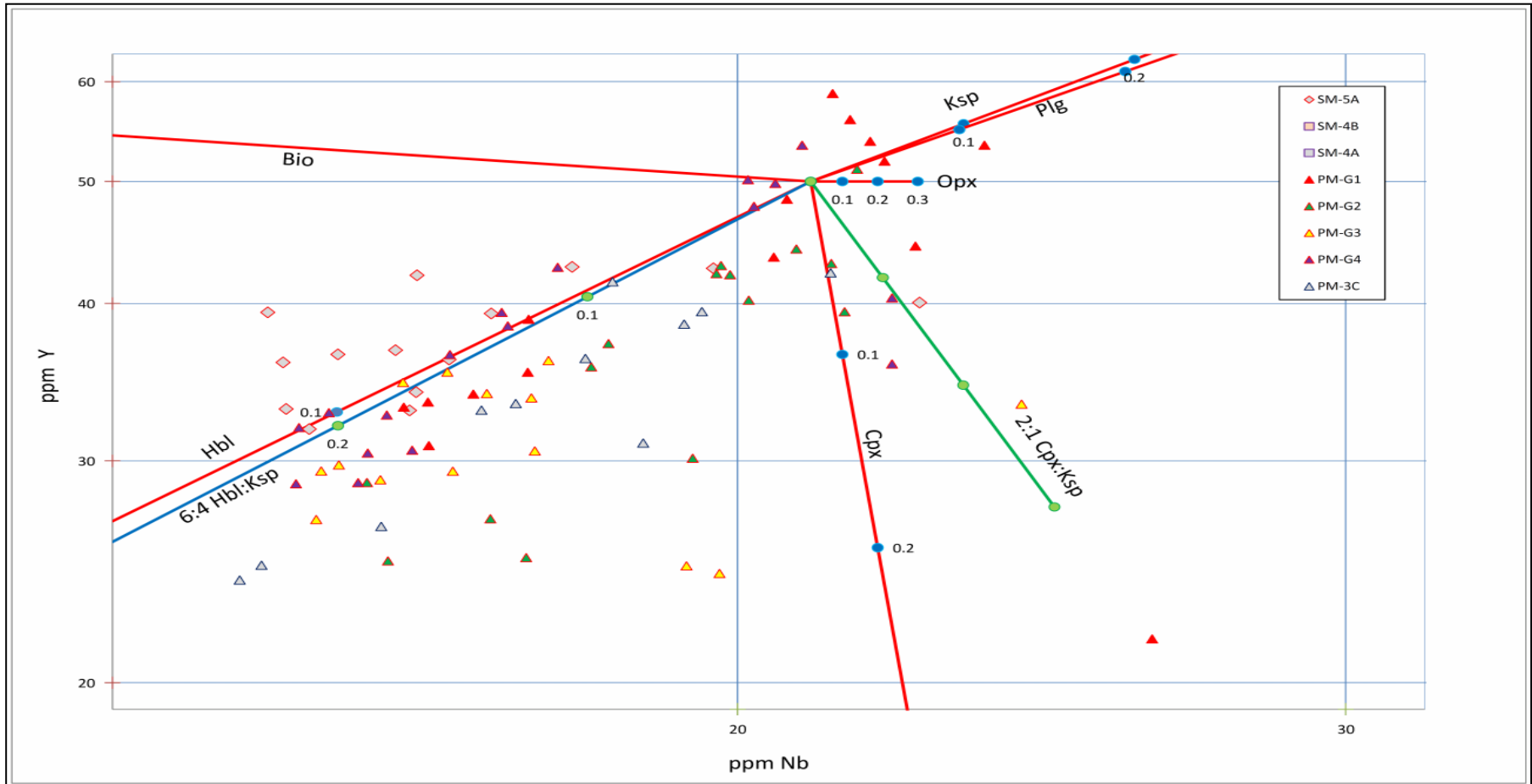


Fig. 4-11: Nb-Y log plot: Plotting Nb concentrations against Y further serves to illustrate that the second stage of fractional crystallization was dominated by K-feldspar + hornblende rather than K-feldspar + clinopyroxene. Since the K-feldspar and K-feldspar + hornblende vectors were sub-parallel (though in opposite directions), the data points for YTT-derived samples fall in a narrow band rather than spreading out vertically.

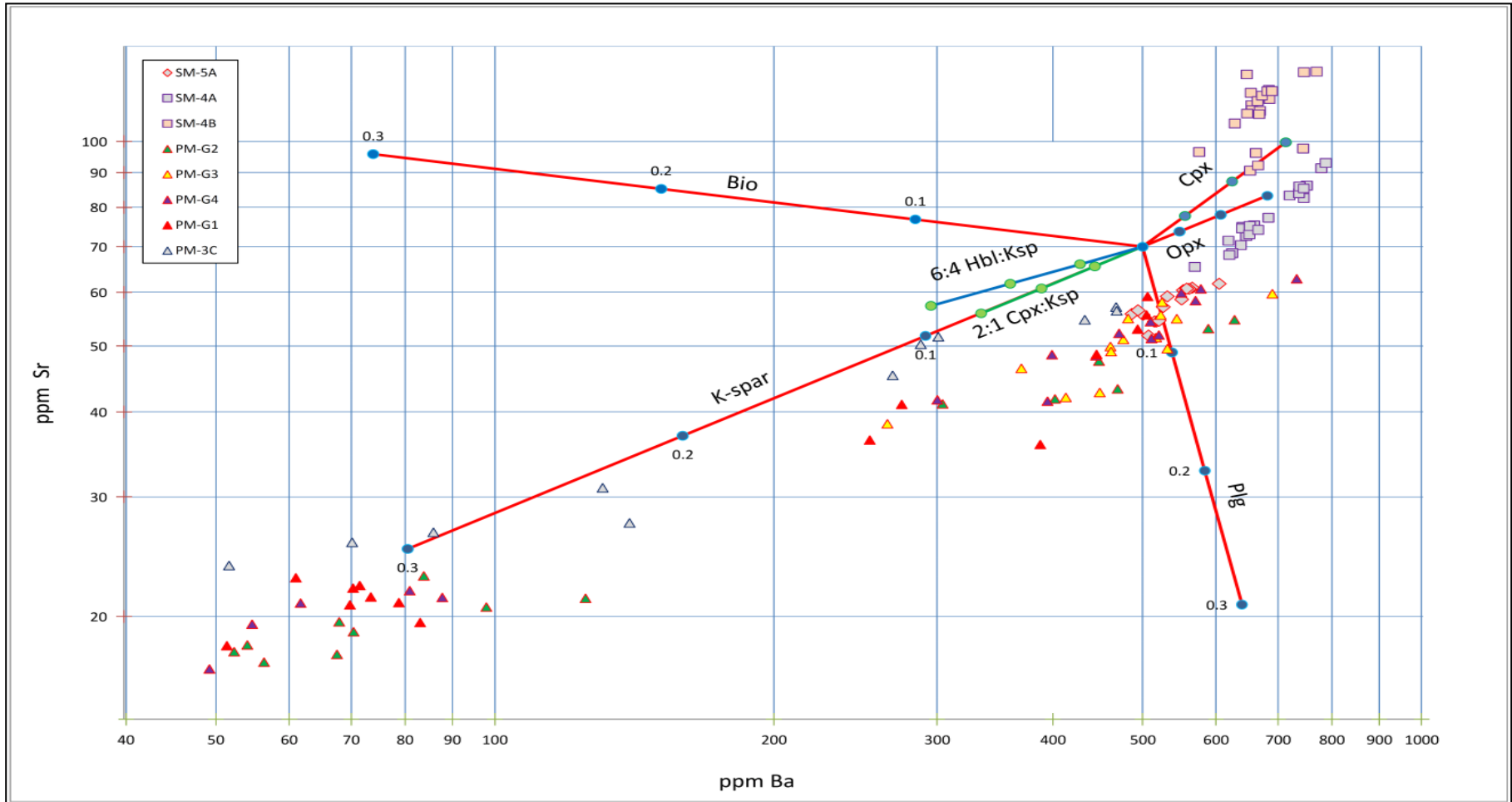


Fig. 4-12. Ba-Sr log plot. On a plot of Ba concentration against Sr, all tephra samples other than those from Sianok Canyon plot on one trend. Note that the proposed vectors for both stages of fractional crystallization are sub-parallel.

Since both Ba and Sr were absorbed by the crystallization of plagioclase, the data all plots linearly (decreasing Sr with decreasing Ba). Sianok SM-4A plots along the same trend, but SM-4B plots above it.

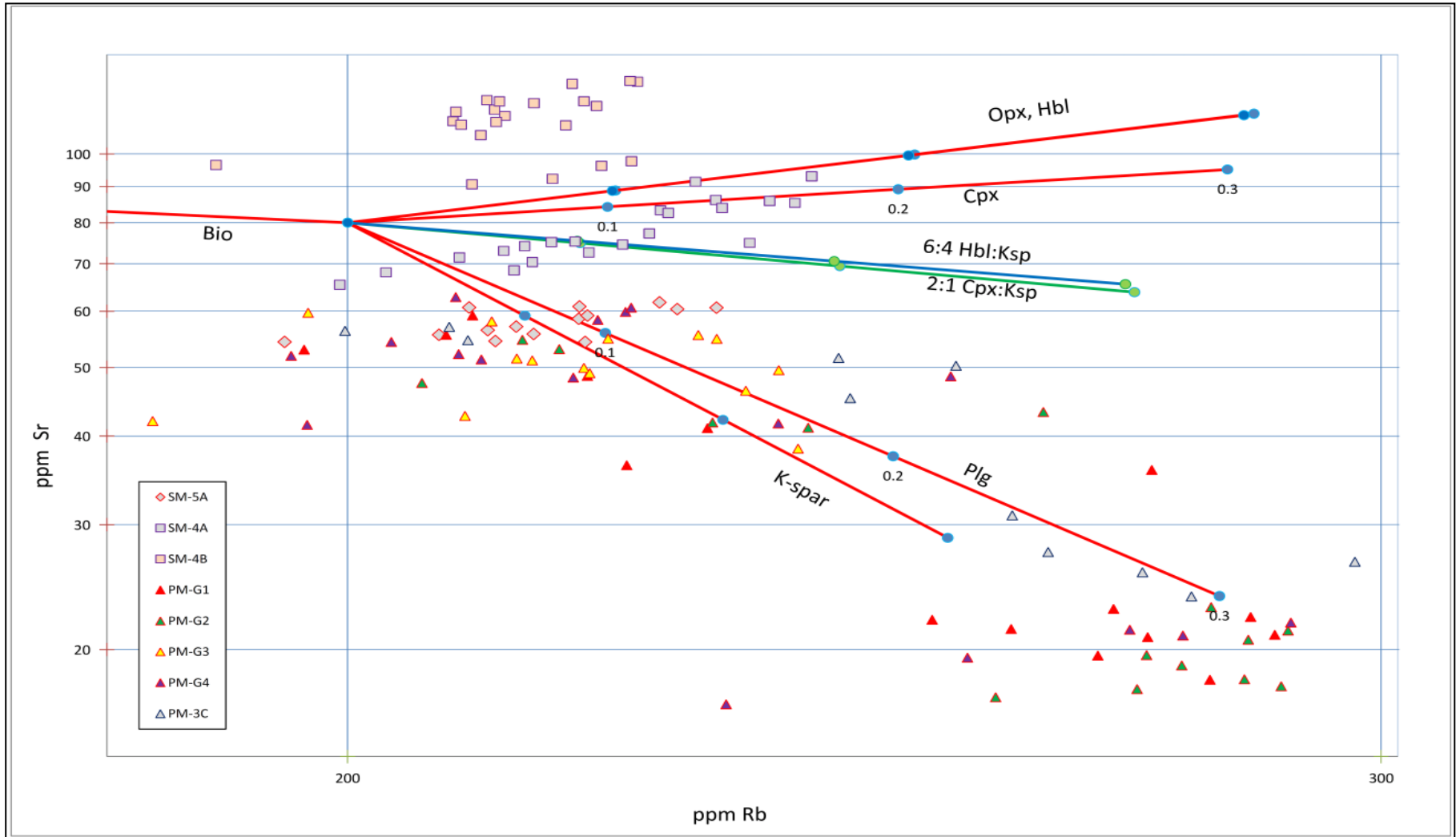


Fig. 4-13 Rb-Sr log plot: A plot of Rb concentrations vs. Sr illustrated the difference between the Sianok tuffs from the YTT derived tuffs and tephra.

The superimposed of the vectors for the proposed two stage fractional crystallization model onto the Ba-Y plot shown in fig 4-14.

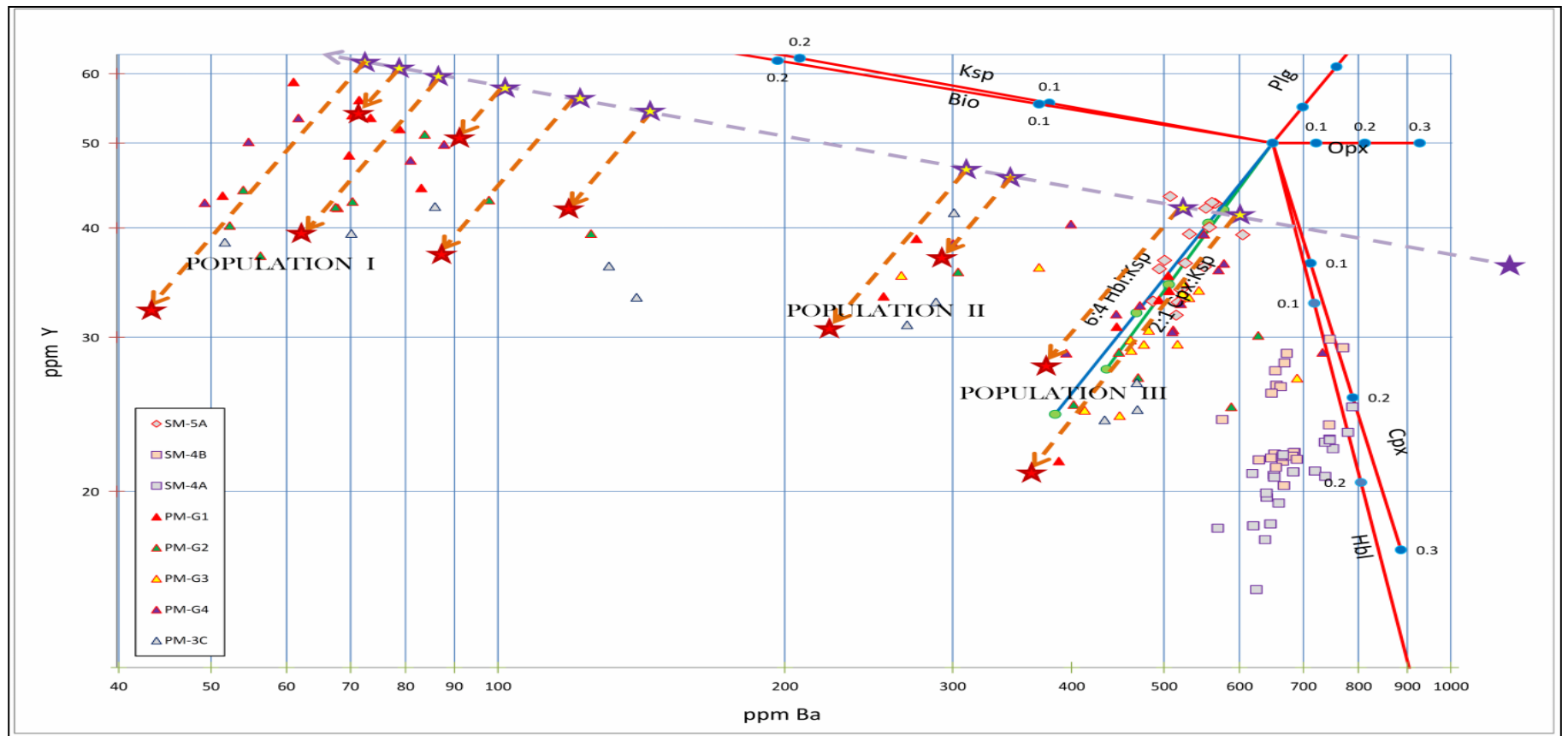


Fig. 4-14 Ba-Y log fin plot: The purple star (off the chart) represented the original, parent melt. It became separated into four or more distinct reservoirs (probably convecting layers or strata) within the magma chamber. All of these layers evolved through the fractional crystallization of K-feldspar (and possibly quartz) to different degrees, following the dashed purple arrow. The yellow stars represented the melt in each of the reservoirs when the second stage of fractional crystallization begins (which is not necessarily simultaneous across all reservoirs).

Note that Population I, being the most evolved, the most silica rich and the most viscous, was the most inhomogeneous of the reservoirs. The second stage of fractional crystallization began when hornblende begins to crystallize (orange dashed arrows). Since each population contains glass shards which have Y concentrations falling within a continuous range, we postulated that this second stage of differentiation was actually due to short-range diffusion effects in an unstirred melt, with the most Y-depleted shards representing glass closest to the crystallizing hornblende and the most Ba-depleted shards closest to crystallizing K-feldspar. The red stars represented the final composition of glass shards after both stages of differentiation. Since multiple populations were found within single layers of tephra, multiple reservoirs were tapped during eruption, with the resultant ash being a mixture of shards from different reservoirs.

Ba and Y (fig. 4-14) could be used to distinguish between the two different stages of fractional crystallization. The first stage involved the crystallization of K-feldspar, causing the differences between each of the reservoirs. Reservoir I, the most evolved, would be the most silicic, the most viscous and therefore the most inhomogeneous. The second stage would involve short-range effects of the crystallization of a mixture of minerals, the most likely being K-feldspar and hornblende (Hbl) or clinopyroxene (Cpx). It was not possible to differentiate between the effects of crystallization of clinopyroxene and hornblende on this plot because the partition coefficients of hornblende and clinopyroxene are very similar – both absorb Y while excluding Ba. The table of partition coefficients to model Rb-Sr, Ba-Sr, Ba-Y, Na-Y and Ba-Nb could be seen in table A2-4.

CHAPTER 5

“Do or do not, there is no try”
– Yoda.

5.0 CONCLUSION AND FUTURE WORK

A detailed study was conducted to diminish uncertainty that create controversy discrepancy on the origin and the age of distal tephra layers in Peninsular Malaysia. This study was motivated by the importance of tephra as time markers in the local Quaternary stratigraphy. A detailed mapping was carried out to acquire as much data as possible from the best location in Peninsular Malaysia with the most plentiful occurrences of tephra. This study provided evidence of widespread distribution of tephra in Lenggong compared to previous study, which has been neglected by local researchers since the discovery of Kota Tampan tephra in the 1930s. Ninety four tephra localities consisted of up to five layers of intercalation of fresh and reworked layers of tephra were reported. Kota Tampan area in Lenggong was believed to be located next to paleolake. The shore of the paleolake was believed to be about 70-75 m higher from current sea level (Zuraina, 1988). Reworked tephra that have been found in the area might have been deposited in the lacustrine depositional environment. This tephra deposits might be eroded from large landslide off Gunung Hong that obstructed Perak River during formation of Chenderoh Lake (Tjia, 1990). Lenggong was covered with plantations that that contributed to the preservation of fresh tephra.

Samples for dating determination have been selected from 4 m thick of fresh tephra in Lenggong, and also from the 9 m thick of Kuala Pelus fresh tephra to get the best prospect from Peninsular Malaysia tephra. Contradictory to previous finding, the results of

this analysis could be correlated with two major eruptions in Sumatra. The results of (PM-G2, PM-G4 and KP2) could be correlated with 52 k.a. Maninjau eruption, which was a new finding for tephra origins in Peninsular Malaysia. Result for KP1 was well correlated with the 75 k.a. YTT eruption. These tephra findings were useful for local and regional stratigraphy.

The major elements analysis was conducted on six main areas in Peninsular Malaysia. Samples were acquired from Padang Sanai - PM-3C which was located at Kedah, Gelok in Perak – (PM-G1, PM-G2, PM-G3 and PM-G4), Gua Badak (PM-B1 and PM-B2) and Bukit Sapi (PM-S1), Kuala Pelus in Perak – (PM-P1, PM-P2, PM-P3 and PM-P4), Kuala Kangsar in Perak – (PM-Q1 and PM-T1), and Kg. Dong in Pahang (PM-D1). The trace and rare earth elements analysis were conducted for PM-G1, PM-G2, PM-G3 and PM-G4 and PM-3C samples. A detailed geochemical analysis was conducted to identify glass shards populations due to crystal fractionation that shows three populations exist in Peninsular Malaysia tephra. The significance of this finding is to prove that major and trace elements can be a useful tool to distinguish tephra. Comparison of these signatures with the tephra units of unknown origin may be used to correlate them to specific eruptions. It was determined that using the major and trace element ratios of $\text{Na}_2\text{O}-\text{K}_2\text{O}$, Sr-Ba, $\text{Na}_2\text{O}-\text{Al}_2\text{O}_3$, $\text{CaO}-\text{K}_2\text{O}$, Ba-Y linear and log, Ba-Nb log, Nb-Y log, Ba-Sr log, Rb-Sr log and Ba/Y log plots were useful in separating eruptions that have similar overall trace element chemistry. The outcome from the geochemical analysis suggested that tephra from Kg. Dong and Kuala Kangsar could be originated from different sources compared to other Peninsular Malaysia tephra. Kg. Dong and Kuala Kangsar tephra Kg. Dong tephra consisted less K_2O whereas Kuala Kangsar consisted less Al_2O_3 (figs. 4-4 and 4-5). From the SiO_2 -Sr and K_2O -Sr plots, it was abundantly clear that no correlation between Sianok with any PM

tephra (figs. 4-6 and 4-7). Gelok samples consisted of PM-G1, PM-G2, PM-G3 and PM-G4 appeared to match very well with SM-5A Tuff (figs. 4-5 to 4-14).

In conclusion, this study proved trace elements could be used to correlate between the undifferentiated tephra with the tephra of known eruptions. Data from other studies could be used and plotted with data from this study e.g., studies on tephra recovered from the Indian Ocean. This study provided widespread and important stratigraphic marker in understanding Late Pleistocene paleoenvironments of Lenggong area. This research would also contribute to Peninsular Malaysia Pleistocene stratigraphy details. By publishing tephra dating results and geochemical data, tephras in Peninsular Malaysia would be differentiated, and, subsequently, this study would benefit the establishment of the time marker in the stratigraphy for the Late Pleistocene of Peninsular Malaysia region.

One major hindrance to this study was the lack of Kg. Dong, Kuala Kangsar and Kuala Pelus REE and trace element data that would provide more information on Peninsular Malaysia geochemistry. The trace and major elements were treated separately, even though there was a big effort made to analyze particular glass shards for both major and trace elements. More cross plots could have made of major vs trace elements, e.g., SiO_2 -Yb or SiO_2 -Sr and more data could have been used for geochemical modelling. Future work should include a detailed examination on glass shards morphology e.g., grain size and shapes study or possibly more dates from other localities in Peninsular Malaysia. More detailed study would provide better understanding about the origin of Peninsular Malaysia tephra.

BIBLIOGRAPHY

- Abdul Latiff, R., 1994. Geologi Am Kawasan Lenggong-Lawin, Perak. Unpublished BSc. Thesis, University of Malaya.
- Aksu, A.E., Jenner, G.; Hiscott, R.N.; Isler, E. B., 2008, Occurrence, Stratigraphy and Geochemistry of Late Quaternary Tephra Layers in the Aegean Sea and the Marmara Sea, *Marine Geology*, v. **252**: 174-192.
- Alexander, J. B., 1968. The Geology and mineral resources of the neighbourhood of Bentong, Pahang and adjoining portions of Selangor and N. Sembilan. *Memoir Geol. Surv. Dept. West Malaysia*. No. 8.
- Alloway, B.V., Pribadib, A., Westgate, J.A., Birdd, M., Fifielde, L.K., Hogg, A., and Smith, I., 2004. Correspondence Between Glass-FT and ¹⁴C Ages of Silicic Pyroclastic Flow Deposits Sourced from Maninjau Caldera, West-Central Sumatra. *Earth and Planetary Science Letters*, v. **22**: 121-133.
- Arth J. G. (1976) Behavior of trace elements during magmatic processes – a summary of theoretical models and their applications. *J. Res. U.S. Geol. Survey*, v. **4**, 41-47.
- Basir Jasin, Ahmad Jantan, Ibrahim Abdullah, Uyop Said, 1987. Tephra Beds at Kg. Temong, Kuala Kangsar, Perak. *Warta Geologi*, v. **13**, No. 5, 205-211.
- Bellivier, O., Bellon, H., Sebrier, M., Sutanto, and Maury, R., 1999, K-Ar age of the Ranau Tuffs: Implications for the Ranau Caldera Emplacement and Split Partitioning in Sumatra, *Tectonophysics*, v. **312**, 347-359.
- Bennett, J. D., McC, D., Bridge, Cameron, N. R., Djunuddin, A., Ghazali, S. A., Jeffrey, D. H., Kartawa, W., Keats, W., Rock, N. M. S., Thomson, S. J. and Whandoyo, R. (1981) “ Geologic map of the Banda Aceh Quadrangle, Sumatra”. Geol. Res. And Dev. Cent., Bandung Indonesia.
- Chesner, C. A.: The Toba Caldera Complex, *Quaternary Int.*, v. **258**, 5–18, doi:10.1016/j.quaint.2011.09.025, 2012.
- Chesner, C. A., Westgate, J.A., Rose, W.I., Drake, R., Deino, A., 1991. Eruptive History of Earth's Largest Quaternary Caldera (Toba, Indonesia) Clarified, *Geology*, v. **19**, 200-203.
- Chesner, C. A., and Rose, W. I. 1991. Stratigraphy Of The Toba-Tuffs And The Evolution of The Toba-Caldera Complex, Sumatra, Indonesia. *Bulletin Of Volcanology* v. **53** (5): 343-356.
- Clift, P.D. and Fitton J.D., 1998. Trace and Rare Earth Element Chemistry of Volcanic Ashes from sites 918 and 919: Implications for Icelandic Volcanism. *Proceedings of the Ocean Drilling Program, Scientific Results*, v. **152**, 67-84.
- Debaveye, J., Dapper, M.D., Paepe, P.D., Gijbels, R., 1986. Quaternary Tephra Deposits in The Padang Terap District, Kedah, Peninsular Malaysia. *Geosea V Proceedings Vol. I, Geol. Soc. Malaysia, Bulletin* **19**, 533-549.
- Dehn, J., Farrel, J.W., and Schmincke, H.U. 1991. Neogene tephrochronology from site 758 on Ninety East ridge: Indonesian arc volcanism of the past 5 Ma. *Proceedings of the Ocean Drilling Program, Scientific Results* v. **121**, 273-295.
- Eastwood, W. J., N. J. G. Pearce, J. A. Westgate, W. T. Perkins, H. F. Lamb, and N. Roberts (1999), Geochemistry of Santorini tephra in lake sediments from southwest Turkey, *Global Planet. Change*, v. **21**: 17 – 29.
- Froggatt, P. C, 1983. Toward a comprehensive Upper Quaternary tephra and ignimbrite stratigraphy in New Zealand using electron microprobe analysis of glass shards. *Quat. Res.*, v. **19**, 188-200.

- Gafoer, S., Amin, T.C. & Pardede, R. 1993. Peta Geologi Lembar Baturaja, Sumatera (Geological Map of Baturaja Sheet, Sumatra). Pusat Penelitian dan Pengembangan Geologi, Bandung, Scale 1 : 250 000.
- Garson, G.D., 2012. Cluster analysis. Asheboro, NC: Statistical Associates Publishers.
- Garver, J.I., 2008, Fission-track dating. V. Gornitz, (Ed.), Encyclopedia of Earth Science Series, Kluwer Academic Press, 247-249.
- Hanan, M. A., Totten, M.W, Hanan, B.B., Kratochovil, T., 1998. Improved Regional Ties to Global Geochronology Using Pb-Isotope Signatures of Volcanic Glass Shards from Deep Water Gulf of Mexico Ash Beds: *Gulf Coast Association of Geological Societies Transactions*, v. **48**, 95-106.
- Henderson, P., 1996. The rare earth elements: introduction and review. New York, Chapman and Hall, 1-19.
- Huber, H., Koeberl, C. and Egger, H., 2003. Geochemical study of lower Eocene volcanic ash layers from the Alpine Anthering Formation, Austria. *Geochemical Journal*, v. **37**, 123-134.
- Hunt, J.B. and Hill. P. G (1993) Tephra geochemistry: a discussion of some persistent analytical problems. *The Holocene*, v. **3**: 271-278.
- Ishizaka, K. and Yanagi, A., 1980. Sr Isotopic Composition of Toba Rhyolitic Ignimbrite and Tuff. *Phys. Geol. Indonesian island Arcs*, 154-164.
- Jansen, W.; Slaughter, M. (1982). Elemental mapping of minerals by electron microprobe. *American Mineralogist*, v. **67** (5-6): 521-533.
- Kastowo, Leo, G.W., Gafoer, S., & Amin, T.C., 1996. Peta Geologi Lembar Padang, Sumatra Barat (Geological map of Padang Sheet, West Sumatra). Pusat Penelitian dan Pengembangan Geologi, Bandung, Scale 1: 250 000.
- Kent A.J.R., Darr C., Koleszar A.M., Salisbury M.J. and Cooper K.M. (2010) Preferential eruption of andesitic magmas through recharge filtering. *Nature Geoscience* v. **3**, 631-636.
- Knott, J.R., Sarna-Wojcicki, A. M., Montañez, I.P., Wan, E., 2007, Differentiating the Bishop ash bed and related tephra layers by elemental-based similarity coefficients of volcanic glass shards using solution inductively coupled plasma-mass spectrometry: *Quaternary International*, v. **166**: 79 – 86.
- Krukowski, S.T., 1988. Sodium metatungstate: a new heavy mineral separation medium for extraction of conodonts from insoluble residues: *Journal of Paleontology*, v. **62**, no. 2, 314-316.
- Kuehn, S.C. and Froese, D.G., 2010, Tephra from ice – A simple method to routinely mount, polish, and quantitatively analyze sparse fine particles: *Microscopy and Microanalysis*.
- Kuehn, C. Stephen., Froese, D.G., Carrara, P.E., Foit, F.F., Pearce, N.J.G., Rotheisler P., 2009. Major- and Trace-Element Characterization, expanded Distribution, and a new Chronology for the latest Pleistocene Glacier Peak tephra in western North America. *Quaternary Research* v. **71**, 201-216.
- Le Maitre R.W., Bateman P., Dudek A., Keller J., Lameyre Le Bas M.J., Sabine P.A., Schmid R., Sorensen H., Streckeisen A., Wooley A.R. and Zanettin B. (1989). A classification of igneous rocks and glossary of terms . Blackwell, Oxford.
- Liritzis, I. and Laskaris, N., (2011). A new mathematical approximation of sunlight attenuation in rocks for surface luminescence dating. *J. of Luminescence*, v. **131**, 1874- 1884.
- Lowe, D.J., 2011. Tephrochronology and its application: a review. *Quaternary Geochronology* v. **6**, 107-153.

- Machida, H. 2002. Quaternary Volcanoes and Widespread Tephra of the World. v. **6**; No. 2, 3-17.
- Ninkovich, D., Shackleton, N.J., Abdel-Monem, A.A., Obradovich, J.D., Izett, G., 1978, K–Ar age of the late Pleistocene eruption of Toba, north Sumatra. *Nature* v. **276**: 574–577.
- Ninkovich, D., Sparks, R., and Ledbetter, M. 1978b. The exceptional magnitude and intensity of the Toba eruption, Sumatra: An example of the use of deep-sea tephra layers as a geological tool. *Bulletin of Volcanology* v. **41** (3): 286-298.
- Nishimura, S. and Stauffer, P. H., 1981. Fission-Track of Zircons from the Serdang Tephra, Peninsular Malaysia. *Warta Geologi*, v. **7**, No. 2, 39-41.
- Nishimura, S., Ikeda, T. and Ishizaka, K., 1980. Geochemistry in Volcanic Rocks of Krakatau, Indonesia. *Phys. Geol. Indonesian Island Arc*, 109- 113.
- Nishimura, S., Thio, K. H. and Hehuwat, F., 1980. Fission-Track Ages of Tephra and Tuffs from Bayat and Karansambung, Central Jawa, *Phys. Geol. Indonesian Arcs*, 81-87.
- Norddhal, H. and Haflidason, H. 1992. The Skogar Tephra, a younger Dryas marker in North Iceland. *Boreas*, v. **21**: 23-41.
- Pattan, J. N., Pearce N. J. G., Banakar, V. K. and Parthiban G., 2002, Origin of Tephra in the Central Indian Ocean Basin and its Implications for the Volume Estimate of the 74,000 Year BP Youngest Toba Eruption. *Current Science*, v. **83**, No. 7, 889-893.
- Pearce, N. J. G., Bendall, C. A., and Westgate, J. A. 2008a. Comment on "Some numerical considerations in the geochemical analysis of distal microtephra" by A.M. Pollard, S.P.E. Blockley and C.S. Lane. *Applied Geochemistry* 23 (5): 1353-1364.
- Pearce, N.J.G., Westgate, J.A., Perkins, W.T., Preece, S.J., 2004, The application of ICP-MS Methods to Tephrochronological problems: *Applied Geochemistry*, v. **19**, 289-322.
- Pearce, N.J.G., Westgate, J. A, Perkins, W. T., 1995, Developments in the Analysis of Volcanic Glass Shards by Laser Ablation ICP-MS: Quantitative and Single Internal Standard-Multi Element Methods. *Quaternary International*, v. **34-36**: 213-227.
- Pearce, J.A., 1983, The Role of Sub-Continental Lithosphere in Magma Genesis at Active Continental Margins, in Hawkesworth, C.J., and Norry, M.J., eds., *Continental Basalts and Mantle Xenoliths*. Nantwich, United Kingdom, *Shiva*, 230-249.
- Pearce J.A. and Norry M.J. (1979) Petrogenetic implications of Ti, Zr, Y and Nb variations in volcanic rocks. *Contrib. Mineral. Petrol.* v. **69**, 33-47.
- Pillay, A. E., 2001. Analysis of archaeological artifacts: PIXE, XRF or ICP-MS? *Journal of Radioanalytical and Nuclear Chemistry*, v. **247**, No. 3, 593-595.
- Purbo-Hadiwidjono, M.M.; M.L. Sjachrudin, S. Suparka (1979). "The volcano–tectonic history of the Maninjau caldera, western Sumatra, Indonesia". *Geol. Mijnb* (**58**): Pages 193–200.
- Rollinson, H.R., 1993, Using geochemical data: evaluation, presentation, interpretation: England, Pearson Education Limited, 352.
- Rose, W.I., and Chesner, C.A., 1987, Dispersal of ash in the great Toba eruption, 75 ka, *Geology*, v. **15**: 913-917.
- Ruslan, Z. H, 2008. Characterization of Late Pleistocene Volcanic Ash at Lenggong, Perak. Unpublished B.Sc. Thesis, University of Malaya.

- Sarna-Wojcicki, A. M., 2000, Tephrochronology, in Noller, J. S., Sowers, J. M., and Lettis, W. R., eds., *Quaternary Geochronology: Methods and Applications*: Washington, D.C., *American Geophysical Union*, 357-377.
- Saunders, A.D., 1998. Trace and REE chemistry of Volcanic Ashes from Sites 918 and 919: Implications of Icelandic, *Proceedings of the Ocean Drilling Program, Scientific Results*, v. **152**.
- Savage N.M., 1988. The use of sodium polytungstate for conodont separations: *Journal of Micropaleontology*, v. **7**, No. 1, 39-40.
- Scrivenor, J. B. 1930. A recent rhyolite-ash with sponge-spicules and diatoms in Malaya. *Geological Magazine* 67 (9): 385-393.
- Scrivenor, J. B. 1931. The Geology of Malaya. London, Macmillan. 52-101.
- Shane, P.A.R., 2000. Tephrochronology: A New Zealand case study, *Earth-Science Reviews*, v. **49**: 223-259.
- Simkin, T. & Siebert, L. 1994. *Volcanoes of the World*, Geoscience Press, Tucson, Arizona, 349.
- Stauffer, P.H., Nishimura, S. & Batchelor, B.C., 1980. Volcanic ash in Malaya from catastrophic eruption of Toba, Sumatra, 30,000 years ago. In: Nishimura, S. (ed.) *Physical Geology of Indonesian Island Arcs*. Kyoto University, 156-164.
- Stauffer, P. H and Batchelor, B., 1978, Quaternary Tephra and Associated Sediments at Serdang, Selangor. *Warta Geologi*, v. **4**, No. 1, 7-10.
- Stauffer, P. H and Batchelor, B., 1973, Late Pleistocene Age Indicated for Tephra in West Malaysia. *Geol. Soc. Malaysia Newsletter* No. 40, 1-4.
- Storey, M., Roberts, R.G., Saidin, M., 2012. Astronomically calibrated $^{40}\text{Ar}/^{39}\text{Ar}$ age for the Toba supereruption and global synchronization of late Quaternary records, *PNAS*, v. **109**, No. 46, 18684–18688.
- Sun, S.S. and McDonough, W.F., 1989. Chemical and Isotopic Systematics of oceanic basalts: implications for Mantle Composition and Processes. *Spec. Publ. Vol. Geol. Soc. Lond.* , No. 42, 313-345.
- Sun, S.S., 1980. Lead isotopic study of young volcanic rocks from mid-ocean ridges, ocean islands and island arcs. *Phil. Trans. R. Soc. London* v. **297**: 409-446.
- Taylor, J.R., 1982. *An Introduction to Error Analysis*. Mill Valley, California, University Science Book, 270.
- Tjia, H.D. and Muhammad, Ros Fatimah, 2008. Blast from the Past Impacting on Peninsular Malaysia. *Geol. Soc. Of Malaysia, Bulletin* **54**: 97- 102.
- Tjia, H.D., 1976. Enapan Gunungapi Muda di Trengganu. *Warta Geologi*, v. **2**, No. 6, 121-123.
- Ukstins Peate, I., Kent, A.J.R., Baker, J.A. and Menzies, M.A., 2008. Extreme geochemical heterogeneity in Afro-Arabian Oligocene tephra: Preserving fractional crystallization and mafic recharge processes in silicic magma chambers. *Lithos*, v. **102**: 260-278.
- Van Bemmelen, R. W. 1970. The Geology of Indonesia. In "General Geology of Indonesia and Adjacent Archipelagos 1A (second ed.)." *M. Nijhoff (Eds.)*, The Hague, 732.
- Ward, P.A. III, Carter, B.J., and Weaver, B., 1993, Volcanic ashes; time markers in soil parent materials of the Southern Plains: *Soil Science Society of America Journal*, v. **57**, no. 2, 453-460.
- Westgate, J.A., N.J.G. Pearce, W.T. Perkins, S.J. Preece, C.A. Chesner and R.F. Muhammad, 2013. Tephrochronology of the Toba tuffs: four primary glass populations define the 75 ka Youngest Toba Tuff, northern Sumatra, Indonesia, *Quaternary Science*, v. **28**. p. 772-776.

- Westgate, J.A., Philip A.R.S., Nicholas J.G.P, William T.P., Ravi Korisettar, Chesner, C.A., Martin A.J.W, and Acharyya, S.K., 1998. All Toba Tephra Occurrences Across Peninsular India Belong to the 75,000 B. P. Eruption. *Quaternary Research* v. **50**: 107-112.
- Westgate, J.A., Perkins, W.T., Fuge, R., Pearce, N.J.G. , Wintle, A.G., 1994. Trace element analysis of volcanic glass shards by LA-ICP-MS: application to tephrochronological studies, *Applied Geochemistry* v. **9**: 323-335.
- Westgate, J.A., Gordon, M.P., 1981. Correlation techniques in tephra studies. Publishing Company, Dordrecht, 73–94.
- Wintle AG, 2008. Luminescence dating: where it has been and where it is going. *Boreas* **37**(4): 471-482.
- Wohlfarth, B., Bjorck, S., Possnert, G. Lemdahl, G. Brunnberg, L., Ising, J., Olsson, S. and Svensson, N.O., 1993. AMS dating Swedish varved clays of the last glacial/interglacial transition and potential/difficulties of calibrating Late Weichselian ‘absolute’ chronologies. *Boreas*, v. **22**, 113-128.
- Zuraina, M. and Tjia, H. D., 1988. The Geological and Archaeological Evidence for a Late Pleistocene Site, Kota Tampan, Perak, The *Journal of Malaysian Branch of the Royal Asiatic Society*, v. **61**.

APPENDIX I

Table A1-1. Glass fission-track ages of tephra beds from the Gelok and Serdang localities, Peninsular Malaysia.

Sample number	Date irradiated	Spontaneous track density t/cm^2	Corrected Spontaneous track density t/cm^2	Induced track density $10^5 t/cm^2$	Track density on muscovite detector over dosimeter glass $10^5 t/cm^2$	Etching conditions HF:temp:time %: °C: s	D_s μm	D_i μm	D_s/D_i or $D_i/D_s\#$	Age ($\pm 1\sigma$) ka
Gelok 2*	11/02/2010	112.02 \pm 1.08 (108)		2.86 \pm 0.02 (42870)	3.75 \pm 0.03 (14393)	24: 22: 120	6.52 \pm 0.16 [60]	8.15 \pm 0.12 [497]	0.80 \pm 0.02	47 \pm 5
Gelok 2**	11/02/2010		140.03 \pm 1.35 (108)	2.86 \pm 0.01 (42870)	3.75 \pm 0.03 (14393)	24: 22: 120	6.52 \pm 0.16 [60]	8.15 \pm 0.12 [497]	1.25 \pm 0.04#	59 \pm 7
Gelok 4***	11/02/2010	93.2 \pm 1.32 (50)		1.78 \pm 0.01 (22555)	3.75 \pm 0.03 (14393)	24: 21.5: 180	6.90 \pm 0.35 [31]	6.85 \pm 0.11 [405]	1.01 \pm 0.05	59 \pm 9
Serdang***	13/06/1988	78.65 \pm 1.11 (50)		2.86 \pm 0.02 (19976)	7.25 \pm 0.06 (14081)	26: 21: 145	nd	nd	nd	64 \pm 11
Serdang***	13/06/1988	77.18 \pm 1.25 (38)		2.63 \pm 0.01 (35475)	7.25 \pm 0.06 (14081)	26: 21: 160	nd	nd	nd	64 \pm 11

Notes:

- The population-subtraction method was used; details are given in Westgate *et al.* (2007).
- Ages calculated using the zeta approach and $\lambda_D = 1.551 \times 10^{-10} \text{yr}^{-1}$.
- Zeta value is 301 ± 3 based on 6 irradiations at the McMaster Nuclear Reactor, Hamilton, Ontario, using the NIST SRM 612 glass dosimeter and the Moldavite tektite glass (Lhenice locality) with an $^{40}\text{Ar}/^{39}\text{Ar}$ age of $14.34 \pm 0.08 \text{Ma}$ (Laurenzi *et al.*, 2003, 2007).
- Standard error ($\pm 1\sigma$) on age estimate is calculated according to Bigazzi and Galbraith (1999).
- Area estimated using the point-counting method (Sandhu *et al.*, 1993).
- D_s = mean spontaneous track diameter,
- D_i = mean induced track diameter. Number of tracks counted is given in brackets. Number of tracks measured in given in square brackets.
- nd = not determined.

* Age is uncorrected for partial track fading.

** Sample corrected for partial track fading by the track-size (DCFT) method (Sandhu and Westgate (1995)).

APPENDIX II

Table A2-1: The major elements data for Peninsular Malaysia that were used in this study.

Sample	SiO ₂	TiO ₂	Al ₂ O ₃	FeO	MnO	CaO	MgO	Na ₂ O	K ₂ O	Total
PM-G1-1	77.3	0.03	12.5	0.86	0.14	0.68	0.07	3.36	4.96	99.85
PM-G1-2	77.3	0.03	12.5	0.96	-0.01	0.89	0.07	3.08	5.09	99.87
PM-G1-3	77.6	0.09	12.3	0.88	0.06	0.74	0.03	3.44	4.73	99.86
PM-G1-4	77.6	0.09	12.5	0.93	0.09	0.70	0.07	3.17	4.63	99.84
PM-G1-5	77.4	-	12.5	0.96	0.02	0.70	0.05	3.40	4.83	99.86
PM-G1-6	77.4	0.06	12.6	0.86	0.05	0.79	0.04	3.21	4.93	99.88
PM-G1-7	77.2	0.1	12.6	0.99	0.09	0.71	0.02	3.34	4.73	99.83
PM-G1-8	76.8	0.19	12.6	0.86	0.15	0.77	0.09	3.40	4.94	99.84
PM-G1-9	77.3	0.09	12.6	0.90	0.06	0.89	0.08	3.17	4.82	99.91
PM-G1-10	77.8	-	12.6	1.00	0.08	0.76	0.03	3.09	4.61	99.96
PM-G1-11	77.4	-	12.6	0.91	0.12	0.66	0.06	3.14	5.08	99.89
PM-G1-12	77.5	0.05	12.6	0.92	0.07	0.66	0.06	3.21	4.68	99.76
PM-G1-13	77.2	0.06	12.8	0.91	-0.01	0.87	0.04	3.16	4.85	99.84
PM-G1-14	77.4	-	12.7	0.94	-0.02	0.82	0.08	3.18	4.85	88.88*
PM-G1-15	77.3	0.04	12.7	1.00	-0.04	0.68	0.05	3.33	4.88	99.92
PM-G2-1	77.5	-	12.5	0.89	0.01	0.67	0.04	3.41	4.81	99.79
PM-G2-2	77.2	0.17	12.7	0.99	-0.07	0.87	0.05	3.25	4.77	99.89
PM-G2-3	77.4	-	12.6	0.96	0.20	0.68	0.05	3.23	4.79	99.89
PM-G2-4	77.6	-	12.5	0.80	0.09	0.66	0.07	3.42	4.85	99.98
PM-G2-5	77.4	0.08	12.5	0.89	0.02	0.71	0.02	3.27	5.01	99.84
PM-G2-6	77.3	0.13	12.7	1.02	0.05	0.84	0.08	3.11	4.62	99.84
PM-G2-7	78.1	-	12.3	0.77	-0.02	0.67	0.01	3.33	4.72	99.85
PM-G2-8	77.7	0.14	12.5	0.94	0.04	0.71	0.02	3.17	4.64	99.87
PM-G2-9	77.5	0.12	12.6	0.89	0.14	0.74	0.06	2.99	4.85	99.87
PM-G2-10	77.1	0.14	12.6	0.98	0.12	0.93	0.08	3.16	4.73	99.87
PM-G2-11	77.2	-	12.5	0.90	0.10	0.88	0.07	3.12	5.08	99.90
PM-G2-12	77.9	0.08	12.3	0.96	0.05	0.64	0.06	3.19	4.73	99.88
PM-G2-13	77.3	0.13	12.4	1.06	0.06	0.87	0.09	3.18	4.82	99.89
PM-G2-14	77.5	0.09	12.3	0.96	0.15	0.69	0.05	3.20	4.89	99.82
PM-G2-15	77.9	-	12.4	0.85	0.11	0.68	0.10	3.26	4.66	99.90
PM-G3-1	77.3	0.09	12.6	0.98	0.03	0.86	0.09	3.13	4.71	99.86
PM-G3-2	77.2	-	12.6	0.94	0.01	0.86	0.04	3.18	5.06	99.87
PM-G3-3	77.7	0.01	12.5	0.91	0.00	0.82	0.06	3.22	4.69	99.83
PM-G3-4	77.2	0.08	12.8	1.03	0.11	0.71	0.05	3.19	4.68	99.86
PM-G3-5	77.0	0.18	12.8	0.91	0.13	0.79	0.07	3.28	4.76	99.86
PM-G3-6	77.6	-	12.4	0.95	0.06	0.80	0.04	3.24	4.90	99.94
PM-G3-7	77.0	0.05	12.7	1.02	0.09	0.84	0.08	3.15	5.05	99.91
PM-G3-8	77.3	0.01	12.6	0.98	0.03	0.82	0.07	3.21	4.89	99.83
PM-G3-9	77.7	0.08	12.4	0.83	0.07	0.76	0.06	3.12	4.78	99.83
PM-G3-10	77.1	0.08	12.6	0.99	0.07	0.78	0.06	2.95	5.29	99.85

Sample	SiO ₂	TiO ₂	Al ₂ O ₃	FeO	MnO	CaO	MgO	Na ₂ O	K ₂ O	Total
PM-G3-12	77.3	0.04	12.6	0.88	0.08	0.84	0.10	3.24	4.86	99.88
PM-G3-13	77.5	0.04	12.8	0.96	0.04	0.76	0.07	2.55	5.13	99.86
PM-G3-14	77.2	-	12.6	1.01	-0.01	0.79	0.07	3.30	4.91	99.92
PM-G3-15	77.4	-	12.6	0.97	0.00	0.88	0.08	3.19	4.80	99.89
PM-G4-1	77.6	-	12.8	0.87	0.05	0.87	0.02	2.86	4.85	99.88
PM-G4-2	77.4	0.13	12.4	0.95	0.06	0.75	0.06	3.37	4.73	99.88
PM-G4-4	77.5	0.06	12.6	0.99	0.05	0.79	0.07	3.29	4.55	99.91
PM-G4-6	76.8	0.21	12.7	0.89	0.07	0.90	0.11	3.08	5.09	99.88
PM-G4-7	77.4	0.1	12.4	0.88	0.11	0.68	0.07	3.51	4.69	99.86
PM-G4-8	77.1	0.06	12.5	0.95	0.14	0.72	0.05	3.45	4.85	99.82
PM-G4-9	77.3	0.03	12.6	0.84	0.06	0.64	0.06	3.48	4.80	99.74
PM-G4-10	77.4	-	12.6	0.87	0.11	0.84	0.03	3.22	4.79	99.85
PM-G4-11	76.9	0.03	12.7	0.99	0.10	0.84	0.02	3.27	5.01	99.92
PM-G4-12	77.4	0.06	12.5	0.84	0.03	0.82	0.03	3.11	5.07	99.89
PM-G4-13	77.3	0.05	12.4	0.99	0.01	0.79	0.04	3.34	4.90	99.88
PM-G4-14	77.5	-	12.5	0.94	0.06	0.75	0.07	3.30	4.81	99.89
PM-G4-15	77.4	-	12.7	0.97	0.03	0.77	0.04	3.16	4.82	99.85
PM-G4-16	77.6	0.04	12.6	1.02	0.15	0.74	0.06	3.18	4.56	99.89
PM-G4-17	77.4	0.07	12.6	0.98	0.07	0.91	0.05	3.13	4.72	99.86
PM-G4-18	77.0	0.19	12.5	0.99	0.09	0.85	0.02	3.36	4.89	99.88
PM-G4-19	78.0	-	12.4	0.82	0.10	0.70	0.05	3.23	4.67	99.93
PM-G4-21	77.5	-	12.5	0.79	0.08	0.66	0.05	3.36	4.90	99.80
PM-P1-1	72.0	0.00	11.3	0.73	-	0.79	0.00	3.01	4.95	92.79
PM-P1-2	72.0	0.10	11.2	0.81	-	0.58	0.01	3.20	4.75	92.56
PM-P1-3	72.3	0.00	11.6	0.99	-	0.70	0.08	2.94	4.75	93.36
PM-P1-4	71.7	0.00	11.5	0.88	-	0.72	0.05	3.12	4.71	92.68
PM-P1-5	71.2	0.00	11.7	0.80	-	0.73	0.04	2.72	4.51	91.69
PM-P1-6	74.3	0.12	11.6	0.83	-	0.58	0.04	3.39	4.75	95.57
PM-P1-7	74.3	0.06	11.8	0.90	-	0.68	0.01	2.95	5.00	95.68
PM-P1-8	72.9	0.06	11.9	0.70	-	0.69	0.00	3.03	4.63	93.90
PM-P1-9	71.1	0.05	11.3	0.78	-	0.57	0.09	3.00	4.42	91.29
PM-P1-10	71.7	0.06	11.0	0.77	-	0.59	0.03	3.44	4.46	92.09
PM-P1-11	74.9	0.03	11.1	0.76	-	0.61	0.08	2.52	4.81	94.80
PM-P1-12	73.3	0.08	11.2	0.83	-	0.59	0.07	3.19	4.48	93.77
PM-P1-15	74.8	0.04	12.0	0.74	-	0.65	0.09	2.93	4.77	96.06
PM-P1-16	74.5	0.06	11.9	0.90	-	0.73	0.09	2.87	4.86	95.89
PM-P1-17	72.2	0.01	11.4	1.07	-	0.58	0.07	3.15	4.46	92.93
PM-P1-18	72.9	0.04	11.5	0.67	-	0.61	0.00	3.07	4.86	93.72
PM-P1-20	72.2	0.00	12.0	0.98	-	0.71	0.01	3.23	4.83	93.95
PM-P1-21	73.8	0.05	11.4	0.84	-	0.55	0.05	3.20	4.65	94.60
PM-P2-4	71.1	0.05	11.4	0.94	-	0.76	0.04	2.94	4.57	91.82
PM-P2-5	70.7	0.09	11.2	0.54	-	0.74	0.09	2.90	4.87	91.10
PM-P2-6	70.6	0.11	11.2	0.89	-	0.72	0.08	2.93	4.92	91.37

Sample	SiO ₂	TiO ₂	Al ₂ O ₃	FeO	MnO	CaO	MgO	Na ₂ O	K ₂ O	Total
PM-P2-7	72.3	0.00	11.1	0.64	-	0.50	0.03	2.58	4.66	91.73
PM-P2-8	70.9	0.07	11.2	0.84	-	0.59	0.08	2.66	5.30	91.62
PM-P2-10	70.7	0.00	13.5	0.70	-	0.59	0.09	3.05	4.41	92.97
PM-P2-11	71.7	0.06	11.1	0.64	-	0.67	0.09	2.51	4.21	91.05
PM-P2-12	71.4	0.02	10.5	0.46	-	0.66	0.00	3.00	4.64	90.64
PM-P2-13	70.8	0.07	11.4	0.85	-	0.68	0.00	2.52	5.01	91.36
PM-P2-15	74.5	0.00	11.4	0.56	-	0.61	0.05	2.07	4.70	93.88
PM-P2-16	72.9	0.12	11.5	0.65	-	0.75	0.07	2.89	4.89	93.71
PM-P2-17	71.9	0.09	11.7	0.89	-	0.76	0.03	2.52	5.18	93.01
PM-P2-21	70.8	0.00	11.6	0.77	-	0.75	0.00	3.07	5.05	92.05
PM-P2-22	72.7	0.04	11.6	0.56	-	0.68	0.04	2.97	4.93	93.49
PM-P3-2	70.2	0.04	10.9	0.82	-	0.83	0.14	3.08	5.04	91.04
PM-P3-3	71.2	0.12	10.7	0.79	-	0.59	0.01	3.08	4.36	90.81
PM-P3-5	70.1	0.13	10.9	0.88	-	0.68	0.11	3.03	4.69	90.50
PM-P3-6	66.7	0.00	12.2	0.60	-	0.57	0.00	2.98	7.01	90.13
PM-P3-13	69.7	0.15	10.8	1.01	-	0.75	0.00	3.06	4.73	90.18
PM-P3-17	71.3	0.00	10.8	1.16	-	0.70	0.08	3.45	4.91	92.39
PM-P3-19	70.1	0.09	10.7	0.95	-	0.77	0.00	2.94	4.53	90.08
PM-P4-1	70.8	0.02	10.9	0.77	-	0.92	0.01	3.03	4.66	91.09
PM-P4-5	71.9	0.07	10.6	0.80	-	0.70	0.01	2.60	4.17	90.81
PM-P4-8	71.9	0.00	10.4	0.60	-	0.56	0.03	2.93	4.23	90.65
PM-P4-9	73.4	0.17	9.6	0.79	-	0.66	0.06	2.38	4.19	91.23
PM-P4-11	70.3	0.06	11.0	0.87	-	0.80	0.13	2.71	4.37	90.19
PM-P4-12	71.1	0.08	11.2	0.89	-	0.59	0.03	2.81	4.50	91.23
PM-P4-13	70.9	0.07	11.1	1.03	-	0.56	0.03	3.00	4.29	90.97
PM-P4-14	71.1	0.01	11.0	0.87	-	0.66	0.04	2.93	4.46	91.14
PM-Q5-1	74.1	0.00	11.2	0.78	-	0.69	0.05	3.16	4.80	94.81
PM-Q5-3	72.5	0.06	11.4	1.05	-	0.70	0.07	3.17	5.09	94.07
PM-Q5-7	71.0	0.05	11.4	0.81	-	0.80	0.00	3.09	4.69	91.84
PM-Q5-10	70.3	0.03	10.9	1.10	-	0.73	0.02	3.19	4.84	91.07
PM-Q5-14	70.9	0.00	10.6	0.62	-	0.72	0.06	2.94	5.18	90.96
PM-Q5-16	72.2	0.03	11.1	0.86	-	0.64	0.10	2.74	5.10	92.76
PM-Q5-17	72.1	0.00	10.9	0.99	-	0.77	0.01	3.41	4.69	92.81
PM-Q5-18	73.1	0.11	10.7	0.69	-	0.66	0.00	3.41	4.88	93.55
PM-Q5-21	71.4	0.10	10.5	0.81	-	0.57	0.08	3.47	4.69	91.58
PM-Q5-24	72.9	0.04	11.0	0.94	-	0.69	0.00	3.36	4.89	93.76
PM-Q5-25	72.8	0.08	11.5	0.84	-	0.59	0.09	3.23	4.73	93.83
PM-Q5-26	73.5	0.19	11.6	1.07	-	0.66	0.00	3.47	4.66	95.15
PM-Q5-27	72.4	0.02	11.4	0.85	-	0.67	0.05	3.12	4.93	93.46
PM-Q5-29	73.1	0.00	11.6	0.91	-	0.72	0.03	3.29	5.12	94.74
PM-T5-2	71.3	0.08	11.6	0.91	-	0.45	0.08	3.36	4.75	92.56
PM-T5-4	71.6	0.02	11.0	0.75	-	0.73	0.05	3.22	4.67	91.99
PM-T5-5	70.7	0.00	11.5	0.68	-	0.58	0.05	2.93	4.92	91.38

Sample	SiO ₂	TiO ₂	Al ₂ O ₃	FeO	MnO	CaO	MgO	Na ₂ O	K ₂ O	Total
PM-T5-6	71.6	0.06	11.3	0.90	-	0.64	0.09	3.22	4.72	92.53
PM-T5-7	71.2	0.07	11.3	0.76	-	0.71	0.06	2.96	4.54	91.60
PM-T5-8	72.5	0.08	10.9	0.76	-	0.75	0.04	2.81	4.84	92.65
PM-T5-10	72.8	0.02	11.2	0.69	-	0.62	0.07	3.44	4.74	93.56
PM-T5-11	70.8	0.00	10.5	0.95	-	0.65	0.14	2.92	4.77	90.76
PM-T5-13	72.8	0.00	10.0	0.64	-	0.60	0.06	2.79	4.29	91.17
PM-T5-14	73.2	0.00	9.8	0.80	-	0.53	0.00	2.61	4.09	91.11
PM-T5-15	69.9	0.04	11.4	0.87	-	0.68	0.00	3.47	4.85	91.14
PM-T5-16	70.4	0.14	10.9	0.92	-	0.79	0.09	3.03	4.76	91.09
PM-T5-17	71.2	0.00	11.2	0.80	-	0.75	0.12	3.05	4.75	91.80
PM-T5-18	71.6	0.12	11.0	0.75	-	0.67	0.04	3.24	4.79	92.19
PM-T5-19	69.7	0.14	11.1	0.76	-	0.58	0.16	3.48	4.64	90.55
PM-T5-20	75.3	0.00	10.1	0.66	-	0.52	0.00	2.72	4.17	93.46
PM-T5-21	74.6	0.01	10.7	0.67	-	0.67	0.04	2.73	4.43	93.86
PM-T5-22	73.1	0.06	11.8	1.23	-	0.68	0.07	2.86	4.92	94.64
PM-T5-23	71.8	0.01	10.7	0.67	-	0.56	0.03	3.15	4.30	91.28
PM-T5-24	75.8	0.00	11.1	0.71	-	0.65	0.08	3.31	4.61	96.19
PM-K1-2	70.1	0.10	10.8	1.01	-	0.71	0.08	3.20	4.76	90.74
PM-K1-10	69.9	0.11	11.0	1.01	-	0.75	0.04	2.98	4.82	90.63
PM-K1-13	70.1	0.04	10.7	1.23	-	0.80	0.15	3.17	4.74	90.88
PM-K1-14	70.1	0.00	10.7	0.86	-	0.82	0.07	3.29	4.61	90.47
PM-K1-15	70.3	0.13	10.7	1.01	-	0.77	0.00	3.15	4.57	90.60
PM-K1-17	70.1	0.00	10.7	1.50	-	0.75	0.12	3.19	4.62	90.91
PM-D1-1	75.0	0.07	11.9	0.83	-	0.83	0.02	2.26	4.72	95.70
PM-D1-2	74.0	0.00	11.9	0.81	-	0.80	0.06	2.17	4.46	94.24
PM-D1-3	73.2	0.13	11.8	0.96	-	0.78	0.07	1.76	4.74	93.44
PM-D1-4	75.1	0.05	12.1	0.90	-	0.76	0.06	1.89	4.60	95.40
PM-D1-5	75.1	0.12	12.1	0.97	-	0.8	0.06	2.09	4.72	95.99
PM-D1-6	75.01	0.10	12.1	0.83	-	0.69	0.05	2.23	4.41	95.4
PM-D1-7	73.8	0.00	11.8	0.96	-	0.77	0.05	1.9	4.52	93.76
PM-D1-8	75.2	0.08	11.9	0.79	-	0.66	0.04	2.46	4.86	96.01
PM-D1-9	75.8	0.06	12.0	0.93	-	0.70	0.05	1.94	4.66	96.18
PM-D1-10	74.6	0.14	11.8	0.89	-	0.74	0.04	1.82	4.49	94.53
PM-3C-11a	77.3	0.02	12.9	1.00	-	0.67	0.05	3.06	4.97	95.50
PM-3C-11b	77.7	0.00	12.6	1.00	-	0.69	0.08	3.29	4.65	95.50
PM-3C-13	77.8	0.00	12.7	0.83	-	0.80	0.05	3.10	4.78	95.50
PM-3C-14	72.2	0.01	11.9	0.70	-	0.70	0.06	2.72	4.71	92.96
PM-3C-16	69.1	0.10	12.1	0.64	-	0.75	0.07	2.53	4.28	89.56
PM-3C-17a	73.4	0.10	11.8	0.87	-	0.62	0.03	2.76	4.36	93.88
PM-3C-17b	71.0	0.06	11.7	0.82	-	0.62	0.04	2.96	4.23	91.41
PM-3C-18	73.6	0.00	11.3	0.77	-	0.62	0.03	2.45	4.08	92.78
PM-3C-21	70.0	0.02	11.7	0.90	-	0.60	0.04	2.77	4.50	90.52
PM-3C-22	72.6	0.00	11.7	0.93	-	0.64	0.08	3.07	4.35	93.42

Sample	SiO ₂	TiO ₂	Al ₂ O ₃	FeO	MnO	CaO	MgO	Na ₂ O	K ₂ O	Total
PM-3C-23	72.2	0.00	11.8	0.77	-	0.74	0.05	2.88	4.43	92.79
PM-3C-24a	72.4	0.00	11.4	0.68	-	0.67	0.04	2.82	4.39	92.37
PM-3C-24b	71.3	0.02	11.9	0.82	-	0.78	0.07	2.98	4.49	92.31

Table A2-2: The major elements for Sumatra tephras that were used in this study.

Sample	SiO ₂	TiO ₂	Al ₂ O ₃	FeO	MnO	CaO	MgO	Na ₂ O	K ₂ O	Total
SM-4A-1a	76.4	0.06	11.82	0.65	-	0.69	0.07	3.26	4.22	97.11
SM-4A-1b	76.5	0.04	11.86	0.70	-	0.67	0.06	3.22	4.26	97.26
SM-4A-2a	73.1	0.05	11.95	0.62	-	0.71	0.05	3.28	4.25	93.98
SM-4A-2b	73.5	0.08	11.82	0.65	-	0.67	0.06	3.36	4.21	94.32
SM-4A-3	73.5	0.02	12.06	0.43	-	0.69	0.07	3.14	4.20	94.15
SM-4A-5	71.9	0.05	12.16	0.60	-	0.66	0.09	3.34	4.23	93.00
SM-4A-6	73.4	0.03	11.98	0.48	-	0.65	0.09	3.28	4.28	94.14
SM-4A-7	75.6	0.22	12.68	0.57	-	0.62	0.07	3.29	4.31	97.31
SM-4A-8	74.8	0.18	11.97	0.51	-	0.64	0.07	3.21	4.12	95.52
SM-4A-9	76.2	0.14	11.83	0.62	-	0.63	0.07	3.29	4.11	96.92
SM-4A-10a	77.5	0.10	12.05	0.70	-	0.75	0.05	2.23	4.07	97.41
SM-4A-10b	71.3	0.09	12.19	0.44	-	0.65	0.09	3.29	4.19	92.26
SM-4A-11a	73.5	0.10	11.98	0.46	-	0.67	0.07	3.21	4.27	94.29
SM-4A-11b	75.7	0.10	12.07	0.59	-	0.66	0.08	3.30	4.01	96.50
SM-4A-12	71.9	0.09	12.12	0.66	-	0.70	0.07	3.40	4.22	93.13
SM-4A-13	72.2	0.10	12.21	0.58	-	0.65	0.05	3.30	4.25	93.38
SM-4A-14	71.2	0.00	12.19	0.65	-	0.63	0.07	3.21	4.19	92.15
SM-4A-15	69.5	0.00	12.13	0.63	-	0.69	0.06	2.69	4.32	90.02
SM-4A-16	71.7	0.05	12.30	0.50	-	0.69	0.07	3.28	4.30	92.83
SM-4A-20	73.1	0.01	12.25	0.61	-	0.72	0.04	3.35	4.25	94.28
SM-4A-21a	75.8	0.05	12.32	0.65	-	0.69	0.10	3.51	4.20	97.28
SM-4A-21b	75.1	0.09	12.40	0.54	-	0.69	0.07	3.01	4.21	96.07
SM-4A-22	75.0	0.09	12.05	0.38	-	0.64	0.07	2.95	4.55	95.71
SM-4A-23	76.3	0.03	12.16	0.68	-	0.68	0.07	3.59	4.11	97.63
SM-4B-1	72.1	0.06	12.21	0.63	-	0.76	0.08	3.32	3.90	93.05
SM-4B-2a	73.6	0.09	11.99	0.66	-	0.73	0.09	3.36	3.92	94.44
SM-4B-2b	75.2	0.14	12.11	0.58	-	0.70	0.08	3.47	4.00	96.25
SM-4B-3	75.9	0.07	12.34	0.70	-	0.71	0.10	3.52	4.12	97.42
SM-4B-4	72.7	0.18	12.24	0.67	-	0.73	0.09	3.16	3.91	93.65
SM-4B-5	72.4	0.02	12.14	0.70	-	0.73	0.10	3.28	4.04	93.39
SM-4B-6	69.7	0.04	11.68	0.71	-	0.68	0.07	2.96	3.74	89.60
SM-4B-7a	75.3	0.09	12.48	0.65	-	0.73	0.07	3.57	4.11	96.95
SM-4B-7b	74.8	0.04	12.46	0.76	-	0.71	0.11	3.55	4.07	96.53
SM-4B-8	72.5	0.14	12.30	0.66	-	0.70	0.10	3.60	4.14	94.15
SM-4B-9	73.0	0.14	12.20	0.63	-	0.75	0.09	3.43	3.97	94.25
SM-4B-11a	74.8	0.02	12.04	0.46	-	0.75	0.09	3.34	3.96	95.40

Sample	SiO ₂	TiO ₂	Al ₂ O ₃	FeO	MnO	CaO	MgO	Na ₂ O	K ₂ O	Total
SM-4B-11b	72.8	0.15	12.26	0.79	-	0.72	0.09	3.41	3.96	94.14
SM-4B-12a	72.5	0.10	12.17	0.68	-	0.71	0.07	3.28	4.21	93.72
SM-4B-12b	75.2	0.09	12.12	0.54	-	0.73	0.06	3.31	4.23	96.28
SM-4B-13	72.5	0.05	12.19	0.68	-	0.79	0.11	3.37	4.04	93.71
SM-4B-14	75.4	0.14	12.08	0.74	-	0.72	0.09	3.55	3.94	96.64
SM-4B-15	75.4	0.14	12.05	0.60	-	0.77	0.10	3.33	3.98	96.41
SM-4B-17	75.7	0.04	12.26	0.76	-	0.75	0.11	3.40	4.04	97.06
SM-4B-18	74.1	0.00	12.00	0.62	-	0.75	0.08	3.40	4.07	95.05
SM-4B-19	73.7	0.10	12.22	0.67	-	0.73	0.10	3.34	4.00	94.84
SM-4B-20	72.6	0.01	12.28	0.67	-	0.74	0.07	3.46	4.20	93.97
SM-4B-21	74.6	0.09	12.13	0.76	-	0.73	0.10	2.45	4.07	94.87
SM-4B-22	73.0	0.16	12.18	0.72	-	0.77	0.09	3.13	3.99	93.99
SM-5A-2	77.2	12.70	0.80	0.10	-	0.78	0.08	3.26	5.02	99.91
SM-5A-3	77.2	12.35	0.86	0.01	-	0.82	0.09	3.18	5.25	99.85
SM-5A-4	76.8	12.65	0.97	0.12	-	0.87	0.06	3.24	5.25	99.94
SM-5A-5	77.3	12.56	0.90	0.00	-	0.82	0.02	3.23	4.95	99.84
SM-5A-6	77.2	12.47	0.92	0.15	-	0.72	0.07	3.18	5.04	99.86
SM-5A-7	76.8	12.58	0.98	0.16	-	0.90	0.09	3.21	5.12	99.87
SM-5A-8	77.2	12.39	0.89	0.05	-	0.84	0.04	3.25	5.23	99.90
SM-5A-9	77.0	12.41	0.93	0.02	-	0.84	0.06	3.35	5.18	99.85
SM-5A-10	77.0	12.59	0.74	0.10	-	0.86	0.09	3.03	5.35	99.89
SM-5A-12	77.1	12.67	0.83	0.08	-	0.72	0.05	3.17	5.12	99.82
SM-5A-13	77.1	12.48	0.82	0.01	-	0.81	0.08	3.24	5.22	99.87
SM-5A-14	76.9	12.47	0.90	0.11	-	0.75	0.07	3.32	5.31	99.87
SM-5A-15	77.3	12.60	0.89	0.06	-	0.77	0.03	3.08	5.05	99.86

Table A2-3 showed the rare-earth elements (REE) data for Lenggong (PM-G1, PM-G2, PM-G3 and PM-G4), Padang Sanai (PM-3C), Toba (SM-5A) and Sianok (SM-4A and SM-4B) that were used in this study. Concentrations were measured in ppm.

Sample	Zr	Rb	Sr	Y	Nb	Ba	La	Ce	Pr	Nd	Sm	Eu	Gd	Tb	Dy	Ho	Er	Tm	Yb	Lu	U
PM-G1-1	76.7	281	18.1	43.5	20.5	51.4	22.9	44.6	5.26	21.0	5.26	0.22	6.92	1.04	6.77	1.47	5.03	0.81	5.63	0.92	6.56
PM-G1-2	87.6	220	48.6	30.9	16.3	446.1	30.2	53.2	5.45	20.3	4.35	0.32	5.53	0.70	6.33	1.17	3.79	0.61	3.65	0.65	4.46
PM-G1-3	97.9	288	21.0	51.9	22.1	78.8	25.8	50.3	5.90	23.5	5.34	0.32	7.86	1.17	8.43	1.87	5.76	1.05	6.31	0.95	6.90
PM-G1-4	82.1	274	20.8	48.4	20.7	69.8	24.7	45.9	5.73	21.4	4.70	0.31	6.82	1.00	7.38	1.66	5.79	0.93	6.22	0.99	6.45
PM-G1-5	94.5	259	21.4	53.4	23.6	73.5	28.0	54.8	6.28	25.2	6.22	0.28	8.88	1.22	8.63	1.87	6.56	1.06	7.31	1.07	7.62
PM-G1-6	93.9	210	59.2	33.9	16.8	506.4	32.8	58.5	6.14	23.5	4.89	0.56	6.98	0.76	5.09	1.18	3.97	0.55	4.23	0.63	4.62
PM-G1-7	81.8	268	19.6	44.4	22.5	83.1	22.1	41.9	4.91	18.1	4.89	0.21	6.63	0.87	7.25	1.57	5.06	0.76	5.31	0.87	6.19
PM-G1-8	82.4	285	22.2	56.0	21.6	71.5	27.7	56.8	6.69	23.3	8.15	0.10	7.51	1.33	8.96	1.63	5.03	0.97	8.67	1.26	7.77
PM-G1-9	101.8	208	55.6	35.3	17.4	505.2	35.2	60.5	6.66	23.6	4.90	0.47	6.72	0.89	5.99	1.33	4.46	0.77	4.57	0.71	4.82
PM-G1-10	93.4	230	41.1	38.9	17.4	274.9	28.0	50.3	5.48	22.3	5.10	0.50	5.32	0.81	7.01	1.47	4.09	0.76	4.26	0.86	4.85
PM-G1-11	99.0	270	22.8	58.7	21.3	61.0	29.8	56.0	6.86	26.7	5.89	0.24	8.87	1.33	9.78	2.19	7.27	1.12	7.58	1.27	7.53
PM-G1-12	90.6	252	22.0	53.8	21.9	70.3	27.0	51.2	6.06	23.5	5.19	0.41	8.24	1.20	9.52	2.06	6.82	0.99	6.53	1.19	7.56
PM-G1-13	107.8	274	35.8	21.7	26.4	387.9	23.9	99.0	4.49	16.4	4.46	0.30	7.26	0.52	2.95	0.79	2.22	0.45	2.48	0.40	4.76
PM-G1-14	91.4	197	53.0	33.1	16.0	494.1	32.3	57.8	6.10	23.4	4.67	0.46	6.53	0.77	5.32	1.24	4.09	0.75	4.41	0.64	5.07
PM-G1-15	79.3	223	36.4	33.4	16.3	253.9	25.2	46.2	5.22	19.8	4.96	0.30	6.08	0.70	5.80	1.36	3.75	0.56	4.01	0.67	5.18
PM-G2-1	69.1	288	17.8	40.3	20.2	52.3	19.9	44.7	4.71	20.7	5.11	0.14	6.57	0.88	6.49	1.43	4.82	0.81	5.46	0.69	7.42
PM-G2-2	84.4	217	53.1	25.0	15.8	588.4	33.0	51.9	5.42	20.5	4.18	0.54	6.82	0.66	5.63	1.04	3.72	0.50	3.20	0.50	4.16
PM-G2-3	71.6	274	19.6	42.2	19.9	67.9	20.8	46.9	5.03	19.7	4.45	0.28	7.32	0.95	7.10	1.60	5.40	0.87	5.57	0.85	7.57
PM-G2-4	73.8	284	18.2	44.2	20.8	54.1	23.0	49.8	5.85	20.2	5.44	0.24	7.67	1.00	8.35	1.64	5.36	0.94	6.03	0.87	8.01
PM-G2-5	82.7	289	21.3	39.4	21.5	125.2	22.0	48.5	5.38	20.6	7.98	0.24	6.81	0.83	7.10	1.50	4.84	0.78	5.09	0.73	6.98
PM-G2-6	75.0	231	41.8	25.1	17.4	402.0	24.7	51.3	4.94	17.9	3.70	0.46	5.06	0.68	4.46	0.83	3.21	0.59	3.18	0.49	5.19
PM-G2-7	73.3	277	19.0	42.9	19.8	70.4	22.2	47.7	5.10	19.5	5.09	0.26	7.66	0.98	7.44	1.64	5.06	0.94	5.83	0.86	7.48
PM-G2-8	72.3	273	17.6	42.3	19.7	67.5	22.6	47.0	5.09	19.8	5.09	0.17	6.47	0.97	7.45	1.58	4.93	0.76	5.34	0.96	7.88
PM-G2-9	80.5	240	41.1	35.6	18.1	304.1	27.5	54.5	5.91	23.6	5.08	0.41	7.38	0.84	6.36	1.44	4.22	0.86	4.67	0.77	5.78
PM-G2-10	80.4	206	47.5	28.8	15.6	448.5	28.2	55.4	5.79	21.4	5.07	0.46	6.08	0.66	5.33	0.93	3.45	3.87	3.77	0.58	4.72
PM-G2-11	80.6	263	43.3	27.0	17.0	469.8	27.7	53.6	5.79	19.4	3.36	0.40	6.74	0.69	5.45	1.23	3.49	0.70	4.00	0.51	5.10
PM-G2-12	85.2	281	23.0	51.1	21.7	83.8	25.4	48.8	5.71	23.4	6.15	0.31	8.23	1.44	8.44	1.95	5.90	1.00	6.27	1.07	7.74
PM-G2-13	101.7	214	54.7	30.2	19.4	628.0	33.0	59.4	6.34	22.0	4.79	0.42	6.07	0.79	5.76	1.24	3.81	0.62	3.65	0.64	4.83

Sample	Zr	Rb	Sr	Y	Nb	Ba	La	Ce	Pr	Nd	Sm	Eu	Gd	Tb	Dy	Ho	Er	Tm	Yb	Lu	U
PM-G2-14	65.7	258	17.1	37.2	18.4	56.3	19.5	43.3	4.80	18.6	4.77	0.25	6.89	0.85	6.58	1.41	4.49	0.79	5.38	0.82	7.65
PM-G2-15	79.9	285	20.7	43.0	21.3	97.9	23.4	49.2	5.15	19.8	5.44	0.16	7.18	0.97	7.45	1.56	6.73	0.95	5.67	0.95	7.82
PM-G3-1	86.8	197	59.7	27.0	15.1	690.0	31.7	60.5	5.88	21.9	4.09	0.43	6.24	0.68	5.19	1.16	3.24	0.49	3.76	0.60	4.37
PM-G3-2	88.9	222	54.9	30.6	17.5	482.1	29.6	65.8	6.12	22.2	4.62	0.50	6.69	0.95	5.11	1.19	4.14	0.65	3.94	0.56	5.88
PM-G3-3	78.6	214	51.5	29.5	15.2	516.7	28.5	56.8	5.81	21.1	4.39	0.49	6.60	0.75	5.21	1.15	3.79	0.64	4.01	0.62	4.83
PM-G3-4	92.7	231	54.9	33.9	16.9	544.2	32.9	61.5	6.41	24.4	4.30	0.52	6.79	0.77	5.47	1.21	4.33	0.66	4.27	0.66	5.98
PM-G3-5	94.4	230	55.6	33.7	17.4	522.8	32.9	65.9	6.98	25.0	4.69	0.36	7.37	0.91	6.71	1.28	4.41	0.70	4.80	0.69	5.41
PM-G3-6	89.4	234	46.4	36.0	17.6	369.8	29.9	57.9	6.74	24.4	4.99	0.39	8.23	0.96	7.02	1.36	4.92	0.76	5.83	0.87	6.18
PM-G3-7	94.1	212	58.1	34.6	16.0	524.5	34.6	62.0	6.61	25.3	4.91	0.50	6.80	0.98	6.43	1.30	4.12	0.68	4.11	0.66	4.95
PM-G3-8	79.7	219	49.9	29.8	15.3	461.5	28.6	53.3	5.94	19.7	4.76	0.49	6.12	0.82	4.65	1.12	3.58	0.59	3.79	0.69	4.64
PM-G3-9	78.0	239	38.4	35.3	16.5	265.1	25.1	50.0	5.50	20.2	4.23	0.45	6.20	0.95	5.86	1.41	4.66	0.71	4.59	0.64	5.81
PM-G3-10	88.8	209	42.7	24.4	19.8	449.3	25.9	71.3	5.57	18.6	4.06	0.38	6.73	0.57	4.65	1.08	3.21	0.55	3.40	0.51	5.65
PM-G3-12	90.0	215	51.2	29.4	16.5	476.4	29.8	58.0	5.87	21.8	4.71	0.59	6.80	0.69	5.62	1.27	3.56	0.51	3.98	0.56	4.87
PM-G3-13	91.4	185	42.0	24.8	19.3	413.0	24.7	69.2	5.28	20.1	3.59	0.42	6.44	0.87	4.43	1.06	3.34	0.56	3.78	0.61	5.12
PM-G3-14	139.7	237	49.6	33.3	24.2	531.5	32.6	102.5	6.85	24.1	5.15	0.56	8.57	0.80	6.06	1.32	4.23	0.59	4.06	0.60	6.84
PM-G3-15	79.9	220	49.1	29.0	15.8	462.1	28.1	55.1	5.66	19.6	3.88	0.47	6.34	0.74	4.44	1.03	3.43	0.64	3.81	0.60	4.84
PM-G4-1	99.4	223	59.9	39.4	17.1	550.6	38.2	67.1	7.09	26.8	5.15	0.49	6.84	0.91	6.59	1.35	4.52	0.68	4.57	0.79	5.42
PM-G4-2	88.1	237	41.7	38.4	17.2	300.3	29.6	53.6	6.08	22.0	5.20	0.25	5.93	0.80	5.85	1.76	4.36	0.66	5.21	0.77	5.68
PM-G4-4	85.3	211	51.3	30.6	16.1	511.2	32.0	56.6	5.83	22.5	4.84	0.47	6.37	0.80	5.36	1.18	3.80	0.66	3.93	0.72	4.87
PM-G4-6	83.0	255	19.5	50.2	20.1	54.7	25.7	51.3	5.88	24.3	6.10	0.25	7.00	1.05	8.84	1.72	5.94	0.94	6.70	0.98	7.63
PM-G4-7	87.7	278	20.9	53.4	20.9	61.7	26.9	52.4	6.35	24.3	6.57	0.27	7.08	1.19	8.99	1.84	5.65	1.01	7.29	0.97	8.29
PM-G4-8	71.5	232	16.7	42.7	17.7	49.2	21.4	43.2	4.94	19.7	5.22	0.08	5.39	0.89	6.80	1.44	4.92	0.89	5.34	0.69	6.42
PM-G4-9	95.2	221	58.4	35.8	22.2	570.3	36.8	65.1	6.82	24.9	5.46	0.56	6.25	0.87	5.83	1.22	4.52	0.64	5.20	0.87	5.61
PM-G4-10	89.8	209	62.9	28.8	15.5	733.3	36.3	64.1	6.70	21.5	4.27	0.58	4.95	0.62	4.31	0.93	3.43	0.55	3.48	0.51	4.06
PM-G4-11	84.5	219	48.4	31.9	14.9	445.4	30.9	56.9	5.77	21.0	4.44	0.47	5.12	0.75	5.06	1.21	3.18	0.51	4.47	0.67	5.19
PM-G4-12	85.3	203	54.3	30.4	15.6	510.1	32.0	58.9	6.20	23.0	4.63	0.42	5.02	0.78	5.41	1.12	3.59	0.57	4.14	0.68	4.98
PM-G4-13	80.6	196	51.9	32.8	15.2	520.7	32.4	55.8	6.32	24.5	4.67	0.37	5.69	0.79	5.31	1.24	4.10	0.52	4.09	0.65	5.83
PM-G4-14	100.4	224	60.7	36.4	16.5	577.9	37.6	71.7	7.15	26.4	5.08	0.65	5.91	0.86	5.34	1.20	4.46	0.62	4.64	0.82	5.30
PM-G4-15	94.5	253	48.6	40.4	22.2	399.2	34.4	61.1	6.71	25.4	5.84	0.42	6.39	1.04	6.61	1.52	5.28	0.78	5.25	0.69	6.81
PM-G4-16	84.9	209	52.2	32.6	15.8	471.7	31.2	58.2	5.86	22.0	4.17	0.47	5.03	0.73	5.49	1.15	4.02	0.61	3.91	0.71	4.85
PM-G4-17	68.7	197	41.5	28.8	14.9	394.8	25.8	48.3	5.12	24.4	3.90	0.54	4.70	0.80	5.02	0.95	2.74	0.41	3.14	0.50	4.73

Sample	Zr	Rb	Sr	Y	Nb	Ba	La	Ce	Pr	Nd	Sm	Eu	Gd	Tb	Dy	Ho	Er	Tm	Yb	Lu	U
PM-G4-18	82.8	290	21.8	47.8	20.2	80.9	24.7	50.2	5.81	23.2	4.88	0.23	7.02	1.03	8.25	1.69	5.89	0.84	6.41	1.02	7.82
PM-G4-21	80.6	272	21.3	49.8	20.5	87.8	25.5	50.9	5.71	23.1	5.32	0.25	6.62	1.12	7.32	1.49	5.41	1.00	6.27	0.94	7.85
PM-3C-20	61.1	260	30.9	36.2	18.1	130.7	22.8	42.0	4.86	17.9	3.94	0.38	4.04	0.84	5.10	1.13	3.95	0.52	4.15	0.66	4.83
PM-3C-21	78.0	210	54.6	24.1	14.4	433.1	25.9	46.0	5.22	18.3	3.96	0.48	3.54	0.53	3.80	0.67	2.22	0.43	2.42	0.46	3.22
PM-3C-18	62.8	278	23.8	38.5	19.3	51.7	23.2	42.9	4.79	16.9	5.02	0.15	5.19	0.82	5.59	1.19	3.91	0.62	4.55	0.65	5.11
PM-3C-16	72.6	208	57.1	26.6	15.8	468.1	29.2	53.5	5.86	21.3	3.66	0.47	3.42	0.46	4.09	0.91	2.64	0.40	3.32	0.47	3.56
PM-3C-17	77.7	273	25.7	39.4	19.5	70.2	23.0	40.9	4.93	17.1	4.45	0.36	4.94	0.89	5.79	1.21	3.90	0.66	5.25	0.78	5.29
PM-3C-11	78.6	263	27.5	33.3	17.3	139.8	23.3	43.2	4.89	18.6	4.31	0.14	4.53	0.71	5.29	1.22	3.67	0.66	3.61	0.55	4.82
PM-3C-24	88.8	242	51.6	41.6	18.4	301.0	29.0	51.8	5.72	20.8	4.46	0.73	4.94	0.94	4.73	0.85	3.84	0.66	3.79	0.54	4.59
PM-3C-23	66.0	244	45.3	31.0	18.8	268.7	27.3	49.4	5.37	19.9	4.36	0.33	4.91	0.76	4.48	1.00	3.35	0.55	3.62	0.62	4.44
PM-3C-22	96.2	200	56.3	24.8	14.6	468.8	28.5	50.8	5.29	18.5	3.16	0.41	3.32	0.50	3.52	0.82	2.41	0.51	3.35	0.60	3.61
PM-3C-8	73.1	297	26.6	42.3	21.3	85.9	42.7	52.4	5.95	21.7	5.54	0.19	6.16	0.88	6.18	1.41	4.39	0.85	5.43	0.97	6.07
PM-3C-6	68.6	254	50.3	32.9	16.9	288.1	27.7	51.1	5.52	20.1	4.19	0.39	4.27	0.63	4.97	0.90	3.17	0.57	4.04	0.51	4.71
SM-4A-1	55.9	209	71.4	21.0	8.2	618.9	21.9	41.1	4.34	15.1	3.32	0.20	3.33	0.58	3.04	0.64	2.16	0.34	2.07	0.39	4.41
SM-4A-1b	49.2	215	70.4	17.6	7.9	638.2	21.1	41.6	4.27	13.9	2.84	0.41	2.87	0.47	2.52	0.58	1.79	0.28	2.04	0.29	4.97
SM-4A-2	50.3	234	74.9	19.7	7.8	640.9	21.3	40.6	4.59	17.0	3.39	0.37	3.23	0.51	3.59	0.64	2.07	0.31	1.81	0.34	4.54
SM-4A-3	53.0	219	75.3	19.4	8.4	659.6	21.8	43.3	4.78	16.0	3.01	0.33	3.31	0.44	2.95	0.60	1.68	0.26	2.17	0.36	4.63
SM-4A-4	50.3	199	65.4	18.2	7.7	569.2	19.7	37.6	4.28	15.8	2.56	0.52	2.88	0.40	3.05	0.53	1.68	0.38	2.20	0.30	4.19
SM-4A-5b	51.9	220	72.6	18.4	8.6	646.8	20.8	43.6	4.72	15.7	3.49	0.53	3.08	0.42	2.96	0.63	1.87	0.25	2.08	0.34	4.73
SM-4A-6	46.2	213	68.5	15.5	7.8	624.7	18.5	40.3	3.93	13.7	2.95	0.47	2.08	0.35	2.18	0.45	1.30	0.25	1.49	0.27	4.44
SM-4A-7	61.0	231	86.1	22.4	8.3	752.0	25.6	48.5	5.34	19.3	3.80	0.62	3.25	0.49	3.41	0.76	2.14	0.35	2.44	0.37	5.25
SM-4A-8	64.1	229	91.4	23.4	11.2	779.7	26.5	50.0	5.46	19.9	4.58	0.57	3.54	0.66	3.34	0.54	2.54	0.39	3.02	0.51	5.05
SM-4A-9	61.2	226	83.3	21.1	8.7	720.3	24.9	47.0	5.40	19.0	3.63	0.55	3.12	0.49	3.13	0.58	1.86	0.27	2.84	0.48	5.00
SM-4A-10	56.1	223	74.5	19.9	8.4	640.1	21.4	42.3	4.72	15.5	3.31	0.46	2.92	0.44	3.31	0.54	1.63	0.30	1.97	0.33	4.76
SM-4A-11	51.8	203	68.1	18.3	10.2	620.5	20.1	41.0	4.45	14.6	3.20	0.49	2.66	0.46	3.09	0.63	1.94	0.28	2.13	0.36	4.63
SM-4A-12	60.7	227	82.6	23.0	8.9	746.1	25.8	48.1	5.61	17.8	3.30	0.66	3.52	0.43	3.50	0.66	2.28	0.30	2.72	0.37	4.97
SM-4A-13	57.4	213	73.0	20.9	10.1	651.9	21.6	42.6	4.74	14.5	3.15	0.47	3.29	0.44	3.00	0.72	2.06	0.25	2.20	0.33	4.55
SM-4A-14	61.4	232	83.9	22.8	10.7	737.5	24.7	46.4	5.71	21.0	3.68	0.57	3.44	0.60	2.94	0.72	2.19	0.36	2.40	0.31	4.63
SM-4A-15	60.2	236	85.8	20.8	9.2	738.3	24.4	48.4	5.23	18.3	3.40	0.36	3.49	0.46	3.32	0.69	2.19	0.35	2.55	0.36	5.01
SM-4A-16	56.1	217	75.1	20.8	10.2	652.4	21.7	42.0	4.86	15.5	2.98	0.53	3.04	0.41	2.91	0.63	2.02	0.37	2.42	0.36	4.42
SM-4A-20	62.8	238	85.3	22.9	11.0	746.2	26.2	48.3	5.34	18.5	3.57	0.54	3.63	0.64	3.89	0.70	2.06	0.36	2.91	0.45	5.13

Sample	Zr	Rb	Sr	Y	Nb	Ba	La	Ce	Pr	Nd	Sm	Eu	Gd	Tb	Dy	Ho	Er	Tm	Yb	Lu	U
SM-4A-21	61.3	225	77.2	21.1	11.3	683.5	24.1	43.9	4.87	15.5	3.55	0.54	3.16	0.52	3.40	0.68	2.02	0.31	2.44	0.38	4.58
SM-4A-22	68.8	240	93.0	25.0	11.0	788.2	28.8	52.6	6.06	18.4	4.44	0.75	3.72	0.60	4.19	0.88	2.28	0.41	2.93	0.45	5.15
SM-4A-23	62.1	214	74.1	22.0	10.8	666.5	23.6	42.6	4.67	15.8	3.99	0.49	3.39	0.47	3.00	0.62	1.74	0.33	2.21	0.40	4.48
SM-4B-2	71.6	210	90.6	22.1	10.8	653.1	27.9	52.1	5.58	19.0	3.46	0.49	3.26	0.46	3.32	0.67	2.39	0.27	2.46	0.37	3.97
SM-4B-2b	71.6	217	92.2	21.7	10.9	666.3	27.4	53.2	5.68	20.4	3.51	0.47	3.35	0.54	3.28	0.71	2.11	0.31	2.09	0.36	4.21
SM-4B-4	84.5	215	117.9	27.5	10.2	654.3	31.1	52.3	6.02	20.8	3.27	0.78	3.47	0.47	2.87	0.58	2.26	0.25	2.68	0.38	3.79
SM-4B-5	84.6	211	106.3	21.7	10.8	628.9	26.9	50.2	5.41	19.3	2.94	0.57	2.99	0.49	3.07	0.66	2.16	0.30	2.44	0.32	4.01
SM-4B-6	78.4	224	97.6	23.8	11.7	745.4	31.3	57.0	6.69	22.3	4.06	0.61	3.74	0.55	3.96	0.73	2.25	0.38	2.80	0.45	4.55
SM-4B-7	70.8	213	113.1	21.3	10.4	655.2	28.0	52.5	6.29	20.7	2.90	0.66	3.15	0.49	3.19	0.63	2.10	0.34	2.52	0.42	3.97
SM-4B-8	89.8	209	114.6	21.9	10.8	665.6	29.1	53.6	5.79	17.9	3.18	0.55	2.80	0.45	3.51	0.66	1.88	0.34	2.55	0.38	4.10
SM-4B-9	73.6	212	115.5	22.2	11.3	685.5	30.7	54.8	6.43	22.4	3.98	0.71	3.07	0.54	3.73	0.65	1.90	0.36	2.46	0.38	4.22
SM-4B-10	88.7	208	111.2	26.5	11.6	655.9	28.6	51.7	5.78	19.7	3.67	0.79	3.48	0.48	3.61	0.62	2.06	0.33	2.31	0.34	3.86
SM-4B-11	89.2	218	125.5	21.8	10.3	647.7	28.3	50.9	5.82	19.5	3.06	0.60	3.60	0.46	2.69	0.59	1.87	0.32	2.20	0.39	4.02
SM-4B-12	75.0	221	96.2	26.3	11.0	662.8	22.9	43.3	4.97	15.8	3.57	0.66	2.86	0.38	3.11	0.68	2.10	0.31	2.39	0.32	4.45
SM-4B-13	92.3	212	110.9	28.0	12.4	669.0	29.4	53.3	5.86	21.6	4.02	0.58	3.20	0.56	3.61	0.67	2.02	0.31	2.39	0.38	4.10
SM-4B-14	91.7	221	116.8	28.8	10.6	672.6	28.9	52.7	5.87	21.5	3.25	0.76	3.40	0.48	3.22	0.67	1.94	0.38	2.28	0.41	4.21
SM-4B-15	74.5	211	119.1	22.2	11.6	684.2	28.7	53.9	6.38	20.4	3.66	0.63	2.83	0.51	3.49	0.60	2.05	0.31	2.19	0.35	4.12
SM-4B-16	62.4	190	96.5	24.2	9.7	575.5	24.4	46.2	5.10	16.2	3.28	0.61	3.17	0.38	2.78	0.57	1.75	0.27	1.91	0.34	3.52
SM-4B-17	93.1	212	118.6	22.0	11.4	681.6	30.0	56.4	6.00	20.6	3.97	0.68	3.46	0.54	3.56	0.59	1.91	0.29	2.24	0.29	4.26
SM-4B-18	81.5	218	109.7	20.3	10.5	668.1	27.8	52.9	5.76	22.0	3.64	0.54	3.40	0.48	2.92	0.66	1.70	0.36	2.02	0.31	4.12
SM-4B-19	91.8	219	118.7	21.8	11.2	689.3	30.0	54.4	6.06	21.4	3.37	0.61	3.43	0.58	3.98	0.69	1.78	0.37	2.43	0.35	4.32
SM-4B-20	70.3	209	109.9	25.9	10.5	648.4	28.3	52.1	5.45	18.1	3.83	0.63	3.35	0.46	3.13	0.55	2.22	0.30	2.67	0.33	4.53
SM-4B-21	99.8	224	126.4	29.8	10.9	746.4	32.4	59.2	6.73	22.9	4.25	0.66	3.92	0.54	3.80	0.83	2.38	0.37	2.72	0.42	4.63
SM-4B-22	77.1	223	126.7	29.2	11.9	770.5	31.5	59.8	6.55	22.8	4.22	0.70	3.65	0.57	3.73	0.73	2.33	0.43	3.18	0.42	4.75
SM-5A-1	117	219	60.9	42.7	19.7	566	45.8	67.5	8.34	33.0	7.51	0.59	7.05	1.12	6.80	1.74	5.41	0.84	6.12	1.17	6.13
SM-5A-2	100	219	58.6	36.1	16.5	551	36.7	63.3	6.84	26.0	4.76	0.50	5.05	0.83	5.50	1.37	3.56	0.61	4.35	0.76	4.75
SM-5A-3	92.9	214	57.1	36.5	15.3	526	38.6	58.3	6.71	24.9	5.42	0.57	5.82	0.66	5.79	1.24	4.24	0.67	4.40	0.86	5.08
SM-5A-4	102	207	55.6	36.7	15.9	501	37.8	58.6	6.78	27.2	5.46	0.52	6.05	0.91	6.04	1.33	4.62	0.57	4.84	0.76	4.75
SM-5A-5	87.8	220	54.3	32.9	16.1	517	33.9	58.4	6.13	22.4	4.48	0.52	4.54	0.86	5.18	1.09	3.58	0.54	4.57	0.69	4.75
SM-5A-6	107	228	60.4	42.1	16.2	553	42.8	64.4	7.66	42.7	7.21	0.68	7.18	0.93	7.32	1.43	4.16	0.81	5.16	0.79	6.26
SM-5A-7	86.9	195	54.3	31.8	15.0	515	34.8	58.5	6.26	23.6	4.80	0.39	5.17	0.81	5.45	1.22	3.93	0.63	4.80	0.67	5.36

Sample	Zr	Rb	Sr	Y	Nb	Ba	La	Ce	Pr	Nd	Sm	Eu	Gd	Tb	Dy	Ho	Er	Tm	Yb	Lu	U
SM-5A-8	104	226	61.8	39.3	17.0	605	39.0	67.6	7.42	26.8	5.27	0.70	6.03	0.93	6.42	1.23	3.84	0.60	4.62	0.73	6.65
SM-5A-9	113	231	60.7	42.8	17.9	562	40.4	69.5	7.51	26.3	5.62	0.53	6.85	1.10	7.28	1.46	4.43	1.05	4.37	0.93	5.39
SM-5A-10	131	173	51.8	43.5	34.3	507	47.6	69.5	16.41	29.5	7.61	0.29	5.37	1.04	7.89	1.57	20.76	0.80	6.06	1.33	7.59
SM-5A-11	88.6	220	59.2	39.4	14.6	532	33.8	57.5	7.75	27.8	6.35	0.53	5.24	0.66	5.21	1.08	4.63	0.53	4.44	0.94	4.96
SM-5A-12	88.3	212	54.5	34.0	16.1	521	37.1	59.6	6.70	24.8	4.38	0.57	5.23	0.76	4.83	1.19	3.81	0.52	4.08	0.63	5.47
SM-5A-13	87.8	215	55.7	33.0	14.8	487	33.2	56.0	6.12	21.5	5.09	0.39	5.48	0.76	4.60	0.95	3.65	0.55	3.77	0.67	4.51
SM-5A-14	95.9	211	56.4	35.9	14.8	494	33.8	56.6	6.49	24.2	5.02	0.51	5.31	0.76	5.30	1.05	3.64	0.70	4.11	0.78	4.88
SM-5A-15	112	210	60.7	40.1	22.6	558	39.6	316.5	7.94	31.4	5.42	0.61	9.31	0.95	6.13	1.60	4.97	0.77	4.72	0.94	5.40

Table A2-4: Table of mineral/melt partition coefficients for rhyolitic melts.

Model 1 - Rb-Sr			Model 2 - Ba-Sr			Model 3 - Ba-Y			Model 4 - Nb-Y			Model 5 - Ba-Nb			
Rb	Sr		Ba	Sr		Ba	Y		Nb	Y		Ba	Nb		
Init	200	80	Init	500	70	Init	650	50	Init	21	50	Init	650	19	
Opx			Opx			Opx			Opx			Opx			
1	2.30103	1.90309	1	2.69897	1.845098	1	2.8129134	1.69897	1	1.3222193	1.69897	1	2.8129134	1.278754	
0.9	2.3466502	1.948436	0.9	2.74459	1.890444	0.1	0.9	2.8585336	1.69897	0.9	1.3313708	1.69897	0.9	2.8585336	1.287905
0.8	2.3976493	1.999128	0.8	2.795589	1.941136	0.2	0.8	2.9095326	1.69897	0.8	1.3416013	1.69897	0.8	2.9095326	1.298136
0.7	2.4554672	2.056598	0.7	2.853407	1.998606	0.3	0.7	2.9673506	1.69897	0.7	1.3531997	1.69897	0.7	2.9673506	1.309734
Cpx			Cpx			Cpx			Cpx			Cpx			
1	2.30103	1.90309	1	2.69897	1.845098	1	2.8129134	1.69897	1	1.3222193	1.69897	1	2.8129134	1.278754	
0.9	2.3453232	1.925237	0.9	2.738733	1.867245	0.9	2.8526766	1.561698	0.9	1.3313708	1.561698	0.9	2.8526766	1.287905	
0.8	2.3948389	1.949994	0.8	2.783185	1.892002	0.8	2.8971282	1.40824	0.8	1.3416013	1.40824	0.8	2.8971282	1.298136	
0.7	2.4509751	1.978063	0.7	2.83358	1.920071	0.7	2.9475232	1.234264	0.7	1.3531997	1.234264	0.7	2.9475232	1.309734	
Hbl			Hbl			Hbl			Hbl			Hbl			
1	2.30103	1.90309	1	2.69897	1.845098	1	2.8129134	1.69897	1	1.3222193	1.69897	1	2.8129134	1.278754	
0.9	2.3461469	1.947841	0.9	2.742714	1.889849	0.9	2.8566575	1.51594	0.9	1.1849468	1.51594	0.9	2.8566575	1.141481	
0.8	2.3965833	1.997868	0.8	2.791616	1.939876	0.8	2.9055593	1.31133	0.8	1.0314893	1.31133	0.8	2.9055593	0.988024	
0.7	2.4537633	2.054584	0.7	2.847056	1.996592	0.7	2.9609996	1.079362	0.7	0.8575134	1.079362	0.7	2.9609996	0.814048	
Bio			Bio			Bio			Bio			Bio			
1	2.30103	1.90309	1	2.69897	1.845098	1	2.8129134	1.69897	1	1.3222193	1.69897	1	2.8129134	1.278754	
0.9	2.1976181	1.943357	0.9	2.45371	1.885365	0.9	2.5676532	1.743355	0.9	1.0766388	1.743355	0.9	2.5676532	1.033173	
0.8	2.0820134	1.988371	0.8	2.179532	1.930379	0.8	2.2934757	1.792973	0.8	0.8021033	1.792973	0.8	2.2934757	0.758638	
0.7	1.9509516	2.039404	0.7	1.868695	1.981412	0.7	1.9826389	1.849225	0.7	0.4908605	1.849225	0.7	1.9826389	0.447395	
Gar			Gar			Gar			Gar			Gar			
1	2.30103	1.90309	1	2.69897	1.845098	1	2.8129134	1.69897	1	1.3222193	1.69897	1	2.8129134	1.278754	
0.9	2.3463757	1.948161	0.9	2.74395	1.890169	0.9	2.857893	0.143215	0.9	1.3679768	0.143215	0.9	2.857893	1.324511	
0.8	2.3970678	1.998546	0.8	2.794233	1.940554	0.8	2.9081759	-1.59597	0.8	1.4191293	-1.59597	0.8	2.9081759	1.375664	
0.7	2.4545378	2.055668	0.7	2.851239	1.997676	0.7	2.965182	3.567697	0.7	1.4771213	3.567697	0.7	2.965182	1.433656	

Plg			Plg			Plg			Plg			Plg		
1	2.30103	1.90309	1	2.69897	1.845098	1	2.8129134	1.69897	1	1.3222193	1.69897	1	2.8129134	1.278754
0.9	2.3449114	1.747515	0.9	2.730634	1.689523	0.9	2.8445775	1.740152	0.9	1.3652313	1.740152	0.9	2.8445775	1.321766
0.8	2.3939667	1.573596	0.8	2.766032	1.515604	0.8	2.8799751	1.786189	0.8	1.4133147	1.786189	0.8	2.8799751	1.369849
0.7	2.449581	1.376423	0.7	2.806162	1.318431	0.7	2.9201055	1.838382	0.7	1.4678271	1.838382	0.7	2.9201055	1.424361
Ksp			Ksp			Ksp			Ksp			Ksp		
1	2.30103	1.90309	1	2.69897	1.845098	1	2.8129134	1.69897	1	1.3222193	1.69897	1	2.8129134	1.278754
0.9	2.3312299	1.771766	0.9	2.464692	1.713774	0.9	2.578635	1.744727	0.9	1.3664668	1.744727	0.9	2.578635	1.323001
0.8	2.3649906	1.624958	0.8	2.202791	1.566966	0.8	2.3167341	1.79588	0.8	1.4159313	1.79588	0.8	2.3167341	1.372466
0.7	2.4032653	1.458521	0.7	1.905872	1.400529	0.7	2.0198153	1.853872	0.7	1.4720095	1.853872	0.7	2.0198153	1.428544
Apt			Apt			Apt			Apt			Apt		
1	2.30103	1.90309	1	2.69897	1.845098	1	2.8129134	1.69897	1	1.3222193	1.69897	1	2.8129134	1.278754
0.9	2.3467875	1.948847	0.9	2.744727	1.890856	0.9	2.8586708	0.085572	0.9	1.3679768	0.085572	0.9	2.8586708	1.324511
0.8	2.39794	2	0.8	2.79588	1.942008	0.8	2.9098234	2.080521	0.8	1.4191293	2.080521	0.8	2.9098234	1.375664
0.7	2.455932	2.057992	0.7	2.853872	2	0.7	2.9678153	4.342206	0.7	1.4771213	4.342206	0.7	2.9678153	1.433656
.66Cpx+.34Ksp			.66Cpx+.34Ksp			.66Cpx+.34Ksp			.66Cpx+.34Ksp			.66Cpx+.34Ksp		
1	2.30103	1.90309	1	2.69897	1.845098	1	2.8129134	1.69897	1	1.3222193	1.69897	1	2.8129134	1.278754
0.9	2.3406302	1.874131	0.9	2.647477	1.816139	0.9	2.7614208	1.622647	0.9	1.3430578	1.622647	0.9	2.7614208	1.299592
0.8	2.3848994	1.841757	0.8	2.589914	1.783765	0.8	2.7038569	1.537324	0.8	1.3663532	1.537324	0.8	2.7038569	1.322887
0.7	2.4350877	1.805055	0.7	2.524653	1.747063	0.7	2.6385964	1.440594	0.7	1.3927634	1.440594	0.7	2.6385964	1.349298
.6Hbl+.4Ksp			.6Hbl+.4Ksp			.6Hbl+.4Ksp			.6Hbl+.4Ksp			.6Hbl+.4Ksp		
1	2.30103	1.90309	1	2.69897	1.845098	1	2.8129134	1.69897	1	1.3222193	1.69897	1	2.8129134	1.278754
0.9	2.3401801	1.877411	0.9	2.631505	1.819419	0.9	2.7454485	1.607455	0.9	1.2575548	1.607455	0.9	2.7454485	1.214089
0.8	2.3839462	1.848704	0.8	2.556086	1.790712	0.8	2.6700292	1.50515	0.8	1.1852661	1.50515	0.8	2.6700292	1.1418
0.7	2.4335641	1.816159	0.7	2.470583	1.758167	0.7	2.5845259	1.389166	0.7	1.1033118	1.389166	0.7	2.5845259	1.059846

Table A2-5: Chondrite Standards of Sun and McDonough (1989) used to normalize Trace and Rare Earth Elements (REE).

La	Ce	Pr	Nd	Sm	Eu	Gd	Tb	Dy	Ho	Er	Yb	Lu
0.237	0.612	0.095	0.467	0.153	0.058	0.2055	0.0374	0.254	0.0566	0.1655	0.17	0.0254

Cs	Rb	Ba	Th	U	Nb	Ta	Pb	Sr	Zr	Hf	Eu	Y
0.188	2.32	2.41	0.029	0.008	0.246	0.014	2.47	7.26	3.87	0.1066	0.058	1.57

Table A2-6: Normalizing standards of Pearce (1983) and Sun and Mc Donough (1989) used to normalize the spider diagrams to MORB.

Rb	Ba	Th	K	Nb	Ta	La	Ce	Sr	Nd	Sm	Zr	Eu
2.0	20.0	0.2	0.15	3.5	0.132	2.5	10.0	120.0	7.3	3.3	90.0	1.02

Ti	Y	Yb
1.5	30.0	3.0

APPENDIX III



Fig. A3-1: Picture of Bukit Sapi tephra (PM-S1) in Lenggong, Perak. Outcrop showed more than 2 m thick of tephra. SEM photos from this sample showed fresh and fine glass shards texture (refer fig. 3-10A).

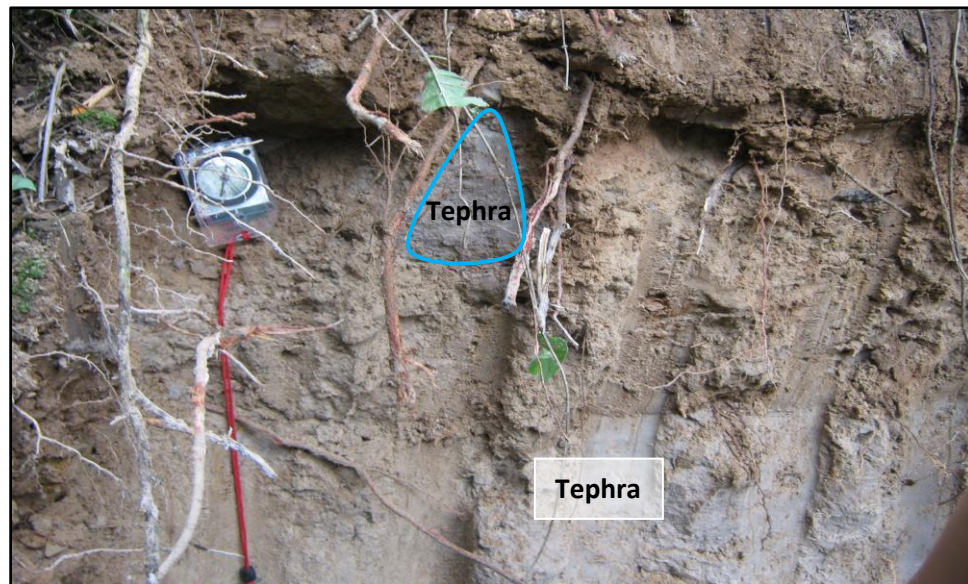


Fig. A3-2: Picture of Gua Badak tephra in Lenggong, Perak. Noted the circled area shown that tephra was transported in a small volume and eventually disappear in this formation.

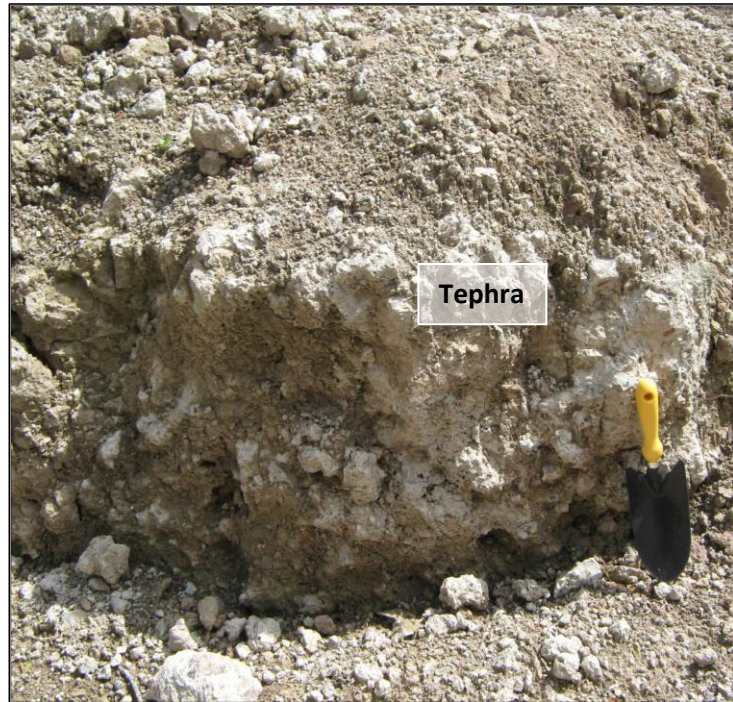


Fig. A3-3: Picture of Temelong tephra in Lenggong, Perak. This tephra was highly reworked and cemented.



Fig. A3-4: Picture of Labit tephra in Lenggong, Perak. Tephra was highly cemented and compacted.



Fig. A3-5: Picture of Lubuk Kawah tephra in Kota Tampan province, located at Lenggong, Perak. Tephra were well-preserved by palm plantations. The thickness of tephra was approximately 0.7 – 1.0 m.

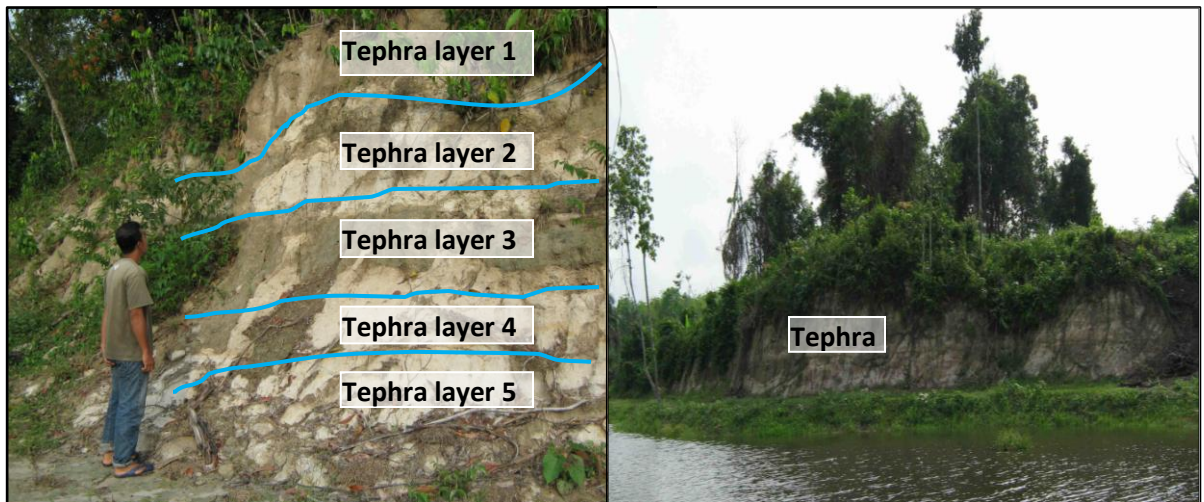


Fig. A3-6: Picture of Sena Halu outcrop in Luat province, located at Lenggong, Perak. Recently, the fresh tephra layers were exposed by man-made lake, consisted of more than 4 layers with the total tephra thickness more than 4 m. Global Positioning System (GPS) location: N 05° 03' 31.2'' E 100° 58' 56.8''.



Fig. A3-7: Picture of Padang Ragut Grus tephra in Lenggong, Perak. This fresh tephra outcrop had been destroyed by animal activities.

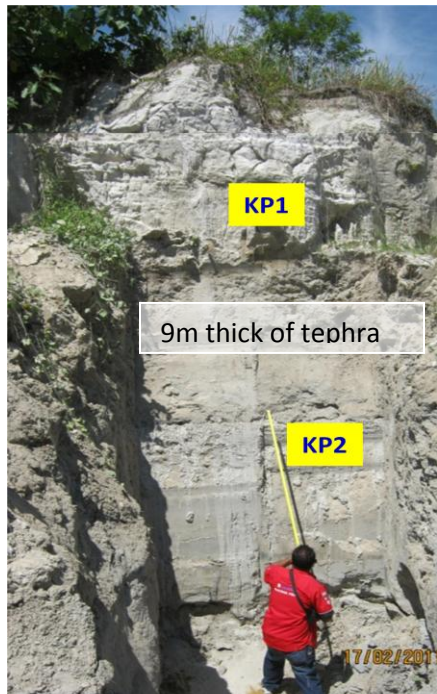


Fig. A3-8: Picture of Kuala Pelus tephra at 'Labu Sayong' mines in Kuala Kangsar district, Perak. Current work suggested that KP1 originated from Toba while KP2 originated from Maninjau eruptions. GPS location: N 04° 53.337' E 101° 00.005'.

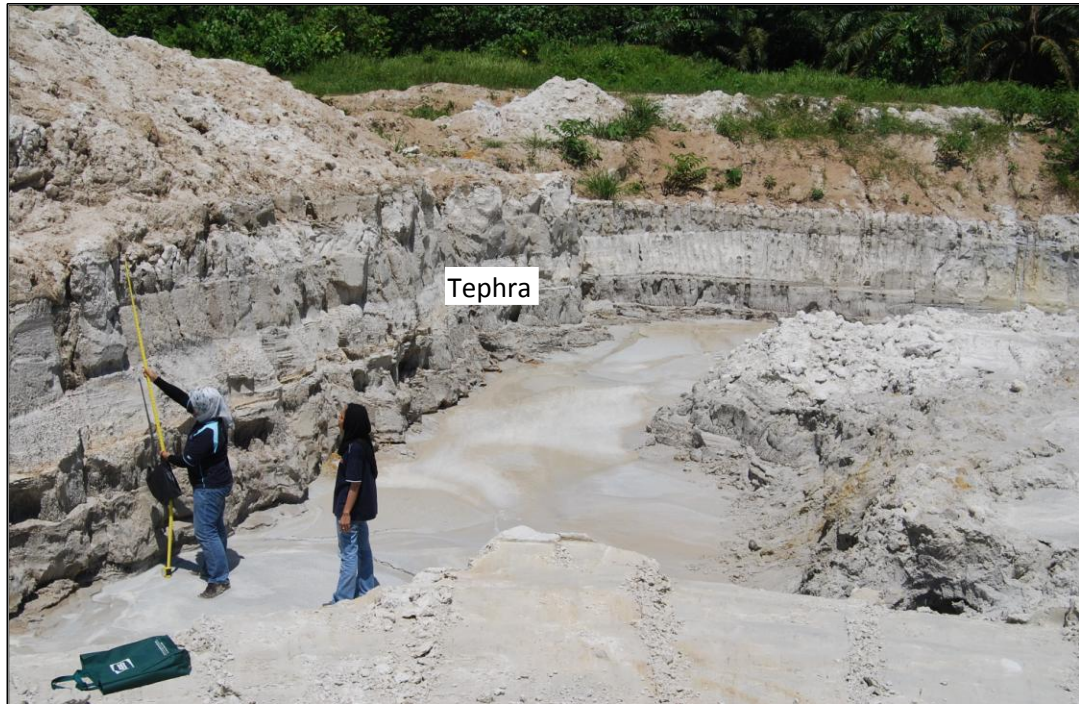


Fig. A3-9: Picture of Kg. Talang tephra (PM-T1) in Kuala Kangsar, Perak. Outcrop was approximately 3.5 m thick displaying 3 distinct tephra layers. GPS location: N 04° 53.750' E 101° 02.024'.



Fig. A3-10: Picture of Kg. Dong sample (PM-D1) at Raub, Pahang. The tephra was deposited at an abandoned paddy field.